ASSESSMENT OF HIGH LATITUDE VARIABILITY AND EXTREME EVENTS IN THE BERING SEA AS SIMULATED BY A GLOBAL CLIMATE MODEL

By

Joshua M. Walston

RECOMMENDED:

_____
Dr. Uma S. Bhatt

_____
Dr. John E. Walsh
Advisory Committee Co-Chair

_____
Dr. Georgina A. Gibson
Advisory Committee Co-Chair

_____
Dr. Uma S. Bhatt,
Chair, Department of Atmospheric Sciences

APPROVED:

_____
Dr. Paul W. Layer
Dean, College of Natural Science and Mathematics

_____
Dr. John C. Eichelberger
Dean of the Graduate School

_____
Date

ASSESSMENT OF HIGH LATITUDE VARIABILITY AND EXTREME EVENTS IN THE BERING SEA AS SIMULATED BY A GLOBAL CLIMATE MODEL

A

THESIS

Presented to the Faculty

of the University of Alaska Fairbanks

in Partial Fulfillment of the Requirements

for the Degree of

MASTER OF SCIENCE

By

Joshua M. Walston, B.S.

Fairbanks, Alaska

August 2014

Abstract

Atmospheric and Oceanic observations of the Arctic and Subarctic are relatively sparse and hinder our ability to analyze short term variability and long-duration anomalies of physical and biological variables over decadal time scales. Earth System Models (ESM's), such as the Community Earth System Model (CESM1), represent a useful tool to advance the understanding and the predictive potential of large-scale shifts in the climate and climate related impacts.

This thesis initially focuses on assessing the skill of the Community Climate System Model (CCSM4), to capture natural variability of the climate system. Subsequently, I examine the impacts of variability and seasonal-scale extremes of the physical environment on the marine ecosystem of the eastern Bering Sea as simulated by an earth system model, the CESM1, which includes the CCSM4 and earth system elements. A performance assessment of key atmospheric components (air temperature, sea level pressure, wind speed and direction) simulated by the CCSM4 over the Bering Sea and Arctic domains suggests a general improvement in model predictions at high latitudes relative to the model's predecessor, the CCSM3. However, several shortcomings, with possible implications for marine ecosystem modeling, still remain in this version of the CCSM. The most important of which includes an under-simulated Siberian High and a large northwest displacement of the Aleutian Low resulting in a negative bias of up to 8 hPa over the Bering Sea. The simulated inter-annual variability of surface air temperature and sea level pressure over the Bering Sea was found to exceed observed variability by ~1.5 to 2 times. The displaced pressure systems and increased variability could have important ramifications for modeling efforts that use CCSM atmospheric output as drivers for marine ecosystem studies.

When the CCSM was combined with other earth system elements to form the CESM, the coupled model was found to simulate strong linear relationships between primary production and air temperature, and between primary production and sea ice area over the fifty-five year period examined (1950-2005). A trend towards warmer air temperatures and reduction in sea ice area was found in every season. With a simulated increase in air temperature, an increase in the occurrence of seasonal positive primary production extremes followed. There were several instances of extremes in the physical environment coinciding with primary production extremes. However, clear, discernable patterns relating seasonal extremes in the physical environment to extremes in the production were hard to come by, suggesting that the complex interaction between the biology and physics was not fully captured by the variables examined. However, it is perhaps more likely that the lack of correspondence was because the important interactions between the biology and physics of the eastern Bering Sea occur on sub-seasonal timescales.

Table of Contents

Page

Page

Page

Page

List of Figures

List of Tables

Acknowledgements

I would like to thank Dr. Georgina Gibson and Dr. John Walsh for serving as co-chairs to my committee. Without their guidance and persistent help this research would not have been completed. Their enthusiasm and passion for the climate sciences has been extremely encouraging throughout my studies. I would also like to thank Dr. Uma Bhatt for taking the time to be a member of my committee. Her willingness to help and the fruitful comments she has given have greatly improved this thesis. I cannot thank my committee enough for their patience throughout the writing process, especially Dr. Gibson and Dr. Walsh. The time they spent revising and editing each part of this thesis, will always be greatly appreciated. Additionally, this research would not have been completed without the funding of the National Science Foundation Arctic Research Program under award number 1049225.

The research comprising this thesis was conducted as a group effort. While I independently completed the data manipulation, analysis, and authored the body of this work, Dr. Gibson and Dr. Walsh provided interpretation, ideas and direction for this research and each manuscript Walston et al. (2014) and Walston et al. (submitted).

1 Introduction

Recent changes to the Arctic environment have been widespread and occurring at rates faster than previously anticipated (Jeffries et al., 2013). Evidence of change has been found throughout the entire Arctic system, including increase in air temperature (Christensen et al., 2007), decreasing summer sea ice extent, volume, and thickness (Walsh et al., 2014), receding glaciers (Hassol et al., 2004), thawing permafrost (Romanovsky et al, 2013) and increased frequency of wildfires (Kelly et al., 2013). The changes seen in the Arctic could be an early indication of broader scale changes with environmental and societal implications on a global scale (Hassol et al., 2004). Large-scale modes of climate variability over spatial and temporal scales are often associated with the changes in the Arctic region. However, the rapid changes in the Arctic have been attributed to positive feedback mechanisms due to recent temperature amplifications caused by anthropogenic forcing (Screen and Simmonds, 2010). Strong evidence suggests that human-induced climate change is continuing to strengthen and climate related impacts are increasing (Melillo, 2014).

Natural changes to the climate system are a result of internal climate variability and exhibit oscillatory characteristics on a range of scales. Common drivers of Arctic and Subarctic climate variability include the Arctic Oscillation (Thompson and Wallace, 1998; AO), the Pacific Decadal Oscillation (Mantua et al., 1997; PDO), and the El Nino Southern Oscillation (Bjerknes, 1969; ENSO). The AO is characterized by anomalous sea level pressure between the Arctic and lower latitudes (> 45°N) on time scales ranging from interannual to interdecadal (Thompson and Wallace, 1998). The anomalous sea level pressure causes alterations to the jet stream, changing the trajectory of storms and modifying air temperature and precipitation patterns over the Arctic, Eurasia and North America (Thompson and Wallace, 1998). The PDO is defined by anomalous

sea surface temperatures (Hunt and Drinkwater, 2005), and similar to the AO, modifies air temperature and precipitation patterns in the Subarctic Pacific basin and North America. The PDO cycles between a negative (cold) and positive (warm) phase over inter-decadal to decadal timescales (Mantua et al., 1997, Hare and Mantua, 2000). Atmospheric circulation in the Subarctic Pacific is largely affected by the phase changes in the PDO. The position and strength of the semi-permanent Aleutian Low pressure center (AL), the dominant atmospheric feature over the Subarctic Pacific domain (Rodionov et al., 2007), corresponds to the negative (weak AL) and positive (strong AL) phases of the PDO. A similar air-sea interaction is observed during ENSO events, which are tropical in origin and exhibits higher frequency variations (interannual). ENSO events are associated with the warming of equatorial Pacific waters and the oscillation of atmospheric pressure over the western tropical Pacific (Bjerknes, 1969), strongly influencing both temperature and precipitation patterns on a global scale (Hollowed et al., 2001). Evidence suggests that ENSO events alter the sea surface temperatures and atmospheric circulation patterns in the Subarctic Pacific through atmospheric teleconnections, and is hypothesized to be a mechanism for decadal variability over the North Pacific (Latif and Barnett, 1994; Alexander et al., 2004; Deser et al., 2004).

Several external forces, which can be both natural and anthropogenic, also contribute to the variation of the climate system. The main external forces include: solar variation, volcanic eruptions, and anthropogenic gases, all of which influence the Earth's radiative balance and thus cause the climate to fluctuate (Myhre et al., 2013). Small changes to either internal or external forces can cause rapid or abrupt changes to the physical environment, and associate extreme climatic events as discussed below. The combination of both internal and external forces driving the variability of the climate system makes it difficult to estimate the relative contribution

individual drivers have on the entire system, and thus climate prediction can be challenging (Deser et al., 2010; Curry and Webster, 2011). Climate models are based on known physical principles to reproduce multiple aspects of the observed climate. These models can be valuable tools to understand and separate out the relative impacts of the various drivers. Such climate models are used to make predictions of climate system dynamics on seasonal and decadal timescales (Flato and Marotzke, 2013). Therefore it is important to analyze the performance of climate models for a range of time scales over global and regional domains.

In addition to the relatively modulated climate variability, even more unpredictable extreme atmospheric events are observed to have a large impact on humans and ecosystems alike (Peterson et al., 2013). Severe, atypical events in physical and ecological systems are largely attributed to the natural variability listed above (Deser et al., 2012; Loikith and Broccoli, 2014). Evidence suggests that extreme weather and climate events have increased in recent decades, and that both may be attributed to increasing anthropogenic forcing (Melillo et al., 2014). As the climate proceeds to change, due to natural and anthropogenic forcing, a shift in its mean distribution can cause extremes of key atmospheric drivers to become more frequent and more intense (Solomon et al., 2007; Walsh et al., 2014). The natural changes to the climate system impact the biota of marine ecosystems. Identifying and understanding the pathways that transfer climate change in the atmosphere and ocean to the marine biota is essential for understanding how ecosystem dynamics will respond to both longer term and shorter term changes (Francis et al., 1998; Stabeno et al., 2005).

The eastern Bering Sea is one of the most biologically productive ecosystems in not only the Arctic but in the world. Approximately 450 species of fish, 50 species seabirds, and 25 species of marine mammals are supported by this extraordinary lower trophic level production (National

Research Council, 1996). The abundant fish and wildlife have sustained the lives and livelihoods of indigenous groups of Asia and Alaska for thousands of years (Stabeno et al., 2005). Native communities continue to use the animals of the Bering Sea for food, clothing, energy, as well as spiritual and cultural traditions (Loughlin et al., 1999). In addition, the Bering Sea is currently the source of nearly 25 million pounds of subsistence food and provides approximately half of all fish and shellfish harvests in the United States with a value exceeding 3 billion dollars annually (Harvey and Sigler, 2013). The Bering Sea marine ecosystem has been shown to be vulnerable to both long duration anomalies and abrupt changes to the physical environment (Mantua et al., 1997; Francis et al., 1998) and episodic weather events (Bond and Overland, 2005). The biological, cultural and commercial significance of the Bering Sea creates an ideal location for examining the ability of global climate models to predict important regional atmospheric dynamics and the response of the marine ecosystem to those dynamics on biologically relevant timescales.

Located in the northernmost extent of the Pacific Ocean, the Bering Sea spans approximately three million square kilometers and serves as the only Pacific connection to the Arctic Ocean. The coastlines of Russia and Alaska frame the Bering Sea from east to west, and the Aleutian Islands, a 1900km island chain, creates a southern border. The eastern Bering Sea is characterized by a remarkably extensive and shallow continental shelf that is less than 200m deep, and encompasses nearly 40 percent of the Bering Sea (National Research Council, 1996). The shelf sharply transitions into a deep basin that ranges between 2500m and 3500m. The circulation of Bering Sea (Figure 1) forms a cyclonic gyre with three well-defined currents dominating the hydrography of the basin: Aleutian North Slope Current (ANSC), Bering Slope Current (BSC), and Kamchatka Current These currents transport freshwater, heat, nutrients and

plankton poleward as water flows from the Gulf of Alaska to the Bering Sea through a series of Aleutian Island passes. As water enters the eastern Bering Sea it joins with the ANSC flowing eastward, north of the Aleutian Islands. Once the ANSC approaches the continental shelf the current turns in a northwest direction to form the BSC along the shelf. Upwelling from the BSC supplies nutrient rich deep water to the euphotic zone, supporting a tremendous amount of primary and secondary production along the entire perimeter of the continental shelf (Springer et al., 1996). At the northern end of the shelf break, south of Cape Navarin, the BSC bifurcates into an eastward and westward extension. The eastward extension crosses onto the shelf and continues northward through the Bering Strait, while the westward extension turns south and connects to the Kamchatka Current. Water then continues south along the Russian coast until it re-enters the North Pacific Ocean through Kamchatka Strait. The eastern Bering Sea shelf is separated from the water masses of the deep ocean basin by relatively persistent shelf-break fronts (Kinder and Schumacher, 1981; Coachman, 1986) that restrict on-shelf transport of water and tracers, including nutrients that would fuel primary production. Sea ice plays an important role in controlling ecosystem dynamics of the Bering Sea. The seasonal presence of sea ice can extend southward over 1,700km and in response to air temperature and geostrophic wind variability, can exhibit strong year-to-year variability (Walsh and Johnson, 1979), impacting both the physical structure of the water column and marine ecosystem dynamics. The timing of sea ice retreat directly affects the temperature and stratification of the water column, determining the conditions in which the spring phytoplankton bloom occurs and therefore controlling which habitat receives the flow of energy (Hunt et al., 2002).

Due to harsh meteorological conditions and its remote location, historical observational data are limited for the Bering Sea. Although, deployed moorings and research vessels provide an

observational record that spans a large portion of the eastern Bering Sea. The observations are discontinuous in time and space. Sparse temporal data prohibits analysis of long-duration physical and biological anomalies over decadal time scales. Such restrictions have made Earth System Models (ESMs) particularly useful tools to advance the understanding of large-scale shifts in the climate and climate related impacts over this region. A number of the purely physical General Circulation Models GCMs have transitioned into more comprehensive representation of an Earth System with the inclusion of an interactive representation of ecosystems and biogeochemistry (Flato, 2011). The Community Earth System Model, version one (CESM1) is an example of such a model. Developed at the National Centers of Atmospheric Research in collaboration with universities and national laboratories, the CESM is one of several climate models that have made significant contributions to national and international climate assessments (Hurrell et al., 2013). At its core the CESM exchanges state information and fluxes between four main climate system components: atmosphere, land, ocean, and sea ice. The latest version now incorporates sophisticated modules capable of representing the physical, biological and chemical processes to better understand the past and present climate and determine the future climate (Hurrell et al., 2013).

Past studies have explored the ability and skill of the CESM over the Arctic domain (de Boer et al., 2012). Here, the CESM1 is used to extend previous work to examine different scales of variability in the Arctic and Bering Sea and to explore the impacts of seasonal scale extremes on the Bering Sea ecosystem. Chapter Two discusses the ability of the CCSM4, the general circulation component of the CESM1, to simulate key atmospheric forcing variables important for marine ecosystems, with an emphasis on high latitude variability over interannual and decadal timescales. Variability of the physical system is further explored in Chapter Three, by

examining the occurrence of interannual and seasonal extremes and the response of lower trophic levels (primary production) of the eastern Bering Sea. Because observations are not sufficient to enable such an assessment of linkages between Bering Sea climate and biology, we have based this study on CESM model simulations. While many of the results obtained here are subject to the limitations of model validity, the results include climate-biological linkages that can guide observational priorities in the Bering Sea region.

Figures

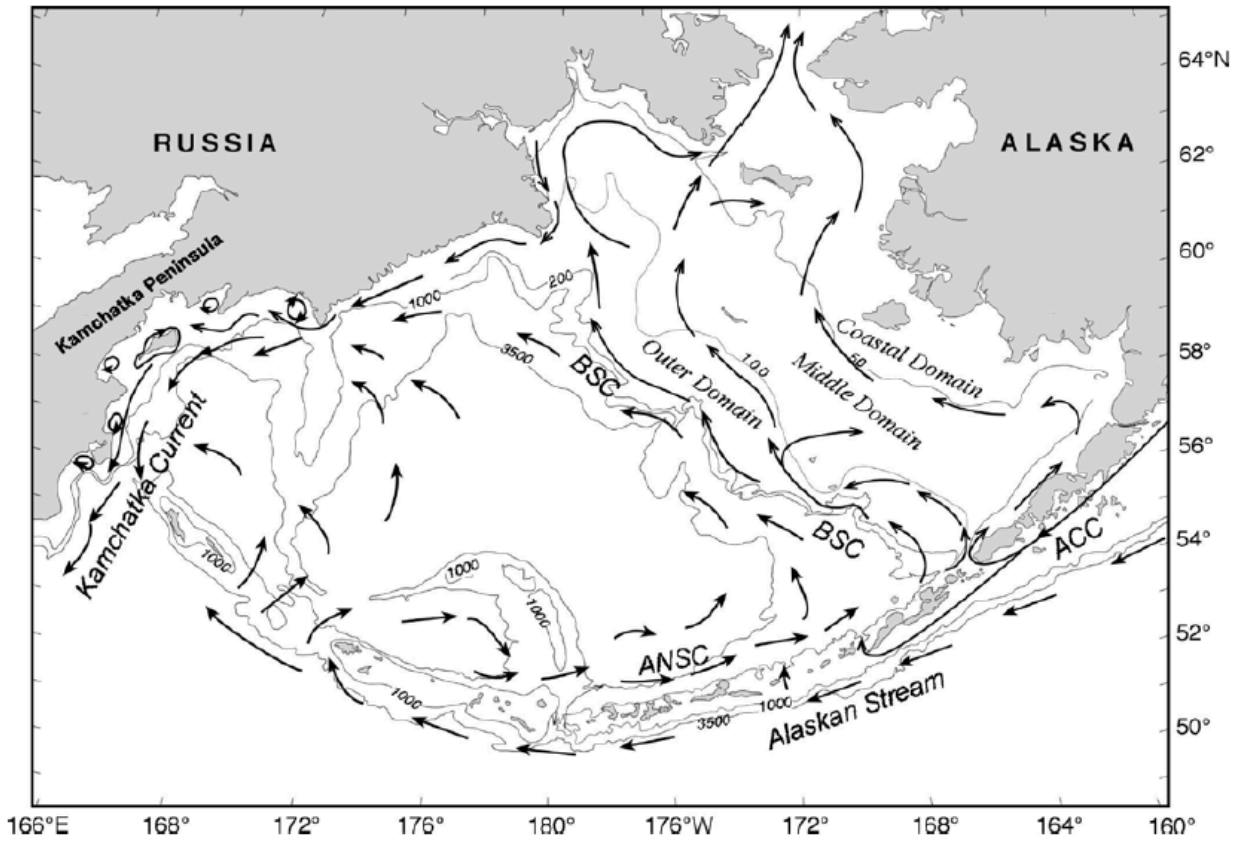

Figure 1.1. Hydrographical reference of the Bering Sea. Schematic of the major circulation features in the Bering Sea–BSC, Bering Slope Current; ACC, Alaska Coastal Current; ANSC, Aleutian North Slope Current. Created by Stabeno et al. 1999 and modified by Hunt et al. 2010.

References

Alexander M A, Lau N C, Scott J D. 2004. Broadening the atmospheric bridge paradigm: ENSO teleconnections to the North Pacific in summer and to the tropical west Pacific-Indian oceans over the seasonal cycle, in Earth's Climate: The Ocean- Atmosphere Interaction, Volume 147, Wang C, Xie S P, Carton J A (eds), AGU, Washington, D. C., pp. 85–104.

Bjerknes J. 1969. Atmospheric teleconnections from the Equatorial Pacific. *Monthly Weather Review* **97**(3): 163–172.

Bond N A, and Overland J E. 2005. The importance of episodic weather events to the ecosystem of the Bering Sea shelf. *Fisheries Oceanography* **14**(2): 97–111.

Christensen J H, Hewitson B, Busuioc A, Chen A, Gao X, Held I, Jones R, Kolli R K, Kwon W T, Laprise R, Magaña Rueda V, Mearns L, Menéndez C G, Räisänen J, Rinke A, Sarr A, Whetton P. 2007. Regional Climate Projections, in: Climate Change 2007: The Physical Science Basis. Contribution of Working Group I to the Fourth Assessment Report of the Intergovernmental Panel on Climate Change, Solomon S, Qin D, Manning M, Chen Z, Marquis M, Averyt K B, Tignor M, Miller H L (eds), Cambridge University Press, Cambridge, United Kingdom and New York, NY, USA.

Coachman L K. 1986. Circulation, water masses, and fluxes on the southeastern Bering Sea shelf. *Cont. Shelf Res* **5**: 23–108.

Curry J A, and Webster P J. 2011. Climate Science and the Uncertainty Monster. *Bulletin of the American Meteorological Society* **92**(12): 1667–1682.

De Boer G, Chapman W, Kay J E, Medeiros B, Shupe M D, Vavrus S, Walsh J. 2012. A Characterization of the Present-Day Arctic Atmosphere in CCSM4. *Journal of Climate*, **25**(8): 2676–2695. DOI:10.1175/JCLI-D-11-00228.1

Deser C, Phillips A S, Hurrell J W. 2004. Pacific inter-decadal climate variability: Linkages between the tropics and the North Pacific during boreal winter since 1900. *Journal of Climate* **17**: 3109–3124.

Deser C, Phillips A, Bourdette V. 2010. Uncertainty in climate change prjections: the role of internal variability. *Climate Dynamics **38***(3): 527–546.

Deser C, Phillips A S, Tomas R A, Okumura Y M, Alexander M A, Capotondi A, Ohba M. 2012. ENSO and Pacific Decadal Variability in the Community Climate System Model Version 4. *Journal of Climate* **25**(8): 2622–2651. DOI:10.1175/JCLI-D-11-00301.1.

Flato G M, Marotzke J, Abiodun B, Braconnot P, Chou S C, Collins W, Cox P, Driouech F, Emori S, Eyring V, Forest C, Gleckler P, Guilyardi E, Jakob C, Kattsov V, Reason C, Rummukainen M. 2013. Evaluation of Climate Models, in: Climate Change 2013: The Physical Science Basis. Contribution of Working Group I to the Fifth Assessment Report of the Intergovernmental Panel on Climate Change, Stocker T F, Qin D, Plattner G K, Tignor M, Allen S K, Boschung J, Nauels A, Xia Y, Bex V, Midgley P M (eds.), Cambridge University Press, Cambridge, United Kingdom and New York, NY, USA.

Flato G M. 2011. Earth system models: an overview. *Wiley Interdisciplinary Reviews: Climate Change* **2**(6): 783–800. DOI:10.1002/wcc.148

Francis R C, Hare S R, Hollowed A B, Warren S. 1998. Effects of interdecadal climate variability on the oceanic ecosystems of the NE Pacific. *Fisheries Oceanography* **7**(1): 1–21.

Hollowed A B, Hare S R, Wooster W S. 2001. Pacific Basin climate variablity and patterns of Northeast Pacific marine fish production. *Progress in Oceanography*, **49**: 257–282.

Hare S R, Mantua N J. 2000. Emperical evidence for North Pacific regime shifts in 1977 and 1989. *Progress in Oceanography* **47**: 103–145.

Harvey H R, Sigler M F. 2013. An introduction to the Bering Sea Project, volume II, in: Understanding Ecosystem Processes in the Eastern Bering Sea II, Ashjian C J, Harvey H R, Lomas M W, Napp J M, Sigler M F, Stabeno, P J, Van Pelt T I (eds). *Deep Sea Research Part II, Topical Studies in Oceanography* **94**: 2–6.

Hassol S J, Berner J, Callaghan T V. 2004. ACIA, Impacts of a Warming Arctic: Arctic Climate Impact Assessment. Cambridge University Press. ISBN 0521617782

Hunt G L, Stabeno P, Walters G, Sinclair E, Brodeur R D, Napp J M, Bond N A. 2002. Climate change and control of the southeastern Bering Sea pelagic ecosystem. *Deep Sea Research Part II: Topical Studies in Oceanography* **49**(26): 5821–5853.

Hunt G L, Drinkwater K F (eds). 2005. Background on the Climatology, Physical Oceanography and Ecosystems of the Sub-Arctic Seas. Appendix to the ESSAS Science Plan. GLOBEC Rport No. 20, viii, 96 p.

Hunt G L, Allen B M, Angliss R P, Baker T, Bond N, Buck G, Byrd G V, Coyle K O, Devol A, Eggers, D M, Eisner L, Feely R, Fitzgerald S, Fritz LW, Gritsay EV, Ladd C, Lewis W, Mathis J, Mordy C W, Mueter F, Napp J, Sherr E, Shull D, Stabeno P, Stepanenko M A, Strom S, Whitledge T E. 2010. Status and trends of the Bering Sea region, 2003-2008, in: McKinnell S M, and Dagg M J (eds.), Marine Ecosystems of the North Pacific Ocean, 2003-2008. PICES Special Publication 4, 393 p.

Hurrell J W, Holland M M, Gent P R, Ghan S, Kay J E, Kushner P J, Marshall S. 2013. The Community Earth System Model: A Framework for Collaborative Research. *Bulletin of the American Meteorological Society* **94**(9): 1339–1360. DOI:10.1175/BAMS-D-12-00121.1

Jeffries M O, Richter-Menge J A, Overland J E (eds). 2013: Arctic Report Card 2013, http://www.arctic.noaa.gov/reportcard.

Kelly R, Chipman M L, Higuera P E, Stefanova I, Brubaker L B, Hu F S. 2013. Recent Burning of boreal forests exceeds fire regime limits of the past 10,000 years. Proceedings of the National Academy of Sciences of the United States, in press. DOI: 10.1073/pnas.1305069110.

Kinder T H, and Schumaker J D. 1981. Circulation over the continental shelf of the southeastern Bering Sea, in: The Eastern Bering Sea Shelf: Oceanography and Resources, Volume 1, Hood D W and Calder, JA (eds.), NOAA, University of Washington Press, Seattle pp. 53–75.

Latif M, Barnett T P. 1994. Causes of Decadal Climate Variability over the North Pacific and North America. *Science*, **266**(5185): 634–637.

Loughlin T, Sukhanova I, Sinclair E. 1999. Summary of Biological and Ecosystem Dynamics in the Bering Sea. Chapter 19 in: Dynamics of the Bering Sea, Loughlin T, Ohtani K, (eds). Unniversity of Alaska Sea Grant, Ak-SG-99-03, Fairbanks. 838 pp. ISBN 1-56612-062-4.

Loikith P C, and Broccoli A J. 2014. The Influence of Recurrent Modes of Climate Variability on the Occurrence of Winter and Summer Extreme Temperatures over North America. *Journal of Climate* **27**(4): 1600–1618. DOI:10.1175/JCLI-D-13-00068.1

Melillo J M, Richmond T C, Yohe G W, (eds.). 2014. Highlights of Climate Change Impacts in the United States: The Third National Climate Assessment. U.S. Global Change Research Program, 148 pp.

Myhre G, Shindell B, Bréon F M, Collins W, Fuglestvedt J, Huang J, Koch J, Lamarque J F, Lee D, Mendoza B, Nakajima T, Robock A, Stephens G, Takemura T, Zhang H. 2013. Anthropogenic and Natural Radiative Forcing, in: Climate Change 2013: The Physical Science Basis. Contribution of Working Group I to the Fifth Assessment Report of the Intergovernmental Panel on Climate Change, Stocker T F, Qin D, Plattner G K, Tignor M, Allen S K, Boschung J, Nauels A, Xia Y, Bex V, Midgley P M (eds.), Cambridge University Press, Cambridge, United Kingdom and New York, NY, USA.

Mantua N J, Hare S R, Zhang Y, Wallace J M, Francis R C. 1997. A Pacific Interdecadal Climate Oscillation with Impacts on Salmon Production. *Bulletin of the American Meteorological Society* **78**(6): 1069–1079.

National Research Council. 1996. *The Bering Sea Ecosystem*. Washington, DC: The National Academies Press.

Peterson T C, Hoerling M P, Stott P A, Herring S (eds.). 2013. Explaining Extreme Events of 2012 from a Climate Perspective. *Bulletin of the American Meteorological Society* **94**(9): S1–S74.

Rodionov S, Bond N, Overland J. 2007. The Aleutian Low, storm tracks, and winter climate variablity in the Bering Sea. *Deep Sea Research Part II* **54**: 2560–2577.

Romanovsky V E, Kholodov A L, Smith S L, Christiansen H H, Shiklomanov N I, Drozdov D S, Oberman N G, Marchenko S S. 2013. State of the Climate in 2012. *Bulliten of the American Meteorological Society* **94**(8): S121–S123.

Thompson D W, and Wallace M. 1998. The Arctic oscillation signiture in the wintertime geopotential height and temperature fields. *Geophysical Research Letters* **25**(9): 1297–1300.

Screen J A, Simmonds I. 2010. The central role of diminishing sea ice in recent Arctic temperature amplification. *Nature Letters* **464**(7293): 1334–1337. DOI: 10.1038/nature09051.

Solomon S, Qin D, Manning M, Chen Z, Marquis M, Averyt K B, Miller H L. (2007). Climate Change 2007: The Physical Science Basis. Cambridge, United Kingdom and New York, NY, USA: Cambridge University Press, p. 996.

Springer A M, McRoy C P, Flint M V. 1996. The Bering Sea Green Belt: Shelf edge processes and ecosystem production. *Fisheries Oceanography* **5**: 205–223.

Stabeno PJ, Schumacher JD, Ohtani K. 1999. The physical oceanography of the Bering Sea, in: Loughlin, T.R., Ohtani, K. (eds.), Dynamics of the Bering Sea. North Pacific Marine Science Organization (PICES), University of Alaska Sea Grant, AK-SG-99-03, Fairbanks, AK, pp. 1-28,

Stabeno P, Hunt G Jr, Napp J, Schumacher J. 2005. Physical forcing of ecosytem dynamics on the Bering Sea. Chapter 30 in The Sea, Vol. 14, A.R. Robinson and K. Brink (eds.). ISBN 0-674-01527-4.

Walsh J E, Johnson C M. 1979. Interannual Atmospheric Variability and Associated Fluctuations in Arctic Sea Ice Extent. *Journal of Geophysical Research* **84**: 6915–6928.

Walsh J, Wuebbles D, Hayhoe K, Kossin J, Kunkel K, Stephens G. 2014. Appendix 3: Climate Science Supplement. Climate Change Impacts in the United States: The Third National Climate Assessment, Melillo J M, Richmond T C, Yohe G W, (eds.), U.S. Global Change Research Program, 735–789. DOI:10.7930/J0KS6PHH.

2 Performance assessment of the Community Climate System Model over the Bering Sea[1]

2.1 Abstract

The Community Climate System Model, version 4 (CCSM4) is evaluated against reanalysis data for the late-twentieth century (1955-2005), with a central focus on the ecologically and commercially important Bering Sea in the subarctic Pacific. Several atmospheric variables including surface-air temperature, sea level pressure, wind strength, and direction were evaluated due to their relevance to large marine ecosystems. Simulated spatial patterns of climatological surface-air temperature over the Bering Sea are generally well simulated despite some subregional biases as large as +3 ºC during autumn and -5 ºC during winter. Interannual variability of simulated surface-air temperature exceeds that of the reanalysis by a factor of nearly 1.5. Model simulations show an under-simulated Siberian high and a large northwest displacement of the Aleutian Low pressure center. Further, sea level pressure over the Bering Sea is under-simulated in winter and fall by more than 8 hPa, and over-simulated in summer by more than 5 hPa. Interannual variability in simulated sea level pressure is nearly twice as large as observed. In general, the CCSM4 shows an improved representation of both monthly mean surface-air temperature and sea level pressure over the subarctic Pacific relative to its predecessor, the CCSM3. Despite these advances, there is still a clear need for improvements in the model's representation of high-latitude atmospheric circulation in order to achieve proper atmospheric forcing of marine ecosystem models.

[1]Walston, J.M., Gibson, G.A.,Walsh, J.E.(2014). Performance assessment of the Community Climate System Model over the Bering Sea. *International Journal of Climatology*.DOI:10.1002/joc.3954.

2.2 Introduction

Marine ecosystems are undergoing rapid changes on local and global scales (Hurrell & Deser, 2010; Overland and Wang, 2007; Wang et al., 2010; Coyle et al., 2011). It is still not clear if the biological regime shifts of Large Marine Ecosystems (LMEs) are caused by anthropogenic forcing; the natural variability of oceanic, atmospheric, and biological coupling; or a combination of these two (Di Lorenzo et al., 2010). Hydrographic and biogeochemical models are commonly used to complement observations when understanding marine ecosystem dynamics, and are increasingly used to predict future states of the marine ecosystems themselves. Such a task clearly requires a credible formulation of the physics, biogeochemistry, and ecology of the oceanic system (Hurrell & Deser, 2010), as well as realistic atmospheric forcing. General Circulation Models (GCMs) attempt to capture the chemical and physical processes that define the earth's climate system on decadal and multi-decadal timescales. Outputs from GCMs are increasingly used to drive finer scale, regional ocean-ecosystem models (Gibson et al., 2013; Ji et al., 2013), in order to understand how variability in atmospheric forcing impacts ecosystem dynamics. For this reason, it is important to analyze the performance of GCMs over regional domains of biological relevance.

The Bering Sea is one of the world's ~64 LMEs, spanning almost three million square kilometers in the Subarctic domain of the North Pacific. This region was selected as a region of focus for this study due to its status as one of the world's most biologically productive marine regions (National Research Council (NRC, 1996). Productivity in the Bering Sea supplies over 25 million pounds of subsistence food to nearly 55,000 Alaskan residents and supports several species of seabirds and marine mammals (Bering Sea Interagency Working Group, 2006). Commercial fisheries in the Bering Sea account for more than half of the marine harvest in

United States waters (North Pacific Fishery Management Council, 2005); meanwhile, the Bering Sea is vulnerable to extreme events, long-duration anomalies, and seasonal or longer fluctuations that could potentially lead to large latitudinal shifts in some marine species (Stabeno et al., 2001; Wang et al., 2010; Overland et al., 2010; Danielson et al., 2011); indeed, ecosystem shifts have already been observed in some parts of the Bering Sea (Grebmeier et al., 2006). As a result, subsistence living and commercial fisheries in the Bering Sea may soon see significant changes as the region responds to climate change. It is important to interpret these changes in the context of the inherently large internal variability in the subarctic. One consequence of this large variability is that the ratio of the greenhouse warming to the standard deviation of temperature is smaller in the subarctic, including the Bering Sea, than in the tropics and in the central Arctic. Hawkins and Sutton (2012) and Kattsov and Sporyshev (2006) have used such a metric to show that the greenhouse signal emerges from the noise of internal variability in later decades over the Bering region relative to the time of emergence elsewhere in the Northern Hemisphere.

Due to the changes that have already been observed in this region and across the Arctic as a whole, a number of modeling efforts aiming to understand and predict changes in this region have been undertaken (Jin et al, 2012, Hermann et al, 2013; Gibson et al 2013). As such, the verification of simulated climate variables relevant to ecosystems and the credibility of GCM simulations of Arctic and Subarctic climates have become a question of increasing importance (e.g., Reichler and Kim, 2008). Various GCMs have been independently developed. The Community Climate System Model (CCSM), developed at the National Center of Atmospheric Research (NCAR), is one of many climate models included in both the Coupled Model Intercomparison Project's fifth phase (CMIP5) and the Intergovernmental Panel on Climate Change (IPCC) Fifth Assessment Report (AR5, Gent et al., 2011). The CCSM is a GCM that

exchanges state information and fluxes between four main components: atmosphere, land, ocean, and sea ice. The CCSM, now in its fourth version (CCSM4), was completed and released to the climate science community in April 2010 (Gent et al., 2011). An analysis of the CCSM4 simulations by de Boer et al. (2012) indicate a well-simulated Arctic climate, with reduced temperature biases compared to its predecessor, the CCSM3. Despite having circulation biases over the Arctic domain (de Boer et al., 2012; Maslowski et al., 2012), Jahn et al. (2012) have reported that the CCSM4-simulated spatial sea ice concentration and extent are accurately captured by the CCSM4.

This study extends on previous assessments of the CCSM4 over the Arctic domain (de Boer et al., 2012; Maslowski et al., 2012). Here, we focus on the performance of key atmospheric components simulated by the CCSM4 over the ecologically and commercially important Bering Sea region in the Subarctic Pacific. We emphasize atmospheric variability, which has received relatively little consideration in model evaluations of the Arctic to date. In addition to assessing the CCSM4's ability to capture the variability inherent in the seasonal cycle of key atmospheric components, we assess the model's ability to capture seasonal and inter-decadal variability in the Subarctic's physical system.

2.3 Model output and validation

2.3.1 CCSM4 output and NCEP/NCAR reanalysis data

Our evaluation was based on the recently released twentieth-century all-forcing simulation runs produced by the CCSM4. These simulations consist of a five-member ensemble, each beginning in 1850 and ending in 2005. Each ensemble was forced by externally imposed variations of solar output, aerosols, volcanic activity, CO2, and other greenhouse gases, at levels specified in the IPCC third assessment report (Gent et al., 2011; Gleckler et al., 2008). This

analysis evaluated key atmospheric forcing variables for a fifty-one-year period from 1955 to 2005. Over the fifty-one-year period a brief analysis comparing all five ensemble runs with one another revealed that while ensemble members showed slight variations, all biases relative to observational data were consistent across all five ensemble members of the CCSM4; thus, only our analysis of the first ensemble run is presented here. Ensemble member similarity is discussed in more detail by de Boer et al. (2012).

Simulated monthly sea level pressure and near-surface-air temperature at a sigma level of 0.992 were used in this analysis. Zonal and meridional winds were calculated from simulated sea level pressure using the geostrophic wind equation; in order to determine any impacts biases may have among associated winds fields. Our region of focus was centered over the Bering Sea, an area between 50°-65°N and 160°E-160°W (Figure 2.1). A larger domain, covering the entire Arctic, was also considered, in order to provide broader spatial context for the Bering Sea results. CCSM4 output features a native spatial resolution of 1.25° longitude x 0.9° latitude. All simulated and calculated monthly mean fields were evaluated for the fifty-one-year period previously mentioned. This sub-period of the twentieth-century simulations of the CCSM4 was chosen due to its consistency with reanalysis output.

To validate the model, output was compared to the National Centers for Environmental Prediction and the National Center for Atmospheric Research (NCEP/NCAR) Reanalysis 1 (Kalnay et al., 1996). The NCEP/NCAR reanalysis directly assimilates observed free-air temperature, sea level pressure, and wind observations into a global model using past data from 1948 to the present. Reanalysis surface-air temperatures are near surface from a sigma level of 0.995. All reanalysis variables have a spatial coverage of 2.5° longitude × 2.5° latitude on a global horizontal grid system. Monthly averaged surface-air temperature and monthly sea level

pressure of the CCSM4 were bi-linearly interpolated to the coarser NCEP/NCAR grid resolution, to allow for comparison with reanalysis data. As such, in our analysis, both model and reanalysis data comprised a 19 × 9 grid (171 points) over our Bering Sea domain.

Since the Arctic and Subarctic Pacific regions compose the focus of this project, we defined seasons for consistency with Arctic temperatures and corresponding sea-ice growth/melt. 'Winter' was considered as January through March (JFM); 'spring,' April through June (AMJ); 'summer,' July through September (JAS); and 'fall,' October through December (OND). Monthly data and model simulations were averaged into these seasonal bins for evaluations of model performance on a temporal scale.

2.3.2 Spatial and temporal evaluation

Spatial evaluations of the CCSM4's simulated surface-air temperature and sea level pressure fields were conducted using climatological annual and seasonal means of the late-twentieth century period. These spatial patterns reveal where discernible climatological features simulated by the CCSM4 are located.

2.3.2.1 Fifty-one-year spatial climatologies

To compute the *fifty-one-year annual mean*, both simulated and reanalysis variables at each of the grid points were averaged over the entire fifty-one-year period, for both the Pan-Arctic and Subarctic Pacific domains. A similar technique was used to determine the *fifty-one-year seasonal mean* for *winter*, *spring*, *summer*, and *fall* at each grid point for the entire fifty-one-year period over the Bering Sea, in the Subarctic Pacific.

2.3.2.2 Fifty-one-year spatially averaged climatological annual cycle

To produce a *fifty-one-year spatially averaged climatological annual cycle* of both simulated and reanalysis variables, the variables were spatially averaged over the 171 grid points in the Bering Sea region by each calendar month for the entire fifty-one-year period. Standard deviations for each calendar month from the climatological monthly mean were evaluated.

2.3.2.3 Long-term interannual time series

To produce a *long-term interannual time series*, simulated and reanalysis variables were averaged over the 171 grid points covering the Bering Sea region, and over a three-month seasonal and a twelve-month annual time step, for the entire fifty-one-year period.

2.3.2.4 Spatial and temporal pattern comparison

Taylor diagrams were developed to concisely summarize the degree of correspondence between simulated and reanalysis data, thereby providing a synthesis of model performance for simulating the monthly and seasonal spatial and temporal climatologies and annual cycles for the fifty-one-year period. Additionally, we have used Taylor diagrams to present a comparison between performance of the CCSM4 and its predecessor, the CCSM3. Taylor diagrams quantify the similarities between two patterns, spatial or temporal, through the correlation coefficient (r), standard deviation (σ), and centered root-mean-squared error (RMSE, Neggers et al., 2012). For additional information on Taylor diagrams, Taylor (2001) provides a detailed description.

2.3.2.5 Taylor diagrams

To quantify the ability of the model to spatially (*spatial climatologies*) and temporally (*temporal climatologies*) represent patterns in temperature and pressure over the Bering Sea, spatial and temporal pattern correlations between the model and the reanalysis *fifty-one-year*

annual mean, *fifty-one-year seasonal mean*, and *long-term interannual time series* were computed. In addition to comparing the *fifty-one-year seasonal mean* of the CCSM4 to the reanalysis, the *fifty-one-year seasonal means* of CCSM4 and CCSM3 were also compared. Accuracy of simulated spatial and temporal patterns without the effect of model bias were quantified using the centered RMSE at each grid point, determined after removing the fifty-one-year monthly, seasonal, and annual spatial and temporal means from both the CCSM4 and the NCEP/NCAR reanalysis. By normalizing the metrics (model metrics divided by the observed (reference) standard deviation), a Taylor diagram is capable of displaying multiple parameters on a single diagram. The reference point (Ref) on each Taylor represents the situation in which the modeled pattern is in perfect agreement with the observed pattern in terms of the correlation, normalized variance (σ^*), and normalized centered RMSE.

2.4 Results

2.4.1 Surface-air temperature

Despite some regional biases, the CCSM4 captures the broad-scale *fifty-one-year annual mean* of temperatures over the high-latitude northern hemisphere. Both simulated and observed climatological mean air temperatures poleward of 40°N had their lowest mean air temperatures over the Canadian Arctic Archipelago and their warmest temperatures near the southern boundary of the domain (Figure 2.2a, 3b). However, the model overestimates temperatures throughout northern Eurasia and the North Atlantic Ocean by as much as 5 °C (Figure 2.2c). With the exception of the Beaufort Sea region of the Arctic Ocean where there is a warm bias of 2°C, the CCSM4 tends to be colder than reanalysis data by 2-4 °C over the majority of the Arctic Ocean, which is consistent with previous assessments of the CCSM4's Arctic atmosphere (de Boer et al., 2012). Despite these biases, over the broad Arctic region, the model was indeed able

to capture the observed spatial gradient in temperatures across the Bering Sea, increasing southwards, from -14 °C over the Russian Arctic to 6 °C south of the Aleutian Islands (Figure 2.2d and 3e).

While the CCSM4 captures broad-scale spatial gradients of temperature across the Bering Sea, a closer examination of the *fifty-one-year annual mean* shows that the model under-simulates temperatures creating a negative (cold) bias throughout the Bering Sea. Robust cold biases are located over the Kamchatka Peninsula at the western boundaries of the Bering Sea (Figure 2.2f), where the model shows a negative 5 °C bias.

Both cold and warm temperature biases are present in each of the *fifty-one-year seasonal means* (Figure 2.3). The largest temperature biases occur in the winter (Figure 2.3i) and fall (Figure 2.3l) seasons. Over the northern inner Bering Sea shelf, winter and fall simulated temperatures are between 3 and 4 °C greater than observed. However, there is also a strong negative bias over the western Bering Sea during winter and fall, with temperatures between 6 and 8 °C colder than observed. Model biases in the spring (Figure 2.3j) and summer (Figure 2.3k) are generally smaller in magnitude—between 1 and 3 °C—and are generally negative throughout most of the Bering Sea domain. For example, during spring, the model under-simulates temperatures in the Russian Arctic by 4 °C, while in the summer, temperatures are under-simulated over the northern Bering Sea by 2 °C.

Over the Bering Sea domain as a whole, the CCSM4 reproduces the observed *fifty-one-year, spatially averaged climatological annual cycle* of temperature (Figure 2.4a) with reasonable accuracy. Consistent with observations, the model simulates temperature minima from December to January, and maxima from July to August. Meanwhile, despite the ability of the CCSM4 to capture the overall annual cycle, the model does exhibit a cold bias from May to September (1-

2 °C) and from November to January (~0.5 °C, Figure 2.4b). As indicated by the error bars, the CCSM4 simulates more interannual variability between months over the annual cycle, most noticeably between November and April.

2.4.2 Sea level pressure

As was the case for air temperature, despite some regional biases, the CSSM4 does capture the broad-scale spatial patterns in atmospheric pressure over the high-latitude northern hemisphere. The dominant features in the *fifty-one-year annual mean* of both the CCSM4 model simulations and reanalysis observations are the semi-permanent regions of high pressure over the subtropical oceans and the southern Asian continent, as well as the persistent Aleutian and Icelandic Subpolar low-pressure centers (Figure 2.5a). Although the simulated high and low pressure systems are spatially accurate, the CCSM4 tends to over-simulate semi-permanent features over the subtropical oceans, but under-simulate the Asian High over northern Eurasia. Both the Azores-Bermuda High in the Atlantic Ocean and the Pacific High in the Eastern Pacific Ocean have as much as a 4 hPa positive bias (Figure 2.5c) in the model compared to the reanalysis. The model does capture the dipole pattern of the low-pressure centers, but the intensity of the simulated Icelandic Low exceeds that of the reanalysis by 6 hPa. The simulated Aleutian Low has a smaller (1-3 hPa) negative bias. While the locations of the simulated Subpolar lows are spatially accurate in a broad sense, there are discrepancies in the fine-scale placement. For example, the Icelandic Low simulated by the CCSM4 is located slightly to the northeast of where it naturally resides; moreover, in the North Pacific, the simulated Aleutian Low is shifted to the northwest and centered over the Kamchatka Peninsula. This assessment of Arctic atmospheric circulation confirms the results noted by de Boer et al. (2012) and Maslowski et al. (2012).

The CCSM's representation of atmospheric circulation found in the *fifty-one-year annual mean* contains several biases, but one of the most prominent shortcomings is the under-simulation of the Beaufort and Siberian high-pressure centers (Figure 2.5a). Simulated monthly mean sea level pressures averaged from 1955 to 2005 over the Arctic (Figure 2.5a) and Subarctic (Figure 2.5d) show a significant mass deficit in high latitudes, resulting from the lack of high pressure in the Beaufort and Chukchi Seas. In the Arctic region, the CCSM4 has a negative sea level pressure bias greater than 8 hPa (Figure 2.5c), apparent in the near-absence of the Beaufort High over the Beaufort Sea. The reduced Siberian High and the misplaced Aleutian Low result in strong negative biases over the Bering Sea in the *fifty-one-year annual mean*. The fifty-one-year simulated monthly mean sea level pressure showed as much as a 6 hPa negative bias over the northern Bering Sea domain, while simulations had nearly no biases in the southern Bering Sea. Despite a lack of biases in the southern Bering Sea domain, the CCSM4 simulated as much as a 2 to 3 hPa positive bias in the North Pacific Ocean (Figure 2.5c, 2.5f).

The pattern in regional bias seen throughout the Bering Sea domain in the *fifty-one-year annual mean* persists throughout the *fifty-one-year seasonal means* (Figure 2.6). The shift in atmospheric pressure in the Subarctic Pacific and the under-simulated Siberian High also create biases in the winter, spring, and fall simulated by the CCSM4, over the entire Bering Sea. In winter and fall, the model underestimates sea level pressure by as much as 10 hPa—the largest difference being north of 55° N (Figure 2.6i and 2.6l). While the location of both the Siberian High and the Aleutian Low are accurately simulated during winter, the reduced Siberian High allows the Aleutian Low to extend further north. Geostrophic approximation (Figure 2.6a) suggests easterly winds over the entire Northern Bering Sea, due to the extension of the Aleutian Low in winter, compared to an observed northeasterly wind (Figure 2.6e). In the spring and

summer, the model continues to underestimate sea level pressure in the northern Bering Sea, though the biases are greatly reduced (< 3 hPa). In spring, a lateral shift displaces the Aleutian Low too far west, resulting in only small biases in the magnitude of pressure, relative to observations over the Southern Bering Sea (Figure 2.6j). However, the westward shift of the Aleutian Low in spring impacts geostrophic winds in the Southern Bering Sea, with a southwesterly wind found in CCSM4 (Figure 2.6b), compared to a northeasterly pattern found in the NCEP/NCAR reanalysis (Figure 2.6f). During summer, the CCSM4 overestimates sea level pressure in the Southern Bering Sea and the North Pacific by as much as 6 hPa (Figure 2.6k), generating strong zonal momentum across the Southern Bering Sea (Figure 2.6c).

Despite some biases, the CCSM4 captures the observed *fifty-one-year spatially averaged climatological annual cycle* (1955-2005, Figure 2.7) of sea level pressure over the Bering Sea with no significant difference from observations found in any of the months. Observations indicate a steady increase in pressure over the Bering Sea domain, from 1007 hPa in January to a maximum in April of 1012 hPa, then decreasing in May, and increasing once more until July. After a second maximum of 1012 hPa in July, sea level pressure steadily decreases to a minimum of 1006 hPa in December. Similarly, the *fifty-one-year, spatially averaged climatological annual cycle* in pressure simulated by the CCSM4 shows an increase in sea level pressure from 1003 hPa in January to a maximum sea level pressure of 1013 hPa in August. The pressure then rapidly decreases to a minimum of 1002 hPa in December. A delay in maximum pressure simulated by the CCSM4 creates a slight negative bias of ~1 to 2 hPa in early spring, and a positive bias of 1 to 2 hPa during late spring and summer (Figure 2.7b).

Simulated sea level pressure biases were greatest in the winter and fall months, with the model showing a strong negative bias of as much as 5 hPa. The CCSM4's sea level pressure

exhibits more interannual variability in all calendar months compared to reanalysis data, which may correspond to an increased number of simulated extreme events in the North Pacific Ocean. As was the case with air temperature, the CCSM4 tends to simulate more interannual variability during the winter and fall months (σ, 5 to 9 hPa) compared to the spring months (σ, 2 to 5 hPa).

2.4.3 CCSM4 spatial and temporal pattern comparison

As discussed previously, the simulated spatial distributions of seasonal surface-air temperature and sea level pressure reproduced by the CCSM4 over the Bering Sea have some biases compared to observations. We now use Taylor diagrams to compare the performance of the CCSM4 to the performance of the CCSM3 to determine whether there has been clear improvement relative to observation.

2.4.3.1 Surface-air temperature

With the exception of spring, the CCSM4 had increased model skill over its predecessor in simulating the *fifty-one-year seasonal mean* (Figure 2.8a). In spring, surface-air temperatures went from an under-simulated spatial variability ($\sigma^* = 0.84$) in the CCSM3 to an over-simulated spatial variability ($\sigma^* = 1.14$) in the CCSM4. While this represents an increase in spatial variability, the normalized standard deviation of the CCSM4 matches the observed spatial variability ($\sigma^* = 1$) with more accuracy than that of the CCSM3. However, an increase in spring spatial RMSE (from 0.29 to 0.33) from the 3rd to the 4th version suggests a slight decrease in model skill in the spring spatial temperature pattern. Despite this minor shortcoming for spring surface-air temperatures, the CCSM4's seasonal simulations are spatially well correlated to the observed pattern (all seasonal r values greater than 0.90). Spatial variability, represented as the normalized standard deviation, is generally well simulated across all seasons.

2.4.3.2 Sea level pressure

The most noticeable enhancements in the model performance of CCSM4 over its predecessor are improvements in spring sea level pressure (Figure 2.8b). Simulated spring pattern correlation for the simulated *fifty-one-year seasonal mean* in sea level pressure improved from a negative correlation ($r = -0.40$) in CCSM3 to a weakly positive pattern correlation ($r = 0.29$) in CCSM4. This increased model skill was reflected in spring sea level pressure RMSE values: CCSM4 decreased from an RMSE of 2.13 in the CCSM3 to an RMSE of 1.14. Spring sea level pressure spatial variability was also found to be more accurate in the CCSM4 ($\sigma^* = 0.92$) compared to the CCSM3 ($\sigma^* = 1.52$), with a normalized spatial standard deviation closely matching the observed. Improvements were also seen in the winter *fifty-one-year seasonal mean* of sea level pressure, a positive step towards an accurately simulated Siberian High pressure center. The CCSM4's winter *fifty-one-year seasonal mean* shows higher pattern correlation, lower RMSE and better spatial variability compared to the CCSM3. However, summer and fall *fifty-one-year seasonal means* did not share similar results. Fifty-one-year summer and fall spatial means (Figure 2.7b) were more spatially accurate in the prior CCSM3 than in the CCSM4. CCSM4 fall sea level pressure showed a 41 % decrease in spatial pattern correlation and a 37 % decrease in spatial variability compared to the CCSM3. Summer sea level pressure displayed the largest spatial shortcomings in both the CCSM3 and the CCSM4, with both model versions generating large spatial variations, resulting in larger RMSE. The summer sea level pressure pattern simulated by the CCSM4 showed a 10 % decrease in pattern correlation and a 3.9 % increase in RMSE, relative to the CCSM3.

2.4.3.3 Spatial climatology

The accuracy of the CCSM4's *fifty-one-year annual mean* over the Bering Sea domain depends on the field being considered. Figure 2.9 shows the climatological annual spatial statistics of simulated surface-air temperature, sea level pressure, and calculated zonal and meridional winds over the Bering Sea. The simulated *fifty-one-year annual mean* of surface-air temperature (Figure 2.9) is the most accurately simulated, based on a pattern correlation of 0.98 and a low centered RMSE of 0.18. The spatial variance of surface-air temperature was also the most accurate ($\sigma^* = 1.03$), closely matching observed spatial variance. The CCSM4's *fifty-one-year annual mean* of sea level pressure averaged over the same period of time was less accurate than simulated surface-air temperature, based on a pattern correlation of 0.51 and a RMSE value of 0.85. Spatial variability of the simulated pressure field was approximately half ($\sigma^* = 0.52$) of what was seen in observations. The wind fields, both zonal and meridional, derived from simulated sea level pressure and averaged over the climatological period, were generally well simulated. The zonal wind was more accurate than the meridional wind, based on a spatial correlation of 0.83 and an RMSE value of 0.85, compared to a meridional wind spatial correlation of 0.57 and an RMSE value of 1.01. However, more spatial variability was found in the zonal wind component, indicated by normalized standard deviations of 1.5.

2.4.3.4 Temporal climatology

The CCSM4's *long-term interannual time series* of surface-air temperature captured the seasonal pattern in the observations (Figure 2.10a) with a high degree of correlation ($r = 0.97$). This high degree of correlation is expected, as the seasonal cycle would inflate the correlation between CCSM4 and reanalysis data. We would not anticipate a similar finding in annual values—in fact, the correlation between the CCSM4 annual pattern and the observed annual

pattern was significantly less (r = 0.31, Figure 2.10c) and displayed increased interannual variability ($\sigma^* = 1.35$) compared to NCEP/NCAR reanalysis data.

Despite a high correlation of seasonal temperatures, the model consistently under-simulated peak summer temperatures by about 1 °C (Figure 2.10a). There was also a tendency for the model to over- and under-simulate peak low temperatures on a decadal timescale. The periods of 1975-1977 and 1988-1992 are most notable. During these time periods, the North Pacific, including the Bering Sea, was experiencing a shift in anomalously cold temperatures to anomalously warm temperatures, which is a characteristic feature of the Pacific Decadal Oscillation (PDO) in the North Pacific. However, the CCSM4 tended to over-simulate temperatures during these years, essentially failing to capture these cold years. This result is expected, as the CCSM4 is not adept at producing the correct timing of such decadal events.

Although the *long-term interannual time-series* of surface-air temperature seasonal patterns was highly correlated to NCEP/NCAR reanalysis data, the CCSM4's *long-term interannual time-series* of sea level pressure seasonal pattern (Figure 2.10b) has a relatively low correlation with observations (r = 0.46). The CCSM4's seasonal pattern of sea level pressure averaged from 1955 to 2005 had a large centered RMSE (roughly 1.7) and a large normalized variance ($\sigma^* \sim 1.91$). Sea level pressure was under-simulated by as much as 4 hPa (Figure 2.10b) throughout the winter in the Bering Sea. Similarly, the *long-term interannual time-series* annual pattern of sea level pressure (Figure 2.10c) averaged over the Bering Sea was weakly correlated to the observed annual pattern (r = 0.03), and had a large centered RMSE (2.02). In addition, the CCSM4 simulates relatively large interannual sea level pressure variability ($\sigma^* = 1.79$) compared to observation (Figure 2.10c).

2.5 Discussion

The accuracy of climate models used to drive marine ocean and ecosystem models is becoming a question of increasing importance. To date, there are numerous available GCMs being used in climate science, though the one most commonly used is the CCSM4. Here, we discuss the performance of CCSM4 in the context of the forcing fields of greatest importance to marine ecosystem models in the Arctic and the Bering Sea.

The following discussion will highlight several priority issues in CCSM4 simulations that should be considered by marine ecosystem modelers. This section is organized as follows: a discussion on the shortcomings of key synoptic features simulated by the CCSM4 that impact sea ice movement, advection and formation in the Arctic Ocean and Bering Sea; the significance of a large lateral shift in the Aleutian Low and its implication to near-surface winds, Ekman dynamics and seasonal wind-mixing events; large seasonal surface-air temperature biases and the resulting consequences of water column stability that affect rates of biological processes; and lastly, a discussion on the increased variability of key atmospheric forcing variables and the impact this increase may have on attempts to realistically simulate ecosystem variability.

2.5.1 Sea level pressure: key synoptic shortcomings and their implications

The physical properties of both the Arctic Ocean and the Bering Sea are dependent upon several key atmospheric forcing variables. Atmospheric circulation is a key forcing variable that drives atmospheric winds, which ultimately drive oceanic currents—thus, atmospheric circulation plays a central role in the evolution of sea-ice movement, growth, and melting in the Arctic (Maslowski et al., 2012). In this respect, the Beaufort and Siberian high-pressure centers are an integral part of the Arctic and Subarctic Pacific cryosphere. Maslowski et al. (2012) and de Boer et al. (2012) found that the Arctic's atmospheric circulation simulated by the CCSM4

has significant biases compared to ECMWF 40-year reanalysis data. Maslowski et al. (2012) suggests that the CCSM4's under-simulated Beaufort High causes a misrepresentation of sea-ice motion in the Beaufort Gyre, and overall sea-ice extent exceeds what is observed. Our assessment confirms the biases found by both de Boer et al. (2012) and Maslowski et al. (2012), though we have also shown that these biases vary on a seasonal timescale in the Subarctic Pacific Ocean, with strong biases resulting from an under-simulated Siberian High in winter and fall and a large northwest displacement of the Aleutian Low in spring and again in the fall over the Bering between 1955-2005. The CCSM4 simulated atmospheric circulation in summer with the least amount of model skill relative to any other season; while simulated winter sea level pressure was the most spatially accurate season, closely matching the observed spatial pattern. It is important to note these seasonal differences between the CCSM4 and the observed, particularly when interpreting seasonal and interannual hydrological-ecosystem processes simulated by coupled atmosphere-ocean-ecosystem models.

The Siberian High and the Aleutian Low are key atmospheric features that play a major role in sea-ice formation and advection in the Bering Sea. The formation of sea ice begins in the Bering Sea, when cold northerly winds first freeze the Chukchi Sea in the western Arctic (Stabeno et al., 2012a). Cold northerly winds typically advance southward due to the Siberian high-pressure center, though we have shown that the CCSM4 under-simulates this important circulation component, especially during the winter and fall months, when sea ice formation is at its maximum. In particular, subtle changes in atmospheric circulation like this have the potential to misrepresent the direction and strength of atmospheric winds simulated by GCMs. For example, while the spatial pattern of pressure was most accurately simulated in winter, an under-simulated Siberian High permits the Aleutian Low to extend further north into the Northern

Bering Sea, contributing to a large negative bias (~7 hPa) and producing a strong easterly wind in the area. Easterly winds have the potential to hamper the advection of sea ice into the Southern Bering Sea (Stabeno et al., 2012b), as well as to affect the timing of sea-ice formation and melt, in turn altering the representation of sea-ice thickness and distribution throughout the Bering Sea.

The Aleutian Low is defined by migrating cyclones propagating from west to east across the North Pacific Ocean, where they eventually reach maximum intensity over the Aleutian Islands in the southern Bering Sea (Rodionov et al., 2007; Pickart et al., 2009; Stabeno et al., 2005). The physical and biological properties of the Bering Sea are highly influenced by this semi-permanent cyclonic feature. The intensity and location of the Aleutian Low plays a key role in establishing pressure gradients, which further determine the strength of the wind stress, and therefore wind mixing, at the ocean's surface. The position and intensity of the Aleutian Low also cause large interannual variability in the formation and the extent of sea-ice over the continental shelf regions of the Bering Sea (Brown and Arrigo, 2013). Our assessment found that the CCSM4 produced a large northwest displacement in the Aleutian Low over the Bering Sea, compared to NCEP/NCAR reanalysis data. The shift in the Aleutian Low implies a decrease in the northerly component of meridional transport and an enhancement to the southerly component of meridional transport along the west coast of Alaska. Enhanced southerly winds would promote an over-simulation of the transport of maritime warm, moist air originating from the Tropical Pacific. The direction of wind over the Bering Sea has also been shown to be important for the transport of water (Danielson et al., 2012) and zooplankton (Gibson et al., 2013) onto the Bering Sea shelf, with increased transport onto the southern shelf during episodes of southeasterly winds.

Spring sea level pressure simulated by the CCSM4 was the most spatially improved season over the CCSM3, representing a significant enhancement of the CCSM4, as this is an important time of year for biological production in the Southern Bering Sea. While simulated spring sea level pressure had only minor biases in the Southern Bering (~1 hPa), a large lateral shift of the Aleutian Low positioned the pressure center too far west. This displacement of the Aleutian Low promotes winds in the wrong direction compared to the observed NCEP/NCAR reanalysis wind direction. The CCSM4 simulated strong southwesterly winds over the entire Southern Bering Sea, compared to a northeasterly wind direction observed in NCEP/NCAR reanalysis. A considerable change in the wind direction has implications for the Ekman dynamics that control vertical exchanges of nutrient-rich deep water through upwelling and downwelling processes associated with Ekman pumping (NRC, 1996). Danielson et al. (2012) concluded that a lateral shift in the Aleutian Low, compared to a latitudinal shift, would likely have a greater effect on a shelf-wide reorganization of oceanic circulation and systematic changes in the physical, chemical, and biological fluxes of the Bering Sea. Therefore, it is clear that we need atmospheric pressure centers to be more precisely simulated, especially during seasons of high biological production and sea-ice formation, and care should be taken in interpreting results of biophysical models that are driven by less than accurate atmospheric models.

Further, wind mixing affects the heat and nutrient fluxes over the Bering Sea shelf (Stabeno et al., 2005). Seasonal wind mixing events have a large impact on the temperature and stratification of the water column (Ladd and Stabeno, 2012), impacting the timing and the abundance of biological production in the Bering Sea (Coyle et al., 2008). The water column is typically well mixed in the winter months from the frequent passing of storms, though these events become less frequent as winter transitions into summer. Summer months typically yield

weaker winds, warmer sea surface temperatures, and strong stratification, leading to a nutrient-limited upper mixed layer (Strom and Fredrickson, 2008; Ladd and Stabeno, 2012). Here, we found that CCSM4 simulates sea level pressure during summer with less skill than in any other season. Robust sea level pressure biases were found in the southern Bering Sea (up to 6 hPa), producing a strong pressure gradient over the majority of the Bering Sea region, resulting in stronger than observed zonal momentum in the southern Bering Sea, which would result in over-prediction of wind mixing (proportional to wind speed cubed) and thus an over simulation of nutrients in the upper mixed layer. The additional supply of nutrients could result in an over-estimation of biological production over the southeastern Bering Sea shelf.

2.5.2 Surface-air temperature: model skill and potential consequences

The CCSM4 sea-surface temperatures, which are closely associated with the overlying surface-air temperature, have previously been shown to be improved relative to the CCSM3, in all oceans except the Arctic (Gent et al., 2011). Our analysis confirmed this finding, concluding that simulated air temperatures remain colder than observations by several degrees throughout most of the Arctic. Despite the biases found in the broad Arctic domain, improved spatial temperature gradients of climatological annual mean temperature were simulated by the CCSM4 over the entire Bering Sea. Warm and cold biases still remain in all seasons throughout the 1955-2005 period, though these biases have improved over the CCSM3 simulated Bering Sea surface-air temperatures. We therefore conclude that spatial temperature patterns over the Arctic and Bering Sea domain are generally well simulated by CCSM4.

In combination with surface wind stress, near-surface air temperatures determine the temperature and stability of the water column over the Bering Sea shelf. Our assessment indicated spatial patterns of seasonal CCSM4 surface-air temperatures were generally well

simulated, though care must be taken when interpreting this result. For example, while the spatial pattern in winter was well simulated and closely matched the observed spatial pattern, robust warm biases of ~4 ^{o}C were seen in the Northern Bering Sea; implying the possibility of warm ocean temperatures delaying the formation of sea ice in the northern Bering Sea. In the southern Bearing Sea, winter temperature biases were not as large, though the majority of the southern shelf exhibited a warm bias (>2 ^{o}C). Warm winter biases such as these may have added consequences for ecosystem dynamics in the Bering Sea. Through brine rejection, sea-ice formation in the northern Bering Sea drives convection, replenishing nutrients in the water column and leading to a possible intense spring phytoplankton bloom (Brown and Arrigo, 2013). It is likewise important to note that while the spring spatial pattern was simulated with less skill relative to other seasons, the magnitude of CCSM4 spring surface-air temperatures were accurately simulated and were found to have only minor biases (>1 ^{o}C) over the entire Bering Sea shelf. As thermally induced stratification is important for the onset of the spring bloom, the model's ability to simulate spring surface-air temperatures is encouraging. Simulated summer surface-air temperatures over both the northern and southern Bering Sea improved from the third to the fourth version of CCSM4 simulations, though the CCSM4 summer still remains too cold. Biological process rates such as phytoplankton growth and zooplankton grazing are temperature sensitive; thus changes to water temperature would affect material and energy flow through the ecosystem (Gibson and Spitz, 2011). During recent warming periods (2001-2005), the northern Bering Sea underwent changes due to the warming of ocean waters, and recent studies suggest the possibility of a shift in the Bering Sea towards a pelagic-dominated marine ecosystem (Grebmeier et al., 2006). For the last few years (2007-2012), however, the Bering Sea has been experiencing low year-to-year variability in sea-ice extent, with high ice coverage (Stabeno et al.,

2012b), suggesting several consecutive years of cold air temperatures and the establishment of cold, dense ocean water (cold pool). The establishment of a cold pool has blocked the northward migration of the Bering Sea ecosystem, favoring the benthic ecosystem. Air temperature at the surface impacts the temperature of the ocean and hence sea-ice formation/retreat, controlling which habitat receives primary production in the Bering Sea (Stabeno et al., 2012b; Hunt et al., 2002; Hunt et al., 2011; Coyle et al., 2011). The persistence of model biases, found in winter and summer here, will therefore hamper efforts to accurately hindcast ecosystem dynamics or project the future state of the Bering Sea ecosystem.

2.5.3 Variability and predictability under atmospheric forcing

Atmospheric features over the North Pacific—and more specifically in the Bering Sea—are known to be highly variable on decadal and multi-decadal timescales (Minobe, 1997; Mantua and Hare, 2002). Large marine ecosystem shifts in high latitude seas indicate that marine ecosystems also vary over similar timescales (Beamish, 1993; Mantua et al., 1997; Hare and Mantua, 2000; Coyle et al., 2008; Grebmeier et al., 2006). If a system model such as the CCSM/CESM is to be used to drive marine biophysical models attempting to realistically capture ecosystem variations, the forcing variations in the physical components must also be compatible, in a statistical sense, with those of the actual system. Here we have found that the CCSM4's simulated annual surface-air temperature and sea level pressure have shown greater interannual variability compared to observed variability—nearly 1.5 to 2 times as much, respectively. This additional variability may lead to additional simulated extreme events in the Bering Sea: for example, extreme warm and cold seasons or years, large-scale wind mixing events, and extremes in sea-ice extent or retreat, all of which may have major impacts on projections of the marine ecosystem in the Bering Sea. On a seasonal basis, the over-simulation

of variability by the CCSM4 is greater for sea level pressure than for surface-air temperature. Seasonal variability of surface-air temperature by the CCSM4 is generally well simulated, however only slightly less than observed.

The CCSM4 tends to capture the range of the cold and warm years seen in observations, but failed to capture the temperature minima observed during well-documented regime shifts in the late 1970s and again in the late 1980s (Mantua et al., 1997; Beamish, 1998). Such regime shifts are often associated with modes of atmospheric and oceanic circulation; the El Niño Southern Oscillation (ENSO), the Pacific Decadal Oscillation (PDO), and the Arctic Oscillation are all examples of such modes. CCSM4 modes of Pacific variability, both ENSO and PDO, have been previously found to be comparable to observations (Deser et al., 2012; Landrum et al., 2013), although Deser et al., 2012 suggests that the PDO connection to the tropical pacific remains weaker than observed. While both Deser et al. (2012) and Landrum et al. (2013) suggest that CCSM4 exhibits a pronounced red power spectra with a comparable power to observations in the decadal or longer time scale, Branstator et al. (2013) suggests that the CCSM4 has the least amount of decadal predictability in the North Pacific when compared to other GCM's. Even though the CCSM4 is expected to capture interannual and decadal variability, we would not expect the CCSM4 to capture the timing of either ENSO or PDO events, nor would we expect the individual year-to-year extremes of the model to match those of the real world for two reasons: primarily, all models of this nature generally have limited success simulating the timescales of variability (Stoner et al., 2009) and the chaotic randomness (internal variations) found in the real world cannot be expected to align temporally with a model's internal variations.

2.5.4 NCEP/NCAR 40-year reanalysis biases

It must be noted that the reanalysis does not directly assimilate surface-air temperature observations (Kalnay et al., 1996), which has lead to a bias in reanalysis surface-air temperature. Previous studies have shown that while the NCEP/NCAR Reanalysis 1 is well correlated with surface observations, the reanalysis is systematically colder (Bromwich et al., 2005; Hankes and Walsh, 2011). Depending on location and season, the reanalysis is 1-6 ºC colder than surface observations, especially in Pan-Arctic regions. The CCSM4 biases relative to NCEP/NCAR reanalysis discussed in section 4.2 remain significant, however ecosystem modelers should acknowledge the biases found in reanalysis products such as the NCEP/NCAR Reanalysis 1.

2.6 Summary and outstanding issues

An assessment of the CCSM4 was performed over the Arctic, with a centered focus on the Bering Sea. A spatial and temporal examination of simulated sea level pressure and surface-air temperature was performed over a climatological period spanning fifty-one-years (1955 to 2005). Key findings are as follows:

- The spatial distribution of surface-air temperature was generally well simulated over the Arctic, though the simulated temperatures remain colder than the NCEP/NCAR reanalysis throughout most of the Arctic region.
- Over the Bering Sea, general temperature patterns, including spatial gradients, were accurately simulated compared to the reanalysis, although a cold bias still remains across the climatological period. In general, all seasons of surface-air temperatures are spatially well simulated, although warm and cold biases also still remain in all seasons across the Bering Sea.

- The Beaufort High was nearly non-existent within simulated climatological monthly mean sea level pressure, corresponding to a large mass deficit in the Arctic domain.
- Across the entire northern half of the Bering Sea, a large northwest displacement of the Aleutian Low and a weaker-than-observed Siberian High resulted in a negative bias of up to 6 hPa. This shift in mass, along with a weaker anticyclone, produced errors in sea level pressure, and by implication, near-surface winds, in all seasons over the entire Bering Sea.
- This analysis indicates that simulated interannual variability of surface-air temperature and sea level pressure over the Bering Sea exceeds that which is observed—nearly 1.5 to 2 times the observed variance, respectively.
- On a seasonal basis, the interannual variability of the CCSM4's simulated sea level pressure exceeds observed variability, however the simulated seasonal interannual variation of surface-air temperatures over the Bering Sea corresponds well with the observed variability.

This assessment implies that changes from the 3rd to the 4th version of the CCSM have generally improved model performance over the Bering Sea. However, the question still remains: is the CCSM4 prepared to force marine ecosystem simulations? In our view there are three main limitations at this stage: the systematic errors in the winds, significant seasonal temperature biases, and the increased interannual variability of key atmospheric forcing variables. Persistence of model shortcomings such as these are not isolated to CCSM4 simulations; for this reason, extensions of such evaluations to other models and marine regions would help to establish the readiness of global models for marine ecosystem studies.

2.7 Acknowledgments

This work was funded by the Arctic Program of the National Science Foundation under award #1049225. The NOAA/OAR/ESRL Physical Science Division, Boulder, Colorado, USA provided the NCEP/NCAR reanalysis data used in model validation. The CCSM4 and CCSM3 model outputs were provided by the National Centers of Atmospheric Research and distributed via the Earth System Grid (ESG). Additionally, we would like to thank Dr. Uma Bhatt of the Geophysical Institute, University of Alaska Fairbanks for her fruitful discussions and two anonymous reviewers whose comments helped improve this paper.

Figures

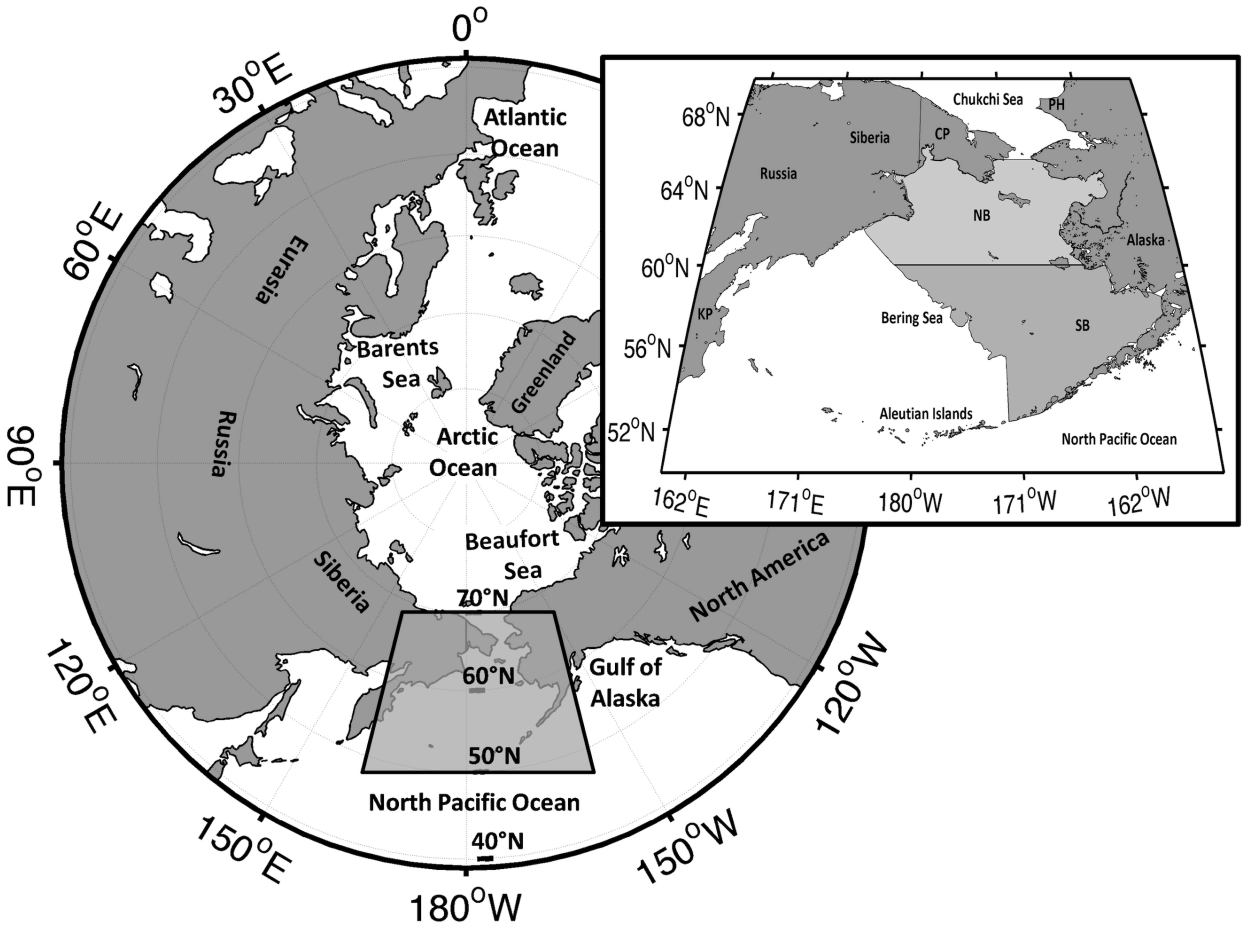

Figure 2.1. Geographic domain used for model assessment. Geographic domain of the study area. The Arctic region extends from 40°N to the pole, and the Bering Sea region in grey extends 50–65°N and 160°E–160°W (KP: Kamchatka Peninsula, PH: Point Hope, CP: Chukchi Peninsula, NB: Northern Bering Sea Shelf, SB: Southern Bering Sea Shelf with a division between the northern and southern Bering Sea at 60°N indicated by the solid black line).

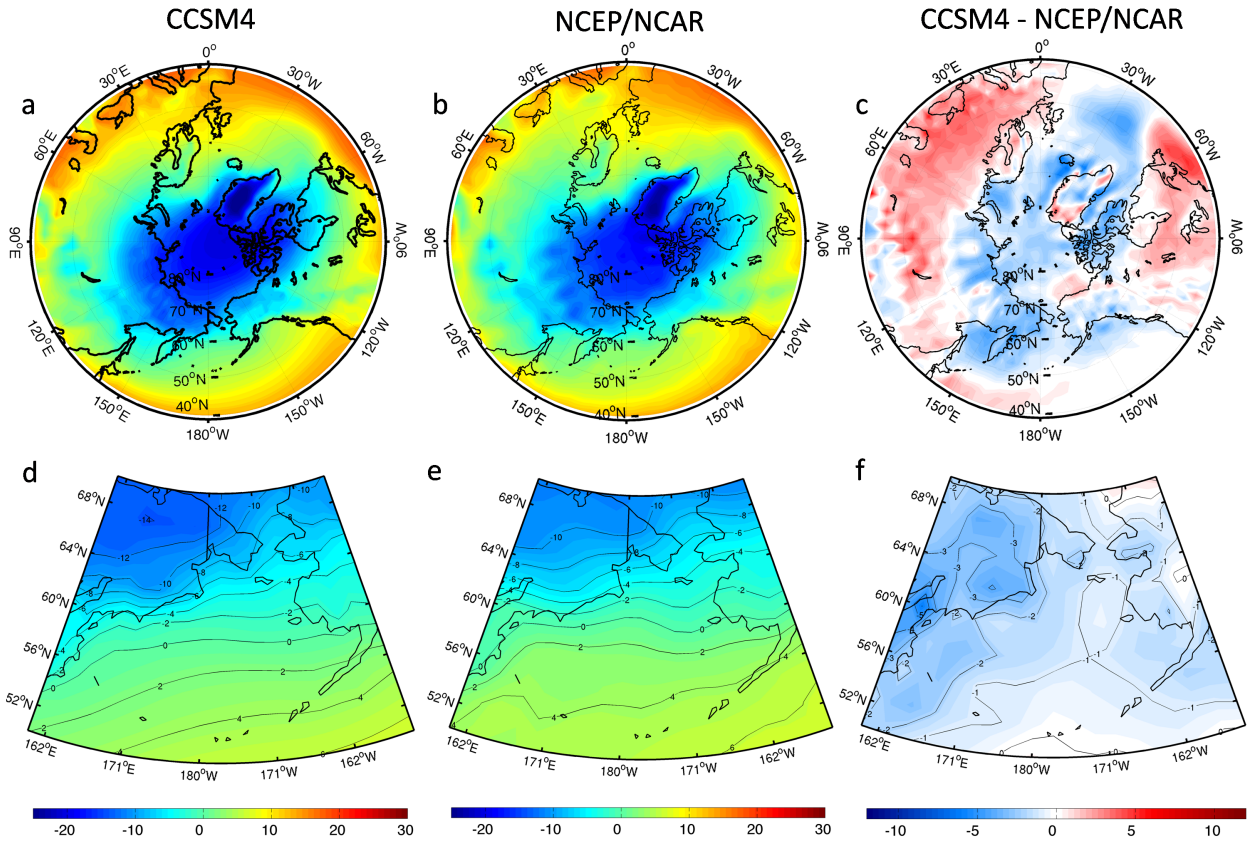

Figure 2.2. Climatological (1955-2005) mean air temperature. Climatological mean temperature fields calculated from monthly mean air temperatures (°C), averaged during 1955-2005 for (a) CCSM4, (b) NCEP/NCAR reanalysis data, and (c) the difference (model minus reanalysis) above 40°N; and for (d) CCSM4, (e) NCEP/NCAR reanalysis, and (f) the difference (model minus reanalysis) over the Bering Sea domain.

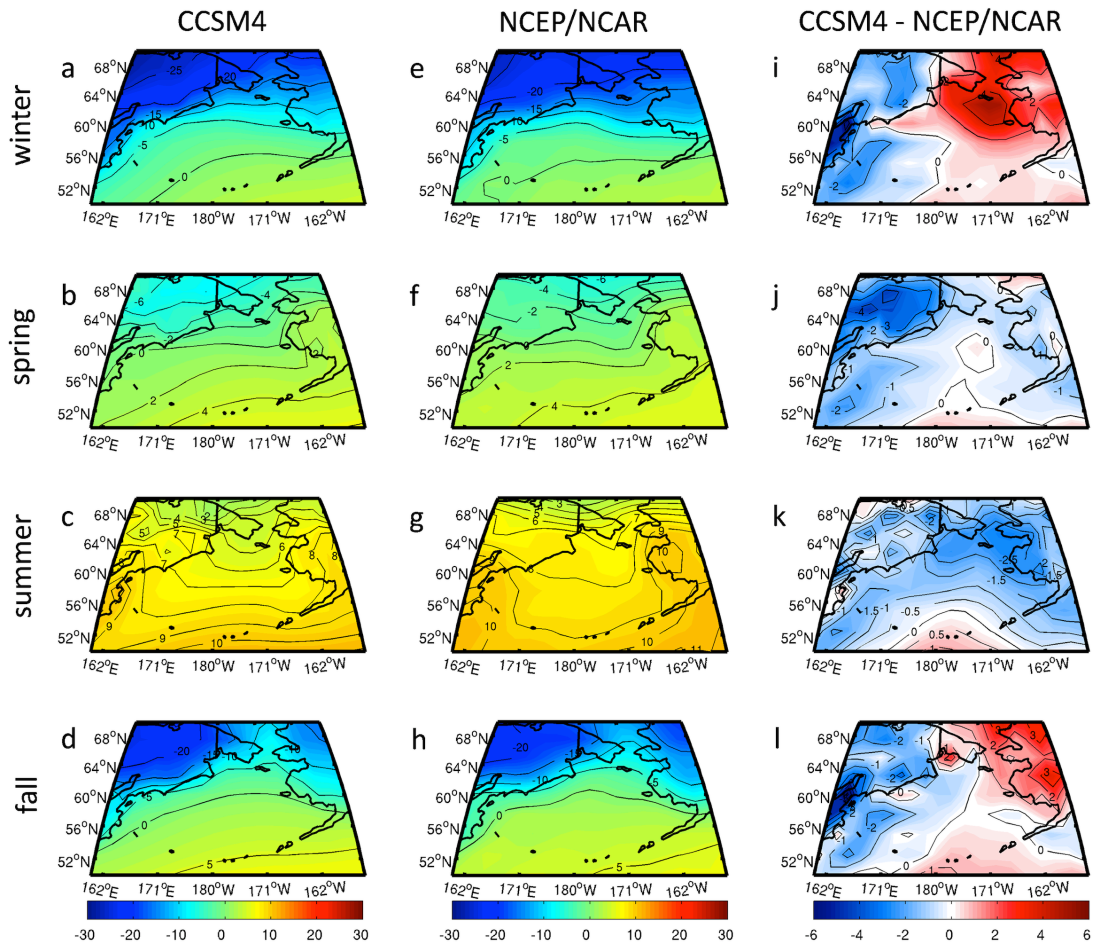

Figure 2.3. Seasonal mean air temperature. Seasonal mean air temperatures (°C) [(a) winter, (b) spring, (c) summer, (d) fall] averaged over 1955-2005 over the Bering Sea domain for (*left*) the CCSM4; (*center*) NCEP/NCAR reanalysis data [(e) winter, (f) spring, (g) summer, (h) fall]; and (*right*) the seasonal difference (model minus reanalysis) [(i) winter, (j) spring, (k) summer, (l) fall].

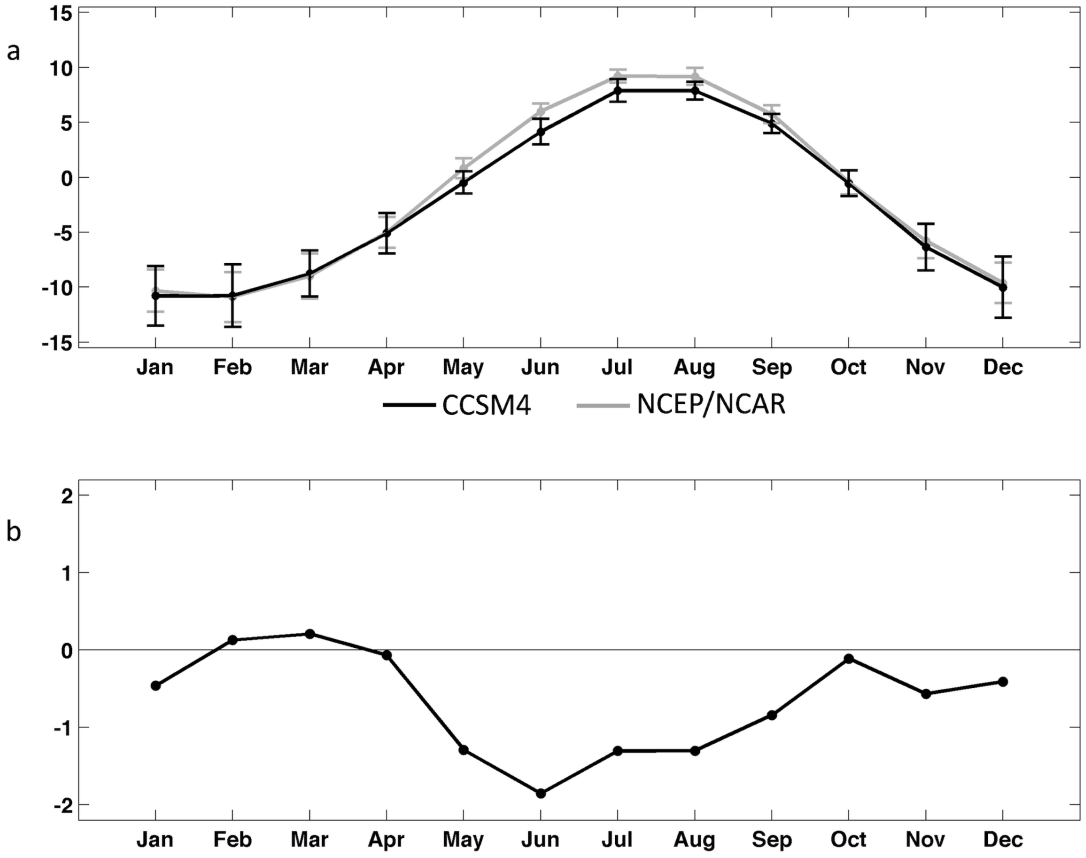

Figure 2.4. Climatological (1955-2005) annual cycle of air temperature. Climatological (1955 to 2005) annual cycle (a) of surface-air temperature (°C) averaged over the Bering Sea from the CCSM4 (black) and NCEP/NCAR reanalysis (grey). The error bars indicate standard deviations of monthly values. The difference between CCSM4 and the NCEP/NCAR reanalysis is shown below (b).

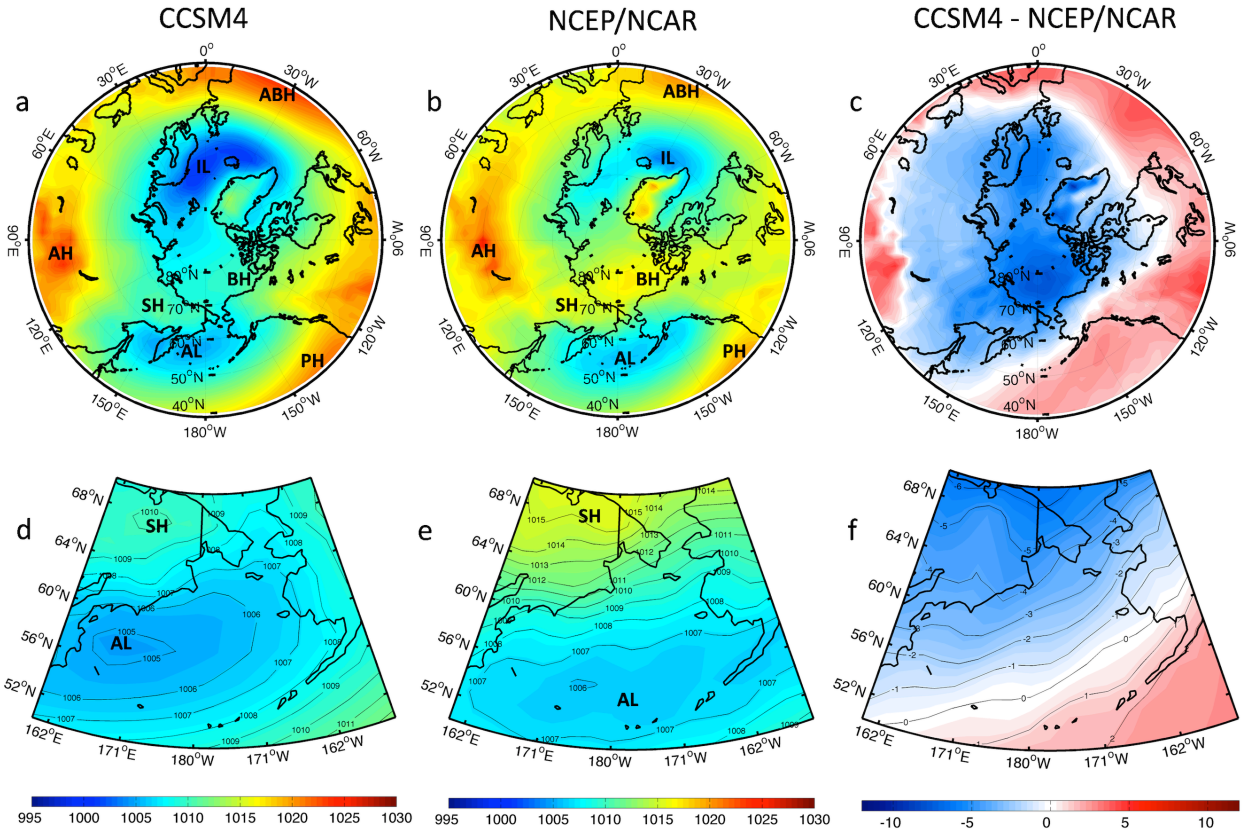

Figure 2.5. Climatological (1955-2005) mean sea level pressure. Climatological mean pressure fields calculated from monthly mean sea level pressure (hPa), averaged from 1955-2005 above 40° latitude for (a) the CCSM4, (b) NCEP/NCAR reanalysis data, and (c) the difference between the two. Similarly for (d) the CCSM4, (e) NCEP/NCAR reanalysis data, and (f) the difference over the Bering Sea domain.

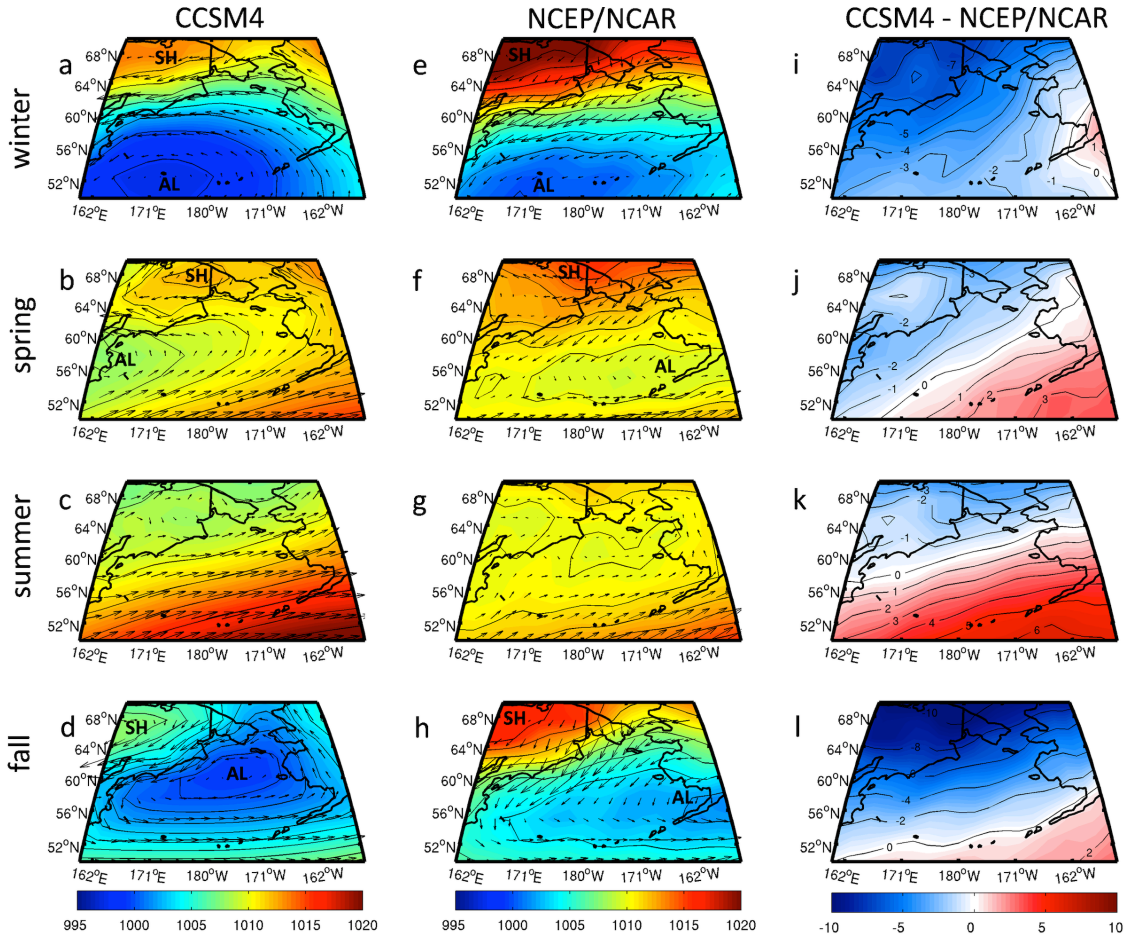

Figure 2.6. Seasonal mean sea level pressure. Seasonal [(a) winter, (b) spring, (c) summer, (d) fall] mean sea level pressure (hPa) averaged from 1955-2005 over the Bering Sea domain from *(left)* the CCSM4, *(center)* NCEP/NCAR reanalysis, [(e) winter, (f) spring, (g) summer, (h) fall]), and *(right)* the seasonal [(i) winter, (j) spring, (k) summer, (l) fall] difference between the two. The Aleutian Low (AL) and the Siberian High (SH) pressure centers are marked in both CCSM4 and NCEP/NCAR Reanalysis. Overlying wind vectors denote geostrophic wind fields for both CCSM4 and NCEP/NCAR Reanalysis data.

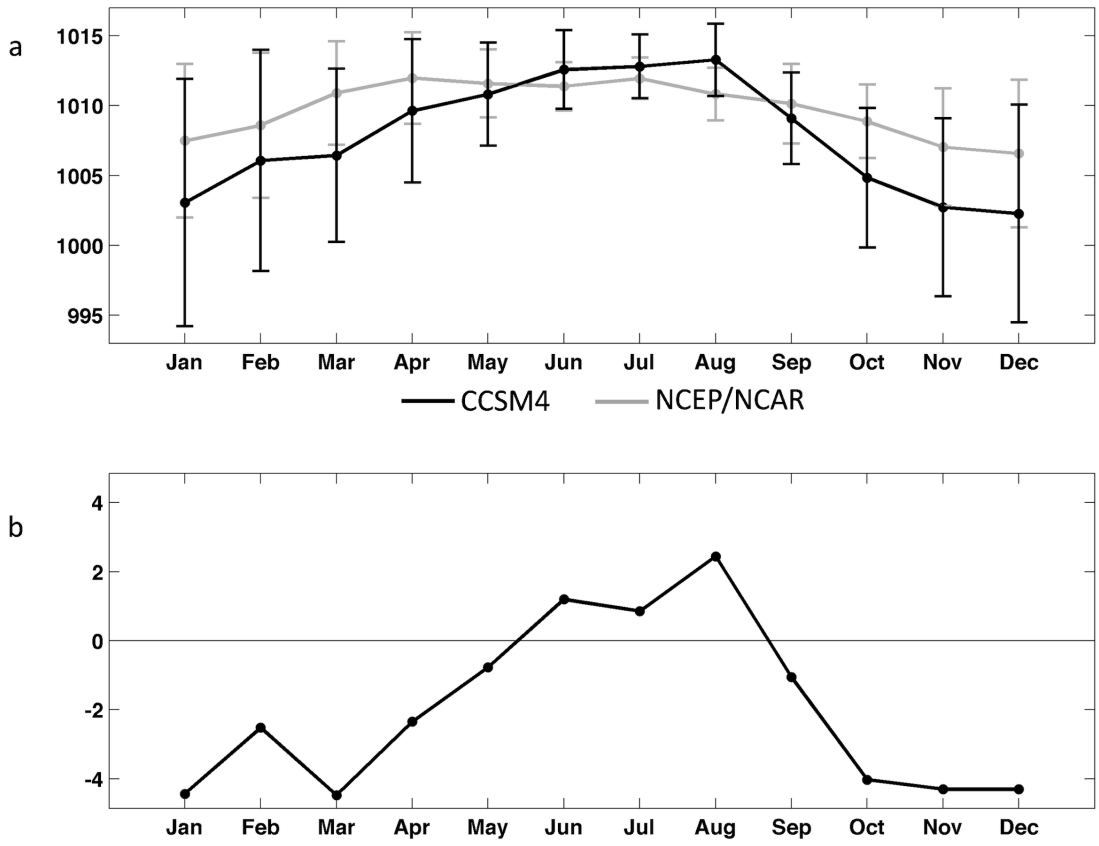

Figure 2.7. Climatological (1955-2005) annual cycle of sea level pressure. Climatological (1955 to 2005) annual cycle of (a) sea level pressure (hPa) averaged over the Bering Sea from the CCSM4 (black) and the NCEP/NCAR reanalysis (grey). The error bars indicate standard deviations of monthly values. The difference between CCSM4 and the NCEP/NCAR reanalysis is shown below (b).

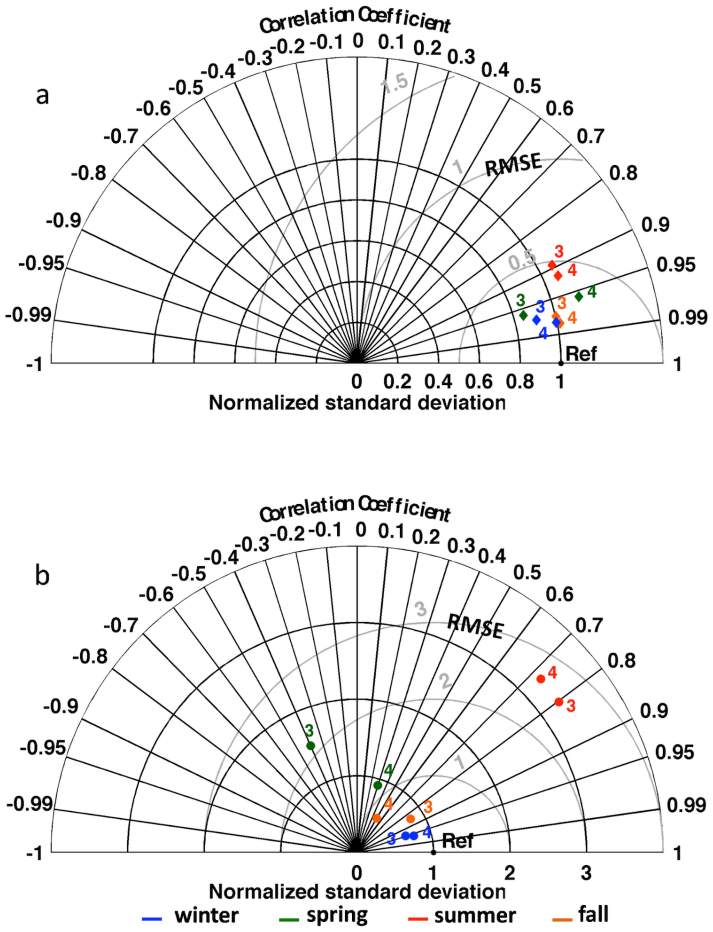

Figure 2.8. Comparison of third and fourth versions of the CCSM spatial pattern statistics. Changes in normalized spatial pattern statistics between the third and fourth versions of the CCSM (a) surface-air temperature and (b) sea level pressure over the Bering Sea. Each version is labeled with version number and the color denotes seasons. All simulated seasonal mean fields are compared to the NCEP/NCAR observational reference (Ref). Isolines indicate the correlation, normalized standard deviation, and the centered RMSE.

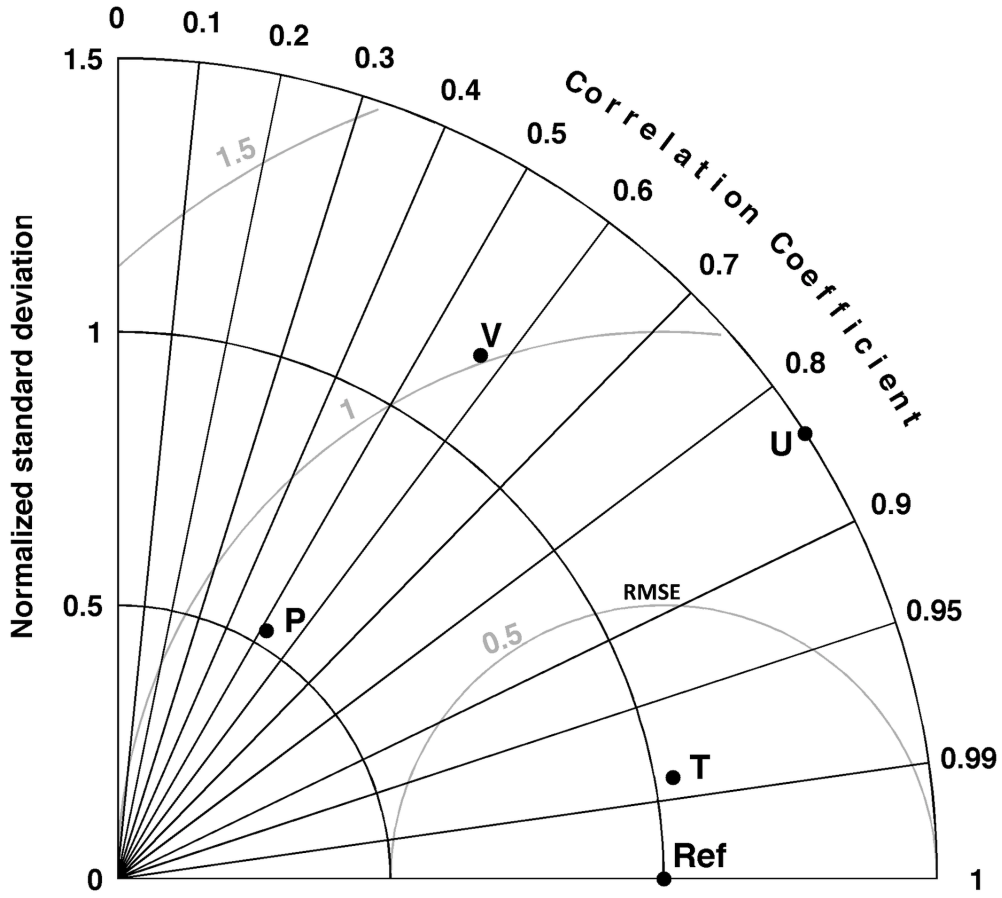

Figure 2.9. Climatological (1955-2005) mean spatial pattern statistics. Spatial pattern statistics describing the climatological mean sea level pressure (P), surface-air temperature (T), zonal (U) and meridional (V) winds over the Bering Sea simulated by the CCSM4. All simulated mean fields are compared to NCEP/NCAR observational reference (Ref). Isolines indicate the correlation, normalized standard deviation, and the centered RMSE.

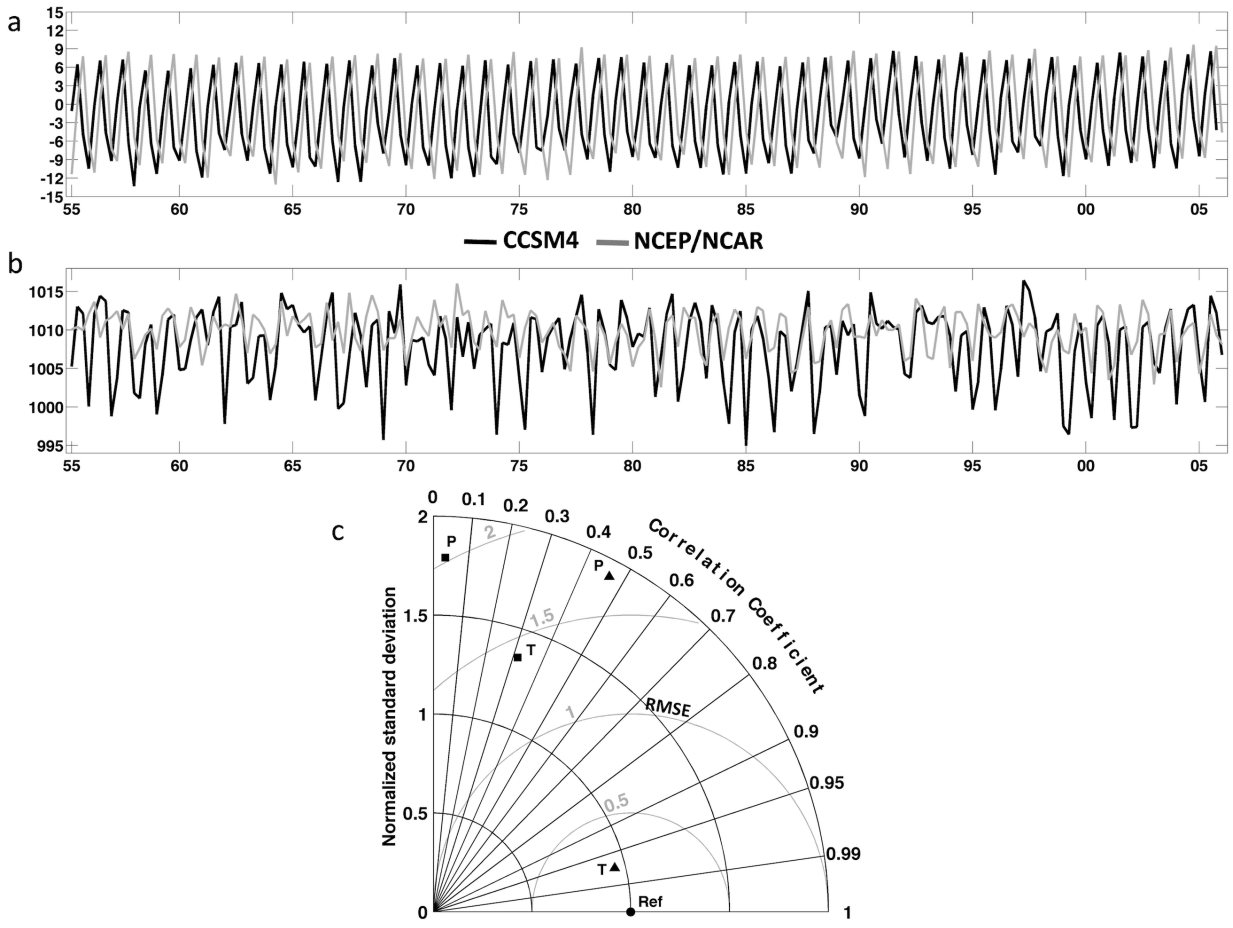

Figure 2.10. Air temperature and sea level pressure temporal pattern statistics. Seasonal mean (a) surface-air temperatures over the Bering Sea domain from 1955-2005, (b) the same for sea level pressure, and (c) the temporal pattern statistics describing the annual (square) and seasonal (triangle) sea level pressures (P) and surface-air temperatures (T) over the Bering Sea, simulated by the CCSM4 from 1955 to 2005. The modeled curve is shifted by three months for clarity purposes. Simulated annual and seasonal cycles are compared to the NCEP/NCAR observational reference (Ref). Isolines indicate the correlation, normalized standard deviation and centered RMSE.

References

Beamish R, Noakes D, McFarlane G, King J. 1998. The regime concept and recent changes in Pacific Salmon Abundanc*e*, Technical Report, pp. 1–3.

Beamish R J. 1993. Climate and exceptional fish production off the west coast of North America.*Canadian Journal of Fisheries and Aquatic Sciences* **50**: 2270-2291.

Bering Sea Interagency Working Group. 2006. Climate change and the Bering Sea ecosystem: an integrated, interagency-multi-institutional approach. AFSC Processed Report, 2006-01. Alaska Fisheries Science Center, National Marine Fisheries Service, NOAA: Seattle, WA, 30 pp.

Branstator G, Teng H, Meehl G A, Kimoto M, Knight J R, Latif M, Rosati A. 2013. Systematic estimates of initial-value decadal predictability for six AOGCMs. *Journal of Climate* **25**: 1827-1846. DOI: 10.1175/JCLI-D-11-00227.1

Bromwich D, Wang S. 2005. Evaluation of the NCEP-NCAR and ECMWF 15- and 40-Yr Reanalyses Using Rawinsonde Data from Two Independent Arctic Field Experiments. Monthly Weather Rev. Special Selection, **133**: 3562–3578.

Brown Z , Arrigo K. 2013. Sea ice impacts on spring bloom dynamics and net primary production in the Eastern Bering Sea. *Journal of Geophysical Research* **118**: 1–20. DOI:10.1029/2012JC008034.

Coyle K, Eisner L, Mueter F, Pinchuk A, Janout M, Cieciel K, Farley E. 2011. Climate change in the southeastern Bering Sea: impacts on pollock stocks and implications for the oscillating control hypothesis. *Fisheries Oceanography* **20**(2): 139–156. DOI:10.1111/j.1365-2419.2011.00574.

Coyle K, Pinchuk A, Eisner L, Napp J. 2008. Zooplankton species composition, abundance and biomass on the eastern Bering Sea shelf during summer: The potential role of water-column stability and nutrients in structuring the zooplankton community. *Deep Sea Research Part II: Topical Studies in Oceanography* **55**: 1775–1791. DOI:10.1016/j.dsr2.2008.04.029.

Danielson S, Weingartner T, Aagaard K, Zhang J, Woodgate R. 2012. Circulation on the central Bering Sea shelf, July 2008 to July 2010. *Journal of Geophysical Research* **117**: C10003. DOI:10.1029/2012JC008303.

Danielson S, Curchitser E, Hedstrom K, Weingartner T, Stabeno P. 2011. On ocean and sea ice modes of variability in the Bering Sea. *Journal of Geophysical Research* **116**: C12. DOI:10.1029/2011JC007389.

De Boer G, Chapman W, Kay J, Medeiros B, Shupe M, Vavrus S, Walsh J. 2012. A Characterization of the Present-Day Arctic Atmosphere in CCSM4. *Journal of Climate* **25**: 2676–2695. DOI:10.1175/JCLI-D-11-00228.1.

Deser C, Phillips A S, Tomas R A, Okumura Y M, Alexander M A, Capotondi A, Scott J D, Kwon Y, Ohba M. 2012. ENSO and Pacific Decadal Variability in the Community Climate System Model Version 4. *Journal of Climate* **25**: 2622–2651. DOI:10.1175/JCLI-D-11-00301.1.

Di Lorenzo E, Schneider N, Cobb K M, Franks P J, Chhak K, Miller A J, Williams J C, Bogard S J, Arango H, Curchister E, Powell T M, Riveiere P. 2010. *An overview of Pacific Climate Variability* Technical Report, pp. 1–10.

Gent P, Danabasoglu G, Donner L, Holland M, Hunke E, Jayne S, Lawrence D, Neale R, Rasch P, Vertenstein M, Worley P, Yang Z, ZhangM. 2011. The Community Climate SystemModel version 4. *Journal of Cimate* **24**: 4973–4991, DOI: 10.1175/2011JCLI4083.1.

Gibson G A, Spitz Y H. 2011. Impacts of biological parameterization, initial conditions, and environmental forcing on parameter sensitivity and uncertainty in a marine ecosystem model for the Bering Sea. *Journal of Marine Systems* **88**: 214-231. DOI: 10.1016/j.jmarsys.2011.04.008.

Gibson G, Coyle K, Hedstrom K, Curchitser E. 2013. A modeling study to explore on-shelf transport of oceanic zooplankton in the Eastern Bering Sea. Journal of Marine Systems. 121: 47–64.

Gleckler P J, Taylor K E, Doutriaux C. 2008. Performance Metrics for climate models. *Journal of Geophysical Research* **113**:D06104. DOI: 10.1029/2007JD008972.

Grebmeier J,Overland J,Moore S, Farley E, Carmack E, Cooper L, Frey K, Helle J, McLaughlin F, McNutt S. 2006. A major ecosystem shift in the northern Bering Sea. Science 311: 1461–1464, DOI: 10.1126/ science.1121365.

Hankes I E, Walsh J E 2011. Characteristics of extreme cold air masses over the North American sub-Arctic. *Journal of Geophysical Research,* **116**. *DOI:*10.1029/2009JD013582.

Hare S, Mantua N. 2000. Empirical evidence for North Pacific regime shifts in 1977 and 1989. *Progress in Oceanography*, **47**: 103–146.

Hawkins E, Sutton R 2012. Time of emergence of climate signals. Geophysical Research Letters, 39: L01702, doi:10.1029/2011/GL050087.

Hermann A, Gibson G, Bond N, Curchitser E, Hedstrom K, Cheng W, Wang M, Stabeno P, Eisner L, Janout M. 2013. A multivari- ate analysis of observed and modeled biophysical variability on the Bering Sea shelf: multidecadal hindcasts (1969–2009) and forecasts (2010–2040). Deep Sea Res. II Topical Stud. Oceanogr. 94: 121–139, DOI: 10.1016/j.dsr2.2013.04.007.

Hunt G L Jr, Stabeno P, Walters G, Sinclair E, Brodeur R D, Napp J M, Bond N A. 2002. Climate change and control of the southeastern Bering Sea pelagic ecosystem. *Deep Sea Research II*, **49**: 5821-5853.

Hunt G L Jr, Coyle K O, Eisner L B, Farley E V, Heintz R A, Mueter F, Napp J M, Overland J E, Ressler P H, Salo S, Stabeno P J. 2011. Climate impacts on eastern Bering Sea foodwebs: a synthesis of new data and an assesment of the Oscillating Control Hypothesis. *ICES Journal of Marine Sciences*. DOI: 10.1093/icesjms/fsr036.

Hurrell J, Deser C. 2010. North Atlantic climate variability: The role of the North Atlantic Oscillation. *Journal of Marine Systems*, **79**: 231–244. DOI:10.1016/j.jmarsys.2009.11.002.

Jahn A, Sterling K, Holland M, Kay J, Maslanik J, Bitz C, Bailey D, Stroeve J, Hunke E, Lipscomb W, Pollak D. 2012. Late-Twentieth-Century Simulation of Arctic Sea Ice and Ocean Properties in the CCSM4. *Journal of Climate,* **25**: 1431-1452. DOI:10.1175/JCLI-D-11-00201.1.

Ji R, Jin O, Varpe. 2013. Sea ice phenology and timing of primary production pulses in the Arctic Ocean. *Global Change Biology*, **19**: 734-741.

Jin M, Deal C, Lee S, Elliott S, Hunke E, Maltrud M, Jeffery N. 2012. Investigation of Arctic sea ice and ocean primary production for the period 1992–2007 using a 3-D global ice–ocean ecosystem model. *Deep Sea Research Part II: Topical Studies in Oceanography*, ***81-84***: 28-35. DOI:10.1016/j.dsr2.2011.06.003

Kalnay E, Kanamitsu M, Kistler R, Collins W, Deaven D, Gandin L, Iredell M, Saha S, White G,Wollen J, Zhu Y, Leetma A, Reynolds R, ChelliahM, EbisuzakiW, Higgins W, Janowiak J, Mo K, Ropelewski C, Wang J, Jenne R, Joseph D. 1996. The NCEP/NCAR 40-year reanalysis project. Bulletin of the American Meteorological Society. 77: 437–471, DOI: 10.1175/15200477(1996)077<0437:TNYRP>2.0.CO;2.

Kattsov V.M., Sporyshev P.V. 2006. Timing of global warming in IPCC AR4 AOGCM simulations. Geophysical Research Letters, 33: L23707, doi:10.1029/2006GL027476.

Ladd C, Stabeno P. 2012. Stratification on the Eastern Bering Sea shelf revisited. *Deep Sea Research Part II: Topical Studies in Oceanography*, ***65***: 72–83. DOI:10.1016/j.dsr2.2012.02.009.

Landrum L, Otto-Bliesner B L, Wahl E R, Conley A, Lawrence P J, Rosenbloom N, Teng H. 2013. Last millennium climate and its variability in CCSM4. *Jornal of Climate*, 26: 1085-1111. DOI: 10.1175/JCLI-D-11-00326.1.

Mantua N, Hare S, Zhang Y, Wallace J, Francis R. 1997. A Pacific Interdecadal Climate Oscillation with Impacts on Salmon Production. *Bulletin of the American Meteorological Society*, ***78***: 1069–1079.

Mantua N, Hare S, 2002. The Pacific Decadal Oscillation. *Journal of Oceanography*, **58**: 35-44. DOI:10.1023/A:1015820616384.

Maslowski W, Kinney J, Higgins M, Roberts A. 2012. The Future of Arctic Sea Ice. *Annual Review of Earth and Planetary Sciences*, **40**: 625–654. DOI:10.1146/annurev-earth-042711-105345

Minobe S, 1997. A 50-70 year climatic oscillation over the North Pacific and North America. *Geophysical Research. Letters*, **24**: 683-686.

National Research Council. 1996. *The Bering Sea Ecosystem* . Washington, DC: The National Academies Press.

Neggers R, Siebesma P, Heus T. 2012. Continuous Single-Column Model Evaluation at a Permanent Meteorological Supersite. *Bulletin of the American Meteorological Society*, ***93***, 1389–1400. DOI:10.1175/BAMS-D-11-00162.1.

North Pacific Fishery Management Council (NPFMC). 2005. Fishery Management Plan for Groundfish of the Bering Sea and Aleutian Islands Management Area, Anchorage, Alaska.

Overland J, Wang M. 2007. Future Climate of the North Pacific Ocean. *Eos Trans. AGU*, **88**: 178–182. DOI:doi:10.1029/2007EO160003.

Overland J E, Alheit J, Bakun A, Hurrell J W, Mackas D L, Miller A J. 2010. Climate controls on marine ecosystems and fish populations. *Journal of Marine Systems*, **79**: 305-315. DOI: 10.1016/j.jmarsys.2008.12.009.

Pickart R, Moore W, Macdonald A, Renfrew I, Walsh J, and Kessler W. 2009. Seasonal Evolution of Aleutian Low Pressure Systems: Implications for the North Pacific Subpolar Circulation. *Journal of Physical Oceanography*, **39**: 1317-1339.

Reichler T, Kim J.2008. How Well do Coupled Models Simulate Today's Climate? *Bulletin of the American Meteorological Society,* **89**: 303-311.

Rodionov S, Bond N, Overland J. 2007. The Aleutian Low, storm tracks, and winter climate variablity in the Bering Sea. *Deep Sea Research Part II,* **54**: 2560-2577.

Stabeno P, Bond N, Kachel N, Salo S. 2001. On the temporal variability of the physical environment over the south-eastern Bering Sea. *Fisheries Oceanography*, **10**: 81–98. DOI:10.1046/j.1365-2419.2001.00157.

Stabeno P, Hunt G Jr, Napp J, Schumacher J. 2005. Physical forcing of ecosytem dynamics on the Bering Sea (Chapter 30). In The Sea: the global coastal ocean interdisciplinary regional studies and syntheses, Vol 14, Robinson AR, Brink K (eds). Harvard University Press: Cambridge,MA. ISBN: 0-674-01527-4.

Stabeno P, Farley E Jr, Kachel N, Moore S,Mordy C, Napp J, Overland J, Pinchuk A, Sigler M. 2012a. A comparison of the physics of the northern and southern shelves of the eastern Bering Sea and some implications for the ecosystem. Deep Sea Res. II Topical Stud. Oceanogr. 65–70: 14–30, DOI: 10.1016/j.dsr2.2012.02.019.

Stabeno P, Kachel N, Moore S, Napp J, Sigler M, Yamaguchi A, Zerbini A. 2012b. Comparison of warm and cold years on the southeastern Bering Sea shelf and some implications for the ecosystem. *Deep Sea Research Part II: Topical Studies in Oceanography*, **65**: 31–45. DOI:10.1016/j.dsr2.2012.02.020.

Stoner A, Hayhoe K, Wuebbles D. 2009. Assessing general circulation model simulations of atmospheric teleconnection patterns. J. Clim. 22:4348-4372. DOI: 10.1175/2009JCLI2577.1.

Strom S, Fredrickson K. 2008. Intense stratification leads to phytoplankton nutrient limitation and reduced microzooplankton grazing in the southeastern Bering Sea. *Deep Sea Research Part II: Topical Studies in Oceanography*, **55**: 1761–1774. DOI:10.1016/j.dsr2.2008.04.008.

Taylor K. 2001. Summarizing multiple aspects of model performance in a single diagram. *Journal of Geophysical Research*, **106**: 7183–7192. DOI:10.1029/2000JD900719.

Wang M, Overland J, Bond N. 2010. Climate projections for selected large marine ecosystems. *Journal of Marine Systems*, **79**: 258–266. DOI:10.1016/j.jmarsys.2008.11.028.

3 Primary production response to seasonal-scale extremes in the Bering Sea simulated by the Community Earth System Model, version 1[1]

3.1 Abstract

The biological response to long-term trends and the co-occurrence of seasonal extremes of the physical environment and primary production in the eastern Bering Sea, as simulated by the Community Earth System Model (CESM1), is presented. This analysis covers the late-twentieth century (1950-2005) and focuses on critical drivers of the eastern Bering Sea ecosystem, including air temperature, sea ice area, wind mixing, and mixed layer depth. Strong linear relationships between both air temperature and sea ice area and primary production during winter and spring were found. The only season that had a positive linear correspondence between wind mixing and primary production was summer. Over the fifty-five year period examined the CESM1 simulates a trend toward warmer air temperatures and a subsequent reduction in sea ice for every season; however, no trends were seen in seasonally averaged wind mixing or mixed layer depth. Corresponding to the air temperature increase over the time considered was an increase in occurrence of positive seasonal extremes in primary production, as well as a reduction in negative production extremes. There were several instances of seasonal production extremes coinciding with seasonal extremes in the physical environment; however, neither these co-occurrences, nor the direction of the biological response to the physics, were consistent throughout the study period.

[1]Walston J M, Gibson G A, Walsh J E. Primary Production Response to Seasonal-Scale Extremes in the Bering Sea Simulated by the Community Earth System Model, version 1. Submitted to the *Journal of Marine Systems*.

3.2 Introduction

Marginal seas in the Arctic and Subarctic are expected to be among the most affected by climate change, as slight changes in the water column can have large effects on physical and biophysical processes (Moran et al., 2012; Lomas et al., 2012). Increasing air temperature (Solomon et al., 2007), declining sea ice volume and extent (Markus et al., 2009), and large shifts in marine ecosystems (Grebmeier et al., 2006) are a few examples of environmental changes in the Arctic and Subarctic regions that are occurring at unprecedented rates. Variations in the physical environment that persist over several decades have been found to explain a substantial portion of biological production variability in the North Pacific Ocean (Beamish, 1993). However, shorter duration extremes on the order of weeks to months in the physical environment, often linked to large-scale modes of variability, can also result in substantial changes in the pelagic ecosystem structure of the marginal seas (Bond and Overland, 2005). Event-scale extremes and long-duration anomalies could potentially have a greater impact on ecosystems and humans than would gradual changes in climate means. Meanwhile, as climatic means change, one may expect the frequency of extremes to change as well, with corresponding impacts on the atmosphere, the ocean, and the biological spheres (Solomon et al., 2007; Stafford et al., 2010). Here we use the Community Earth System Model (CESM) to explore the impact of seasonal extremes in the physical environment, as well as their impact on primary production in the biologically rich marine ecosystem of the eastern Bering Sea.

Since the Arctic and Subarctic domains have been experiencing an increased rate of warming, high-latitude marine and terrestrial ecosystems may experience more stress than lower-latitude marine ecosystems (National Research Council, NRC, 1996). The effects of warming are most noticeable on summer and autumn Arctic sea-ice extent, with September 2012 extent showing a

new record low (Jeffries et al., 2012). Diminishing sea-ice cover and corresponding increased temperatures also have the potential to disrupt the current Arctic marine food web, as sea-ice dynamics drive Arctic Ocean primary productivity (NRC, 1996). While Arctic sea ice continues to decline, the Bering Sea of the Subarctic has actually been experiencing a slightly positive trend over the past 30 years, with a record maximum ice extent in March 2012 (Perovich et al., 2012). The Bering Sea is known to be a highly variable physical system, where the timing and extent of sea ice is crucial for determining the timing of spring biological production (Stabeno et al., 2001). The eastern Bering Sea's broad continental shelf and nutrient-rich currents make it one of the most biologically productive marine ecosystems (NRC, 1996, Loughlin et al., 1999). The ecosystem of the eastern Bering Sea supports both commercial and subsistence livelihoods, and its productivity accounts for more than half of the marine harvest in United States waters and nearly 25 million pounds of subsistence yield (Bering Sea Interagency Working Group, 2006). The eastern Bering Sea, however, is potentially susceptible to event-scale extremes, as well as long duration climate modes (notably, the Pacific Decadal Oscillation, or PDO; the Pacific North American pattern, or PNA; and the El Niño Southern Oscillation, or ENSO) that may alter primary production within the marine ecosystem and hence affect fishery and subsistence yield.

Global circulation models represent a useful tool to explore complex interactions across a range of timescales, from sub-daily to decadal. System models now include sophisticated functions describing ecosystem and biogeochemical processes, which influence carbon-nitrogen cycling, and are becoming more comprehensive and representative of an Earth System (Flato, 2011). These improvements allow a well-rounded diagnosis of climate processes and biophysical feedbacks. The Community Earth System Model version 1 (CESM1) is one such model. The CESM1 builds upon the Community Climate System Model version four (CCSM4) developed

by the National Center for Atmospheric of Research (NCAR) through the incorporation of a marine ecosystem model, interactive carbon-nitrogen cycling, terrestrial biogeochemistry, and atmospheric chemistry processes (Hurrell et al., 2013; Moore et al., 2013). A detailed description that expands upon the major improvements for each model component, in comparison to previous versions, is presented in Gent et al. (2011). Analysis of CCSM4 simulations by de Boer et al. (2012) and Walston et al. (2014) conducted in the Arctic and Subarctic domains, respectively, indicates suitable performance for simulating the climatological mean fields of high-latitude climate. Systematic errors in physical forcing variables, such as sea level pressure and geostrophic winds, as well as increased interannual variability centered over the Bering Sea, have been well documented (Walston et al., 2014).

3.3 Methods

Our study centers around analysis of the historical 20th-century run of the Biogeochemical Elemental Cycling (BEC) model, an ecosystem-biogeochemistry module that runs within the fully coupled ocean component (Parallel Ocean Program version 2, POP2) of the CESM1 (Moore et al., 2004, Smith et al., 2010). A detailed description of the BEC model can be found in Moore et al. (2013). The CESM POP2 is a level coordinate, primitive equation, ocean circulation model (Hurrell et al., 2013) with 60 vertical levels, including 20 in the upper 200 meters (Danabasoglu et al., 2012). The ocean model component has a displaced pole centered over Greenland (80°N, 40°W) in the Northern Hemisphere, with a horizontal grid consisting of 384 latitudes and 320 longitudes. The zonal resolution is approximately 1.11° while the meridional resolution varies from 0.27° at the equator to 0.65° north of 60°N (Gent et al., 2011). Parameterizations for the effects of mesoscale and sub-mesoscale eddies have been included to help re-stratify the ocean mixed layer (Danabasogu et al., 2008; Fox-Kemper et al., 2008; Gent et

al., 2011). Danabasoglu et al. (2012) has provided a detailed description and notable developments for the ocean circulation model relative to previous versions of the CCSM/CESM. The CESM-BEC marine ecosystem component is based on a nutrient-phytoplankton-zooplankton-detritus structure, which explicitly represents the distribution of biological components and their response to physical drivers. There are three phytoplankton functional groups simulated within the CESM-BEC: diatoms, diazotrophs, and small phytoplankton. While the BEC model has been described extensively in a number of previous papers (Moore et al., 2004; Doney et al., 2009), the CESM1 output on which our analysis is based represents the BEC's first public release (Moore et al., 2013).

A fifty-five-year record (1950 to 2005) of air temperature (an indication of sea surface temperature), wind mixing (as measured by cubed friction velocity $(u^*)^3$) over the shelf break, and sea ice area were examined for the occurrence of extreme seasons. These three features are considered key physical drivers and have been observed to fluctuate over intra-annual, interannual, and interdecadal timescales, impacting the marine ecosystem in the eastern Bering Sea over the same timescales. Each of these forces plays an important role in determining the mixed layer depth—the homogenous wind-mixed layer that develops seasonally in the Bering Sea. The depth of the mixed layer provides an indication of how well the water column is stratified and so controls the amount of nutrients and light to primary producers throughout the growing season. Thus, the mixed-layer depth can be regarded as a composite physical variable that can control primary production, so seasonal extremes in mixed layer depth were also considered in our analysis.

The northern and southern portions of the Bering Sea shelf differ in their physical, chemical, and biological oceanographic characteristics (Stabeno et al., 2012a), and as a result, the shelf was

subdivided into north and south domains at 60°N (Figure 3.1) for our analysis. The relationship between air temperature, sea ice area, and primary production was examined over two polygons that divided the eastern Bering Sea. The northern domain covers an area between 60°N-66°N and 174°E-160°W and consisted of 76 model grid points. The southern domain, covering an area between 52°N-60°N and 178°E-158°W, constituted 84 model grid points. To examine the relationship between wind mixing events and primary production, we analyzed wind mixing over the outer shelf between the 50-m and 3500-m isobaths, with a north-south divide at 60°N.

Simulated daily output was summated and/or averaged into seasonal bins for the entire fifty-five year record (1950 to 2005). Since the eastern Bering Sea is located in the Subarctic Pacific, seasons were defined for consistency with Subarctic Pacific temperatures and corresponding sea-ice growth/melt: January through March was defined as 'winter'; April through June was considered as 'spring'; July through September as 'summer'; and October through December was considered 'fall'.

Predictions of production by each phytoplankton group within the model were integrated vertically over the water column and were independently analyzed to determine contributions to total primary production in the eastern Bering Sea. The standardized seasonal and annual departures of total primary production from their 55-year climatological means were determined for both the northern and southern domains. Simulated forcing (air temperature, sea ice area, wind mixing, and mixed layer depth) was also averaged seasonally for the full fifty-five year record. Seasonal anomalies for each environmental forcing variable were calculated and expressed as the standardized departures from each seasonal mean for each respective domain. A simple linear regression model, using ordinary least squares, was used for estimating the correlation between seasonal primary production anomalies and seasonal forcing anomalies.

Linear regression was also used to identify any relationships between primary production and environmental forcing. A two-tailed t-test was used to determine statistical significance. An analysis of variance for linear models was conducted to compare the effect of seasonally averaged forcing on annual primary production in winter, spring, summer, and fall conditions for each north and south domain independently.

Episodic weather events on the order of days to weeks have been shown to influence primary production in the eastern Bering Sea (Napp and Hunt, 2001; Overland et al., 2001; Bond and Overland, 2005); however, we have defined extremes on seasonal and annual timescales in order to distinguish any simulated interannual associations between production and physical forcing. The statistical definition of an extreme is considered as any value of a continuous record that exceeds a statically determined threshold. Here, we define an extreme as any seasonal or annual anomaly that is greater (or less) than or equal to one-and-a-half times the standard deviation. This is less stringent than many definitions of extreme, though our definition results in a sufficient sample size for exploring a biological response to environmental forcing. Using this definition, all extremes for physical and production variables were identified, and the occurrence of extreme production seasons in both the north and south domains was compared to the timing of extreme environmental forcing seasons over the fifty-five year period under consideration.

3.4 Results

3.4.1 Primary production by size class

Relative contributions from the CESM1 autotrophic model components to simulated primary production in the eastern Bering Sea varied throughout the year. Total primary production (Figure 3.2a) shows strong seasonality induced by warming waters, retreating sea ice, and increased light availability occurring during spring and summer in high latitude seas. Small

phytoplankton production contributed approximately 45 percent of the total production from December to March, but contributed less than 20 percent of the total primary production during months of high productivity (June through November; Figure 3.2b). Diazotroph contribution to total production over the Bering Sea domain was negligible throughout the simulation period. Consequently, from here on out our discussion of 'total' primary production considers only small phytoplankton and diatoms. Simulated total annual primary production in the northern domain was consistently higher than in the southern domain. The CESM1 simulates an additional increase in total annual primary production and its interannual variability for the northern Bering Sea during the second half of the fifty-five year period examined, but a comparable trend was not seen in the southern domain (Figure 3.2c). Contributions from small phytoplankton to total annual production also varied from north to south; in the southern domain, smaller cells contributed 13-27% of the total production over an annual timescale, but in the northern domain, they contributed only 4-8% (Figure 3.2d).

3.4.2 Seasonal relationships between physical drivers and primary production

The strength and direction of the relationship between physical forcing and primary production simulated by the CESM1 varied by season. Although many of the correlations between seasonal physical forcing anomalies and seasonal primary production were not statistically significant, there were some notable relationships between physical forcing and production, in both the northern and southern domains of the Bering Sea. In the Northern Bering Sea, a significant and strong positive relationship ($r = 0.87$, $p < 0.05$) between winter air temperature anomalies and winter primary production anomalies (Figure 3.3a) and a strong, statistically significant, negative relationship ($r = -0.94$, $p < 0.05$) between winter sea ice area and winter production anomalies (Figure 3.3c) was evident. Spring temperature (Figure 3.3d)

and spring sea ice area anomalies (Figure 3.3f) had weaker, yet still statistically significant, correlations to spring total primary production anomalies ($r = 0.40$, and $r = -0.54$, respectively). Summer air temperature (Figure 3.3g) and sea ice area (Figure 3.3i) anomalies showed very little correlation to summer primary production, $r = -0.07$ and $r = 0.09$, respectively. Air temperature was also not notably correlated with primary production on a seasonal scale in fall (Figure 3.3j); fall sea ice area anomalies were weakly positively correlated ($r = 0.23$, Figure 3.3l) to fall production anomalies, although the relationship was not determined statistically significant. No relationship was found between anomalies of wind mixing and primary production in winter and fall (Figure 3.3b & k); wind mixing was weakly positively correlated to production in spring and summer, $r = 0.22$ and $r = 0.17$, respectively (Figure 3.3e and h), though neither of these relationships was significant.

Notable associations between seasonal primary production and environmental forcing were also evident in the southern domain, though some of these associations were opposite in direction to those seen in the northern domain. Similar to the northern domain, increases in winter air temperature or decreases in winter sea ice cover were significantly correlated to seasons with increased winter primary production (Figures 3.4a and c, respectively; Table 3.1). In contrast to the northern domain, spring primary production in the southern domain was negatively correlated ($r = -0.34$) with spring air temperature (Figure 3.4d) and was positively correlated ($r = 0.37$) with the amount of spring ice cover (Figure 3.4f); both relationships were statistically significant. Summer and fall temperature (Figure 3.4g and j) and sea ice area (Figure 3.4i and l) did not exhibit notable correlations or significant relationships to seasonal primary production. As was the case in the northern domain, wind mixing was most strongly correlated to primary production in summer ($r = 0.30$, Figure 3.4h) and this was the only seasonal scale

relationship between wind and primary production that could be deemed significant. Wind mixing was weakly positively correlated in fall (r = 0.14, Figure 3.4k), negatively correlated to winter primary production (r = -0.14, Figure 3.4b), and showed no notable correlation to spring primary production (Figure 3.4e).

The impact of seasonally averaged physical forcing on annual primary production simulated by the CESM1 varied by season, forcing variable, and region in the eastern Bering Sea (Table 3.1). In the northern Bering Sea, both winter and spring temperatures had a significant effect on total annual primary production (both with a $p < .05$). Simulated spring sea ice in the northern domain had the most statistically significant relationship to annual primary production ($p < .01$). Furthermore, spring wind mixing was also a significant physical forcing component for total annual primary productivity in the northern domain ($p < .05$). Although several seasonal forcing variables in the north had a statistically significant effect on annual primary production, analogous relationships were not found in the southern domain (Table 3.1). Summer air temperature had the only significant effect on annual primary production in the southern domain ($p < .05$). All other seasonally averaged environmental forcing had little or no statistical significance for annual primary production in the southern domain as simulated by the CESM1. These results suggest that environmental conditions during the early part of the year (winter and spring) have the most significant effect on annual primary production in the northern domain. Annual primary production in the southern domain shows generally weak association with seasonally averaged forcing. However, summer air temperature in the southern domain tends to be the most significant seasonally averaged forcing variable for annual primary production.

3.4.3 Annual and seasonal primary production extremes

Despite a positive correlation (r = 0.59) between annual primary production in the northern and southern Bering Sea (Figure 3.5), the timing of extremes of positive and negative primary production in these two domains did not necessarily coincide; nor were positive and negative production extremes evenly dispersed throughout the multiple decades examined. Over the fifty-five year record, a total of seven extremes in annual primary production were simulated, five of which were years with annual primary production above the extreme threshold; the remaining two were negative extremes (Figure 3.5a). Except for an extreme negative annual primary production in 1955, all extremes in total production were simulated after 1979 in the northern domain. A less discernable trend in total annual production was simulated in the southern domain (Figure 3.5b). However, years of extreme annual production were simulated in the later half of the evaluated period, similar to the north. A total of six extremes in total annual primary production were identified in the southern Bering Sea: three extremes were positive, and three extremes were negative. Extremes in seasonal primary production in the north followed a trend similar to extremes in annual production, with 15 out of 16 seasonal positive extremes all occurring in the latter half of the evaluated period. Negative seasonal production extremes were more irregular throughout the fifty-five year period evaluated and did not follow any clear trend. The CESM1 generated 28 seasonal extremes in the southern domain; 18 were positive extreme production seasons, the majority of which occurred in spring (five) and summer (six). In the southern domain, only four seasonal extremes in primary production occurred during annual extremes in primary production: three extreme high production seasons (summer 1986, summer 1993, and spring 2003) and one extreme low production season (fall 1973).

3.4.4 Relating extremes in primary production to the physical environment

Some seasonal primary production extremes coincided with extreme seasons of physical forcing, although this was frequently not the case. Systematic relationships were found more frequently between seasonal production extremes, seasonal air temperature, and sea ice extremes throughout the fifty-five year record.

3.4.4.1 Seasonal air temperature extremes

Coincident with the general positive air temperature trend that CESM1 predicted for every season over the time period examined, in the northern domain there was a shift from the occurrence of negative seasonal temperature extremes in the first few decades of the time series to positive seasonal temperature extremes throughout the latter couple of decades (Figure 3.6). Of the nine extreme winters in the northern Bering Sea, five were winters with a positive temperature extreme, all of which occurred after 1985 (Figure 3.6a), while the remaining four winters were classified as negative extremes—all four occurring prior to the 1970s. All five winters with positive air temperature extremes coincided with positive extreme winter primary production. While not all extreme cold winters were associated with extreme negative production, all simulated low winter production occurred during winters with below-average winter temperatures. The spring season had the fewest (six) air temperature extremes, all of which occurred after 1995. An extreme low production spring in 1977 coincided with extreme low air temperatures, and a second spring low production extreme in 1984 coincided with near-extreme low temperature. No pattern could be seen in the occurrence of spring positive production extremes and spring positive temperature extremes. Summers classified as extreme were not found to be associated with extreme summer production; however, all simulated positive production extremes occurred during summers with below average summer

temperatures (Figure 3.6c). The CESM1 did simulate extremes in air temperature during fall (Figure 3.6d), but there were no obvious connections between air temperature extremes and the timing of fall production extremes.

Similar to the northern domain, the CESM1 simulated a positive air temperature trend, with an absence of negative extremes in the later half of the 20th century in all seasons, in the southern domain (Figure 3.6e through h). Consistent with this feature, negative temperature extremes (cold seasons) occurred during the first half of the evaluated period, while positive temperature extremes (warm seasons) occurred in the latter two decades. The seasons classified as negative extremes (21 in total) occurred during the first half of the fifty-five year period, and represented nearly twice the amount classified as positive extremes (11 in total) occurring during the later portion of the time series. Four of the five winters classified as negative extremes (Figure 3.6e) corresponded to the timing of extreme negative winter primary production. And while there was little correspondence between spring extreme production (positive or negative) and springs with extreme temperature (positive or negative), below-average spring air temperatures coincided with four out of five positive extremes in spring production (Figure 3.6f). The CESM simulated several temperature and primary production extremes during the summer and fall seasons in the southern Bering Sea (Figure 3.6g and h); however, these seasonal extremes show little relation to the timing of positive or negative primary production extremes. For example, in the more recent past (1998), extreme warm temperatures in summer resulted in extreme negative production, while in the more distant past (1950 and 1967), extreme negative production for this season was the result of near negative extreme temperatures. Positive production extremes in summer and fall do not appear to coincide with negative or positive temperature extremes at any time over the time period examined.

3.4.4.2 Seasonal sea ice extremes

Coinciding with the simulated positive trend in air temperature across the eastern Bering Sea from 1950 to 2005, simulated sea ice area in the northern domain exhibited a steady decline in winter, spring, and fall (Figure 3.7a, b, d). Before 1970, summer in the northern domain was marked by some large positive ice extremes (Figure 3.7c), although standardized ice area anomalies correspond to smaller areal departures in summer than in winter, when actual ice area is much greater. Following the 1970s, summer sea ice was consistently below average; however, no negative extremes were simulated. CESM1 simulated six winters classified as negative extremes for sea ice area for the time period examined—all of which were in the latter two decades. All five positive extreme winter primary production events coincided with five out of six negative extreme winters. Conversely, above-average winter sea ice area results for the first few decades of our time series at near 'extreme' levels, coincided with negative extremes in winter primary production. Four out of six spring sea ice area extremes in the northern domain, all of which were positive, occurred during the earlier part of the record (Figure 3.7b). While above-average spring sea ice area coincided with all three negative spring primary production extremes, as was the case for winter, four out of five positive spring primary production extremes coincided with below-average sea ice area. A total of eight extremes (positive and negative combined) were simulated for fall sea ice area over the northern Bering Sea—more than any other season (Figure 3.7d). However, as was the case for summer, there was no obvious connection between the occurrence of extreme sea ice and extreme primary production during fall.

Prior to the 1970s, positive sea ice extremes—indicating more sea ice than average—occurred in all seasons in the southern Bering Sea (Figure 3.7e through 18h). Three winters with

above-average winter sea ice area in the southern domain coincided with three out of four negative winter primary production extremes (Figure 3.7e). There was a total of six springs with extremes in sea ice area, all of which were positive (Figure 3.7f). In contrast to the northern domain, three out of five spring positive primary production extremes occurred during positive extremes for spring sea ice area in the southern domain. No significant relationships were seen between sea ice extremes and primary production extremes during the summer and fall seasons (Figures 18g and 18h, respectively). For the remainder of the time series, following the 1970s, simulated sea ice area in the southern domain was near average, with no simulated positive extremes. There were no negative sea ice extremes in the southern domain throughout the fifty-five year record.

3.4.4.3 Seasonal wind mixing extremes

Unlike temperature and sea ice area, simulated seasonally averaged wind mixing (Figure 3.8) over the Bering Sea shelf oscillated fairly consistently about the mean over the fifty-five year period examined. Overall, systematic relationships between seasonal wind mixing and primary production in the northern Bering Sea were not discernable. With only six extremes (four positive extreme anomalies and two negative), winter wind mixing had the fewest extremes of all seasons in the northern Bering Sea (Figure 3.8a). Winter production extremes corresponded to periods of both above and below average wind mixing, with no connection to an extreme season of winter wind mixing. Simulated spring wind-mixing extremes were relatively frequent (ten extremes) in the northern Bering Sea (Figure 3.8b). Two of the five springs with extreme positive production were also seasons with extreme wind mixing (1986 and 2004), and a third positive spring production extreme (1979) corresponded to well above average wind mixing. The remaining two positive production extremes (1991 and 2003) occurred when spring wind mixing

was average. One of five negative spring mixing extremes (well below average wind mixing) coincided with extreme low spring production (1984), while the other four spring wind-mixing negative extremes did not coincide with extreme production in either direction. The two remaining extreme low productions in spring occurred when wind mixing was below, or close to, average levels. Summer (Figure 3.8c) had a total of eight simulated extremes: four positive and four negative wind-mixing extremes in the northern domain. Extreme positive summer production coincided with extreme positive wind mixing in 1991, though the remainder of summer extreme production in the north occurred when wind mixing was merely above (1986 and 1990) or below (1950 and 2003) average, and not extremely so. Eight wind-mixing extremes were also seen during the fall (five positive and three negative), but with only one positive extreme wind-mixing season (2001), coinciding with an extreme low season in primary production, and there was little overlap between these extremes and the timing of fall total primary production extremes over the fifty-five year period (Figure 3.8d).

Similar to the northern domain, extremes in wind mixing occurred multiple times in each of the four pertinent seasons throughout the 1950-2005 period, and correspondence between seasonal extremes of wind and extremes in primary production was not consistent. With only six wind-mixing extremes (Figure 3.8e), winter had the fewest seasonal extremes between all seasons. Four of these extremes were positive; two were negative. Both a negative (1965) and a positive extreme wind-mixing season (1967) coincided with extreme production, with the former corresponding to high production and the latter to low. The remaining winter wind-mixing extremes were not coincident with winter production extremes; however, the remainder of winter extreme production in the south occurred when wind mixing during winter was below average (1952, 1954, and 1955). As was the case in the northern domain, wind-mixing extremes were

more numerous in the spring than winter. There were more negative wind-mixing extremes (six) than there were positive (three) over the fifty-five year period. The timing of spring wind-mixing extremes did not overlap with spring primary production extremes. In the southern Bering Sea, summer had the greatest number (eleven) of wind-mixing extremes (Figure 3.8g). While the timing of wind friction velocity extremes did not coincide with the timing of summer total production extremes, the majority of positive total summer primary production extremes occurred in years with above-average summer wind speeds, while all negative summer total primary production extremes occurred during summers with below average wind mixing. The CESM1 simulated a total of seven fall seasons with extreme wind mixing: four positive and three negative. There were no apparent connections between fall wind-mixing extremes and the timing of fall total primary production extremes (Figure 3.8h).

3.4.4.4 Seasonal mixed layer depth

Seasonal mixed-layer depth can be thought of as a composite property of the oceanic surface zone that reflects the balance in the physical environment. Changes in air temperature and salinity due to the formation and melt of sea ice determine the density profile of the water column and act as a stabilizing force, while wind stress imparts energy on the water column and acts to mix the surface ocean. The aggregate effect of these opposing forces determines the depth of the homogeneous upper mixed layer, which by controlling access to nutrients and light, could play an important role in the amount of primary production in any given season.

While the correlation between summer mixed-layer depth and summer production was positive in both the northern and southern domains, the direction of the relationship between spring mixed-layer depth and spring primary production varied between north and south. The positive relationships in the northern Bering Sea in spring ($r = 0.41$, Figure 3.9a) and summer (r

= 0.54, Figure 3.9b) were both statistically significant ($p < 0.05$). Summer mixed-layer depth in the southern domain was also positively correlated to summer production (r = 0.50, Figure 3.9d), and the relationship between these two variables was significant. However, the southern domain spring mixed-layer depth (Figure 3.9c) was only weakly correlated (r = -0.23) to spring production, and the relationship was not statistically significant.

Similar to anomalies in seasonally averaged wind mixing, anomalies in seasonally averaged mixed-layer depth (Figures 20e-h) over the eastern Bering Sea shelf oscillated fairly consistently about the mean over the fifty-five year period examined. In the northern domain, a total of nine spring seasons were classified as having extreme mixed layer depth (Figure 3.9e), four of which were positive events (deeper than usual mixed layer), and the remaining five of which were negative extremes (shallower than usual mixed layer). Three of five positive spring primary production extremes were associated with positive mixed-layer depth extremes during spring (1979, 1986, and 2004). The remaining two positive spring primary production extremes did not show this correspondence; a spring positive production extreme in 1991 occurred during a spring with a below-average mixed layer depth, and the other spring positive production extreme in 2003, during an above-average spring mixed-layer depth. There were no spring negative primary production extremes that coincided with any of the five negative spring mixed-layer extremes. All three negative primary production extremes, however, did occur with average to below-average mixed-layer depth. Compared to spring, summer in the northern domain had fewer extremes (Figure 3.9f). A total of six extremes were simulated over the fifty-five year period: two positive extremes and four negative extremes. While all five summer positive primary production extremes corresponded to above-average mixed-layer depth, only one summer production extreme overlapped with a positive extreme for mixed-layer depth (1990). The four

summers of negative extreme mixed-layer depths did not correspond with summer negative primary production extremes.

In the southern domain, there were fewer spring mixed layer depth extremes, relative to the north, with only six extremes in total (Figure 3.9g). Three of the six extremes were positive and overlapped with neither positive nor negative spring primary production extremes. The remaining three springs were negative mixed-layer depth extremes, one of which corresponded with a positive spring primary production extreme (1967). A total of five positive spring primary production extremes were simulated by CESM1; three of these spring positive production extremes were during springs with below average mixed layer depths (1955, 1957, and 1967). The other two spring positive production extremes were during springs with above-average mixed-layer depths (1952 and 2003). In 1961, the CESM1 simulated a spring negative production extreme during a spring with an above-average mixed-layer depth. Similar to the north, the southern domain had six summers of extreme mixed-layer depth; two of these extreme summers were positive extremes, while the remaining extremes were negative (Figure 3.9h). One positive extreme mixed layer depth, in 2002, coincided with a summer positive production extreme, while three other summer positive production extremes occurred during above-average summer mixed-layer depths (1986, 1989, and 1991). However, the remaining summer positive production extremes occurred with below-average-to-average summer mixed-layer depths (1973 and 1974). While the four summers with extreme negative mixed-layer depths corresponded to neither positive nor negative summer primary production extremes, all three summer primary production extremes did occur during summers with below-average-to-average summer mixed layer depths (1950, 1967 and 1998).

3.5 Concluding discussion

To understand how primary production may respond to future climate change and extreme forcing events, we have examined the impact of seasonal-scale physical forcing toward seasonal and annual primary production over the Eastern Bering Sea, which is a highly productive region of commercial and cultural significance. Our investigation focused on air temperature, sea ice, and wind mixing: three key physical drivers of ecosystem dynamics known to both be highly variable and to impact the marine ecosystem of the eastern Bering Sea (Beamish et al., 1995; Mantua et al., 1997; Bond et al., 2003).

From 1955-2005, the CESM1 simulates a general warming trend (~1.5 °C) over both the northern and southern shelves of the Bering Sea. Over both domains, our analysis indicates this increase in air temperature occurring for every season over the fifty-five year record. This finding indicates that the model simulation is in broad agreement with observations, as a warming trend has been observed in the much of the Arctic and Subarctic regions, and some suggest that the Bering Sea is experiencing an earlier transition from winter to spring (Stabeno and Overland, 2001). However, the magnitude of the CESM1 warming trend is greater than seen in the NCEP/NCAR reanalysis data (Figure 3.10). The natural variability in the CESM1 simulation of air temperature may be result of the exaggerated warming trend seen in the model.

If the recent past, as simulated by the model, is indeed a precursor for the future, our analysis suggests that there will be a greater occurrence of positive seasonal extremes in air temperature as mean temperature increases. A distinct shift in seasonal air temperature extremes, from seasons of extreme negative air temperature anomalies to seasons of extreme positive air temperature anomalies, was exhibited around the 1970s for every season and for both domains of the Bering Sea. Certain modes of natural climate variability (i.e., Pacific Decadal Oscillation, or

PDO, and El Niño Southern Oscillation, or ENSO) are often linked to shifts in the physical environment in the North Pacific Ocean. In the real world, a well-documented shift of the Aleutian Low, the dominating atmospheric feature over the North Pacific, and increased sea surface temperatures had a major impact on the biota of the eastern Bering Sea pre and post 1976/77 (Beamish, 1993; Miller et al., 1994; Francis et al., 1998). Shorter-term shifts in sea surface temperature were also observed in 1997/98 (Napp and Hunt, 2001; Overland et al., 2001). However, as no interannual to decadal pattern in the occurrence of extremes is clear, we speculate that changes in the occurrence of seasonal extremes in the model simulation were more likely caused by the gradual increase in air temperature throughout the time series. Simulated air temperatures were trending towards cooler temperatures during the last few years of time series, implying a reversal to the warming trend. In reality, the Bering Sea has recently been experiencing prominent low-frequency variability, with several years of warm conditions (2001 to 2005) followed by several years of cold conditions (2007 to 2010), with the ecosystem responding differently to each prolonged period of warm (cold) years (Stabeno et al., 2012b).

Review of the CESM1 model simulation suggests that the environmental forcing most important to marine production in the eastern Bering Sea varies with season and domain. The strongest correlations between physical drivers and seasonal production were seen with air temperature and sea ice cover in winter and spring. This correlation is not strong, likely because the formation of sea ice in the eastern Bering Sea depends on the direction and the magnitude of winds, in addition to air temperature. Primary production in the north and south responded similarly to changes in these environmental variables during winter. Generally, an increase in winter air temperature and a reduction in sea ice cover resulted in increased winter production in both the northern and southern domains. The predicted increase in production may be of limited

consequence because production in both domains would be limited by the availability of light and cold temperatures, which slow metabolic processes at this time of the year.

In spring, production in the northern and southern domains responded in opposite directions to increasing temperature or reduced sea ice cover. Warm spring conditions with less sea ice cover in the north promoted above-average spring production, while in the south; above-average spring production coincided with colder springs and above-average sea ice cover. This dichotomy can be understood by noting that the northern Bering Sea, even in spring, is colder and shows more pervasive ice cover than the southern Bering Sea (Brown and Arrigo, 2013). The north is typically cold, with ice cover in early spring, and production at this time is usually in the form of ice edge blooms that occur as sea ice progressively retreats further north, stratifying the water with ice melt and increasing light availability (Niebauer et al., 1990). Warmer temperatures and a reduction in sea ice, as simulated in some years by the CESM1, will enhance this process. In contrast, sea ice cover in the southern Bering Sea exhibits strong year-to-year variability and does not occur every spring. In colder years, when there is greater ice cover, the spring bloom occurs as an ice associated bloom in early spring (Hunt et al., 2002). However, in warmer years when there is no ice cover, production is suppressed by wind-induced deep mixing, and blooms do not occur until the water column is thermally stratified later in the season (Hunt et al., 2002).

Summer wind mixing did appear to be the most important environmental forcing variable to summer production, as an increase in seasonally averaged wind mixing resulted in increased production, although this relationship was greater in the southern domain. Bond and Overland (2005) and Eisner et al. (2014, in press.) suggest that enhanced wind mixing during summer increases primary production in the southern Bering Sea, resulting from increased entrainment at

the base of the mixed layer, sustaining nutrients in the euphotic zone. By summer, thermal stratification is usually well established in the southern domain, and phytoplankton trapped in the upper mixed layer become nutrient limited. Any increase in wind during this time would result in an increase in nutrients, and thus an increase in production.

The relationship between physical extremes and primary production extremes was inconsistent. There did not appear to be a strong correspondence between seasons of extreme forcing and seasons of extreme production as simulated by the CESM1. The lack of correspondence was especially notable during the spring and summer seasons, when production is at a maximum. Winter production did generally coincide with positive extreme temperatures in the northern domain, though winter production is low, and winter production extremes did not generally result in extreme annual production.

The results discussed above may be interpreted in terms of upper ocean stratification and mixed-layer depth. Stratification is initially beneficial to phytoplankton by confining their vertical position to the euphotic zone, allowing access to a sufficient amount of light and nutrients. As such, primary production is more likely to be determined by the intensity of water column stratification rather than any one environmental forcing variable. Over the eastern Bering Sea shelf, the depth of the upper mixed layer is dependent on the stratifying forces of temperature and salinity gradients (due to seasonal heating and ice melt) and by wind-induced mixing. Although not a consistent relationship, we did find a correspondence between simulated extremes in mixed-layer depth and production. In the northern domain, above-average-to-extreme mixed layer depths (deep upper mixed layer) during spring and summer were associated with extreme spring and summer primary production. A similar conclusion was found during the summer in the southern domain; however, positive extreme spring production in the southern

domain favored below-average-to-extreme mixed layer depths (shallow upper mixed layer). The lack of strong correspondence between seasonal mixed-layer extremes and extreme production suggest that a seasonal time resolution may be insufficient for capturing the importance of nutrient entrainment and the rate at which these vertically-mixed nutrients are consumed by biological production.

The importance of seasonal extremes in physical forcing for seasonal and annual production may be underestimated, as certain characteristics of physical drivers may not be represented on a seasonal scale. Water column temperature controls both physical and biological processes and is directly influenced by air temperature. Given the ocean's large heat capacity (Solomon et al., 2007), air temperature extremes over a daily time scale would not be sufficient to warm or cool the water column to have significantly impact on ocean processes. Because of the relatively slow response time of the water column to air temperature, a longer-timescale approach to examining the relationship between air temperature and production is arguably a more appropriate timescale for examining air-sea interaction and the impacts of extreme seasonal heating or cooling on production. Similarly, sea ice formation and retreat can take several months, and seasonal averages for ice cover can capture sea ice dynamics on a timescale important for marine ecosystems. However, it is also important to note that external forces (i.e., wind speed and direction) with influence on sea ice processes can affect the formation and retreat of sea ice over shorter time scales, on the order of days to weeks (Kimura and Wakatsuchi, 2000). Hence, while examining seasonal sea ice extremes and their impact on production is a good first approach, sea ice extremes that vary over shorter timescales may lead to a better understanding of how sea ice extremes impact primary production in the eastern Bering Sea.

The velocity and direction of wind can vary over very short timescales. Wind-mixing events are a result of low-pressure systems crossing the Bering Sea, lasting on the order of a few days to weeks. One can speculate that wind-mixing events would be better represented on a similar time scale. Stabeno et al. (2010) showed that increasing wind strength due to the passing of storms increased primary production, although the impact was dependent on the amount of stratification. Thus, although our results show that wind mixing has a significant impact on production on a seasonal timescale, especially during summer in the southern domain, we may underrepresent this relationship, since the reaction of primary production to event-scale wind mixing (storms) may be not be captured. Stabeno et al. (2010) do suggest a lag time between a wind-mixing event and any increase in new production, though this lag in production is still on the order of days. Such a lag means the production response is not instantaneous and highlights the need to consider the production response over timescales greater than days. Thus, although a three-month seasonal average may underestimate the strength of the relationship between wind events and primary production, a daily timescale is likely too short.

Seasons of extreme production may provide sufficient amounts of energy to increase the chances of species survival in upper trophic levels of the food web, especially during years considered average for production. Simulated seasonal extremes from the CESM1 did not always occur during years of annual production extremes. In high-latitude seas, spring and summer are the largest contributors to primary production, as light and temperature are no longer limiting factors (NRC). Our findings indicate that in both the northern and southern east Bering Sea, positive spring and summer production extremes contribute to positive annual primary production extremes more often than for other seasons. However, the majority of seasonal production extremes occurred during a year when annual production was not at extreme levels.

For example, four out of five spring production extremes in the southern domain occurred during annual production below the extreme threshold.

Despite the lack of correspondence between seasonal extremes and annual extremes (be they positive or negative), extreme production events at any time of year may have important implications for food web dynamics. While total annual primary production is important for the overall productivity of an ecosystem, the timing of primary production can influence which habitat (benthic or pelagic) is the recipient of the newly generated carbon (energy) source (Grebmeier et al., 2006; Hunt et al., 2002, 2011) and can thus alter the structure of the Bering Sea food web. In addition, production extremes may be important at any time of the year, especially during seasons with little contribution to total annual production. Extreme positive production in summer, fall, or winter, for example, may provide an energy source for higher trophic levels (zooplankton and then fish) during a critical time, having a positive impact on their annual production. Therefore, it is important to understand not only how annual production may be impacted by climate change, but also to understand how the occurrence of seasonal production extremes will change, as seasonal production extremes may have the potential to significantly influence the entire marine food web of the eastern Bering Sea.

In summary, the timing and impact of extreme seasonal forcing on primary production simulated by the CESM1 for a fifty-five year period (1950-2005) over the Bering Sea was explored. Results have shown that relationships between simulated extremes are physically and biologically plausible, although simulated seasonal extremes of the physical environment did not always correspond to seasonal primary production extremes. Our results suggest that a seasonal approach to certain key physical drivers (air temperature and, to a certain extent, sea ice area) is suitable for examining the response of biological production, but that the seasonal resolution may

not capture some important characteristics of other principal physical drivers (wind mixing and mixed-layer depth).

3.6 Acknowledgments

This work was funded by the Arctic Program of the National Science Foundation under award #1049225. The CESM1 model output was provided by the National Centers of Atmospheric Research and distributed via the Earth System Grid (ESG). The NOAA/OAR/ESRL Physical Science Division provided the NCEP/NCAR reanalysis data.

Figures

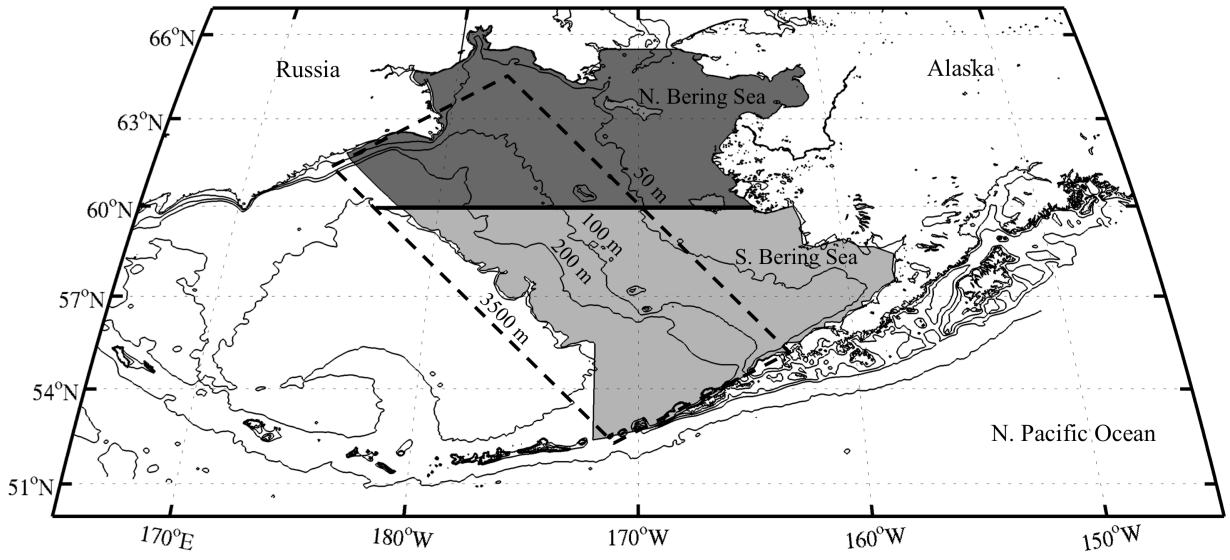

Figure 3.1. Geographical reference of the Bering Sea. The Bering Sea is subdivided into regional polygons at 60°N to define the northern (above 60°N, dark grey) and southern (below 60°N, light grey) domains. Air temperature, sea ice area, mixed layer depth and primary production in its northern domain spans an area between 60°N-66°N and 174°E-160°W, and covers an area between 52°N -59°N and 178°E-158°W in its southern domain. The dashed lines indicate the two wind mixing domains considered; these domains cover an area approximately between the 50-m and 3500-m isobaths with a division at 60°N.

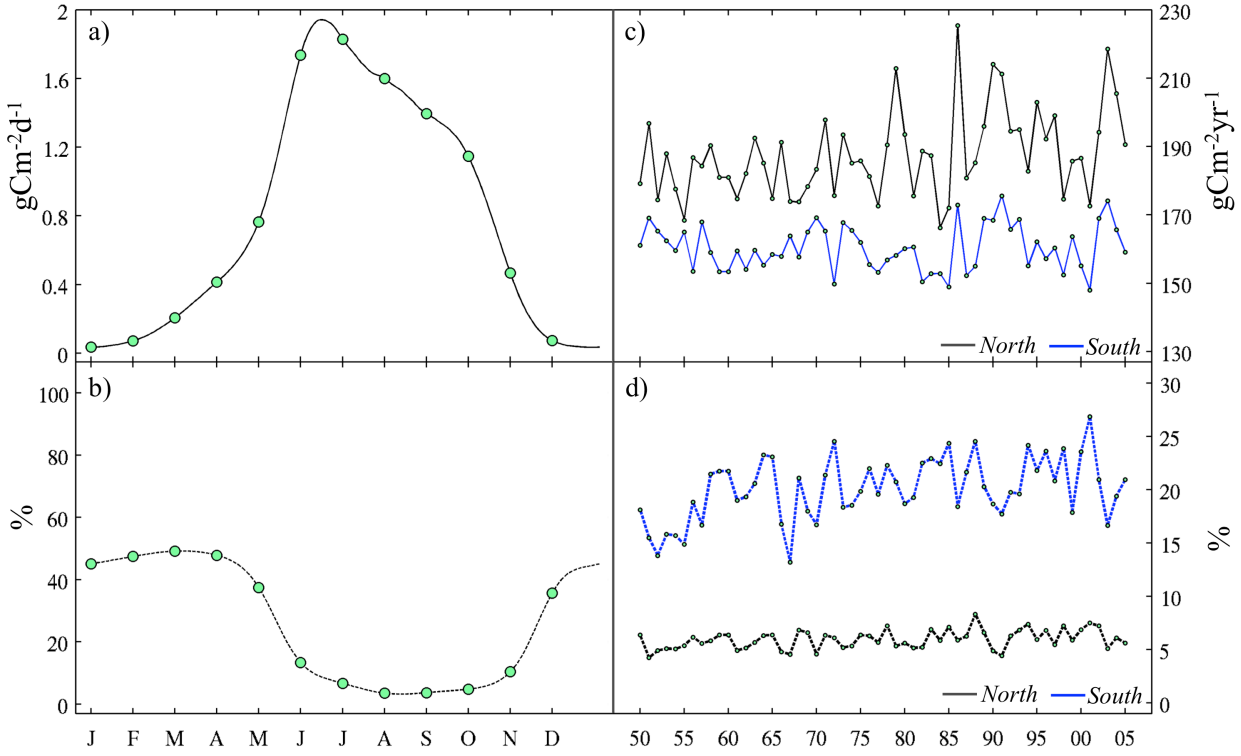

Figure 3.2. Climatological (1950-2005) primary production. Climatological seasonal cycle of daily primary production (a) over both domains of the eastern Bering Sea, with percent of contribution of small phytoplankton (b) simulated by the CESM1 from 1950 to 2005. A comparison of annual primary production estimates simulated by the CESM1 for the 55-year period for the northern and southern domains (c), with percent of contribution of small phytoplankton to the total annual production in both domains (d).

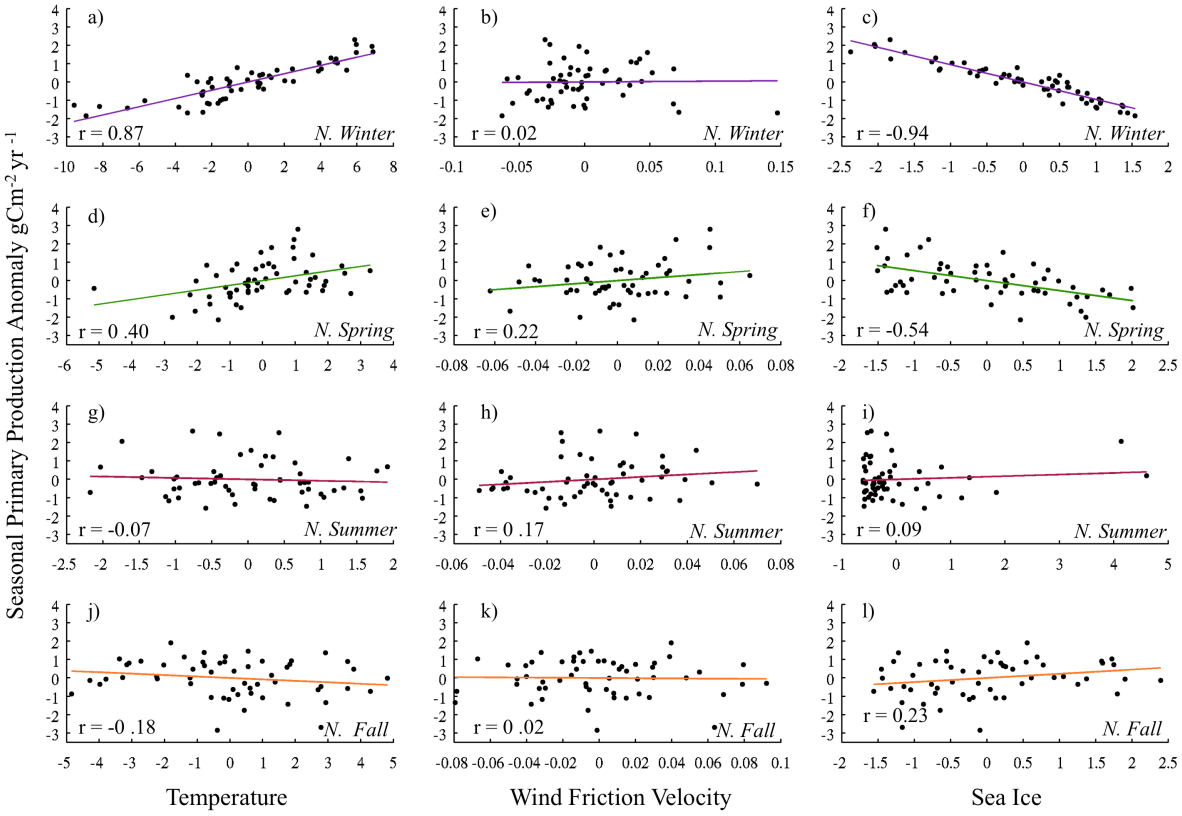

Figure 3.3. Northern Bering Sea linear regression analysis. Simulated relationships between CESM1 (1950-2005) seasonal primary production anomalies and seasonal air temperature (left), wind friction velocity (center), and sea ice area (right) anomalies in the northern Bering Sea. Panels represent a linear regression analysis via the least squares method for each season: winter (purple), spring (green), summer (red), and fall (orange).

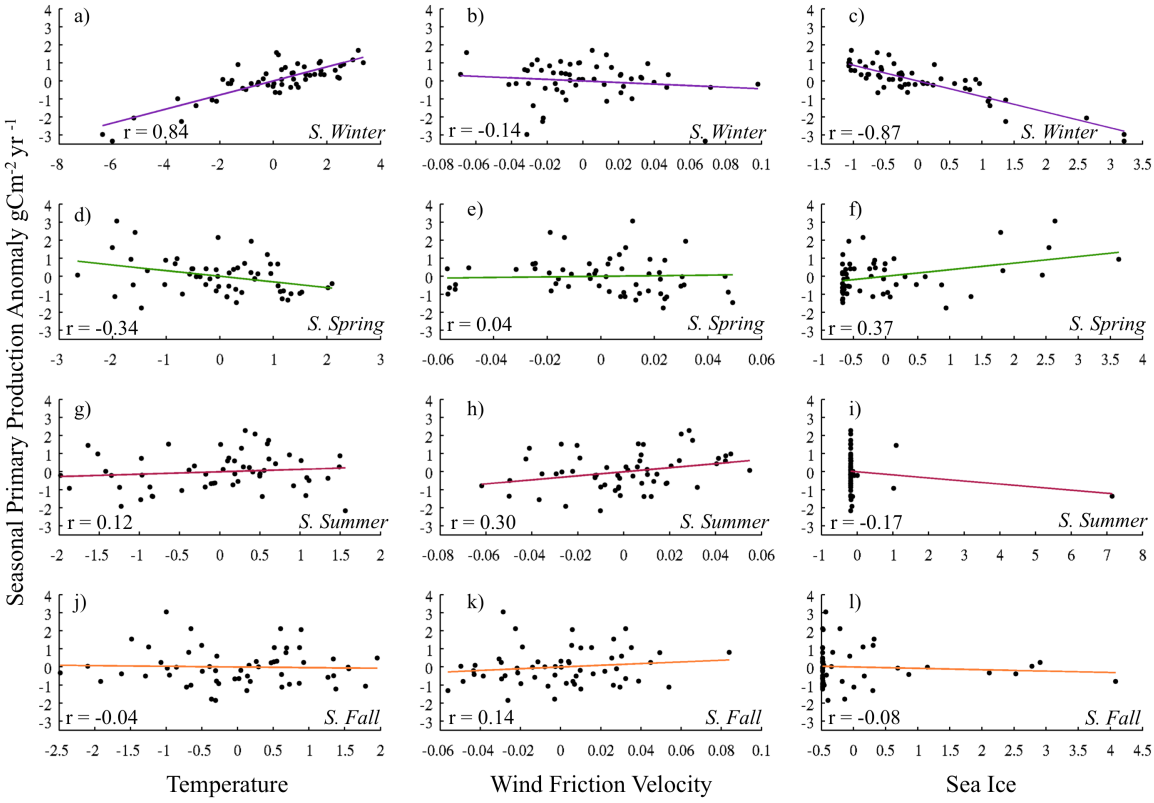

Figure 3.4. Southern Bering Sea linear regression analysis. Simulated relationships between CESM1 (1950-2005) seasonal primary production anomalies and seasonal air temperature (left), wind friction velocity (center), and sea ice area (right) anomalies in the southern Bering Sea. Panels represent a linear regression analysis via the least squares method for each season: winter (purple), spring (green), summer (red), and fall (orange).

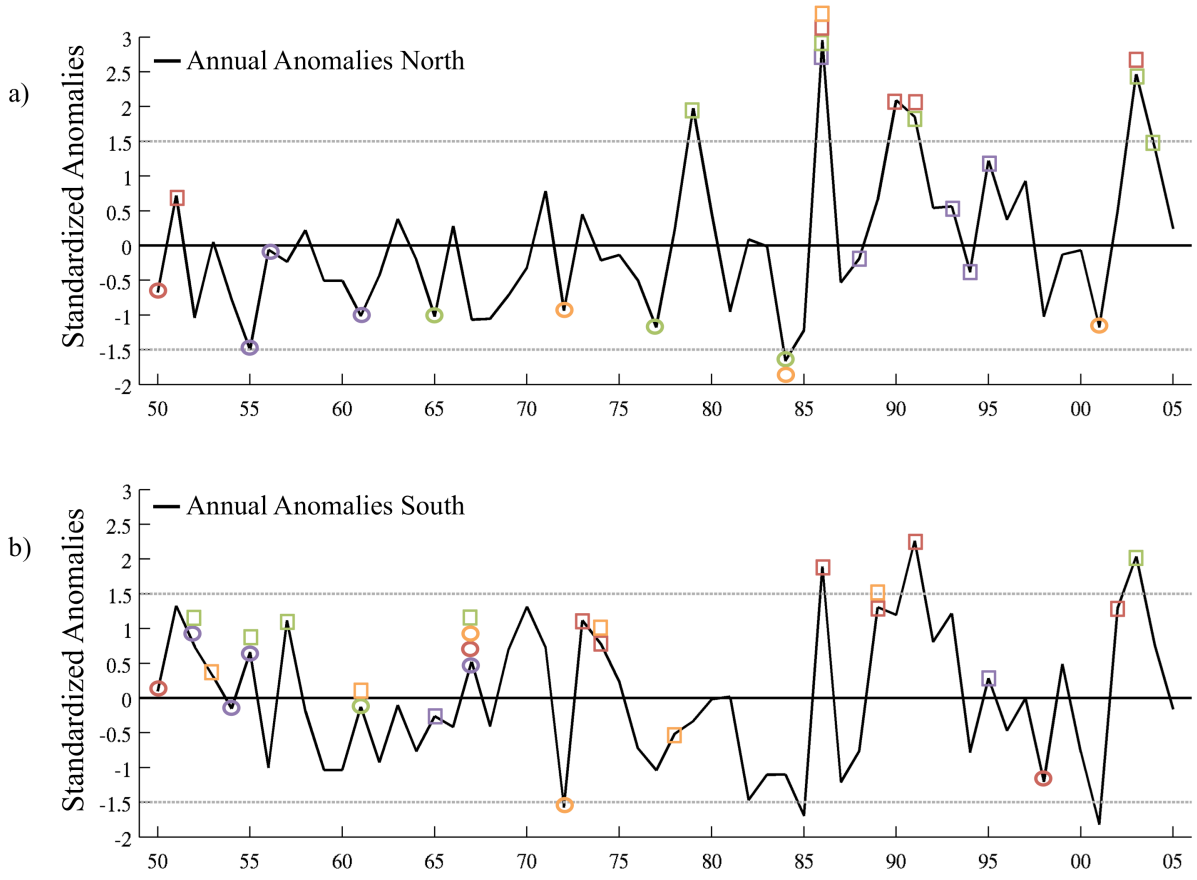

Figure 3.5. Annual primary production anomalies and seasonal primary production extremes. Standardized annual primary production anomalies for both the northern (a) and southern (b) domains of the Bering Sea with and seasonal primary production extremes above and below the extreme threshold simulated by the CESM from 1950 to 2005. Extremes are defined as a year or season greater (less) than or equal to 1.5 times the standard deviation from the annual or seasonal average. A grey dashed line indicates 1.5 times the standard deviation from the annual mean. Seasons above (below) the extreme threshold are labeled with squares (circles) and colored by season: winter is purple, spring is green, summer is red, and fall is orange.

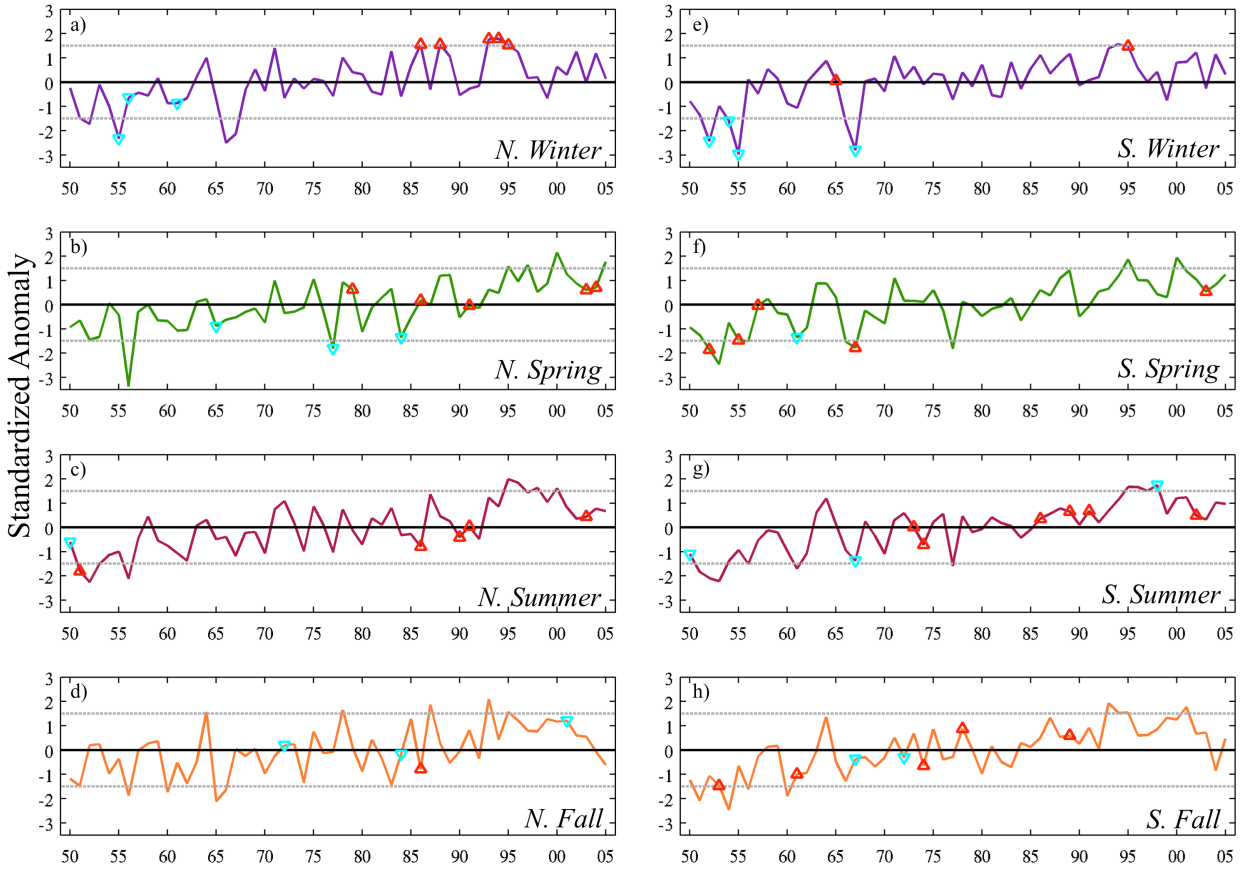

Figure 3.6. Air temperature anomalies and extremes by season. Air temperature anomalies by season (winter: purple, spring: green, summer: red, and fall: orange) with a comparison of seasonal temperature extremes and seasonal primary production extremes for both the northern (left) and southern (right) Bering Sea simulated by the CESM from 1950 to 2005. Extreme production years are marked as red (extreme positive) and cyan (extreme negative) triangles. A grey dashed line indicates 1.5 times the standard deviation from the seasonal mean.

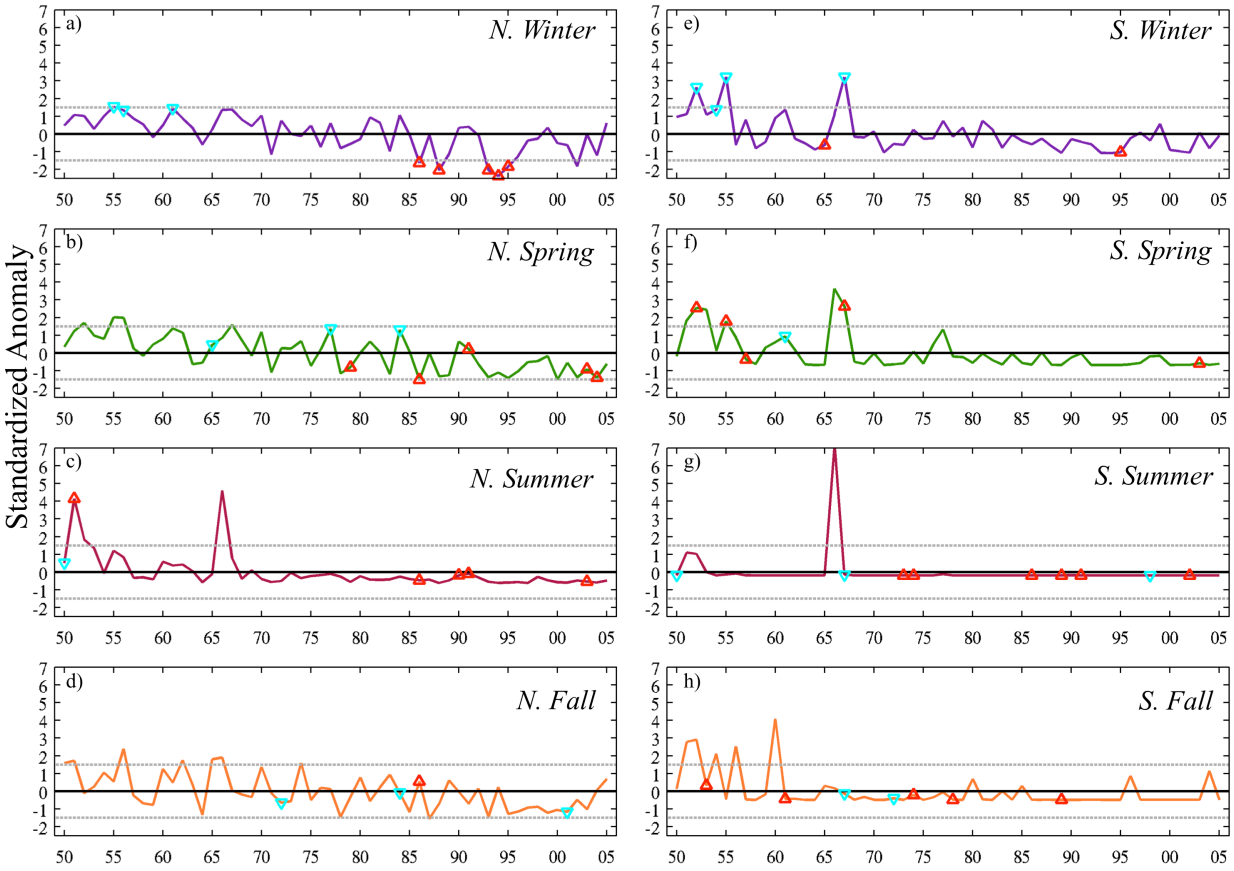

Figure 3.7. Sea ice area anomalies and extremes by season. Sea ice area anomalies by season (winter: purple, spring: green, summer: red, and fall: orange) with a comparison of seasonal sea ice area and seasonal primary production extremes for both the northern (left) and southern (right) Bering Sea simulated by the CESM from 1950 to 2005. Extreme production years are marked as red (extreme positive) and cyan (extreme negative) triangles. A grey dashed line indicates 1.5 times the standard deviation from the seasonal mean.

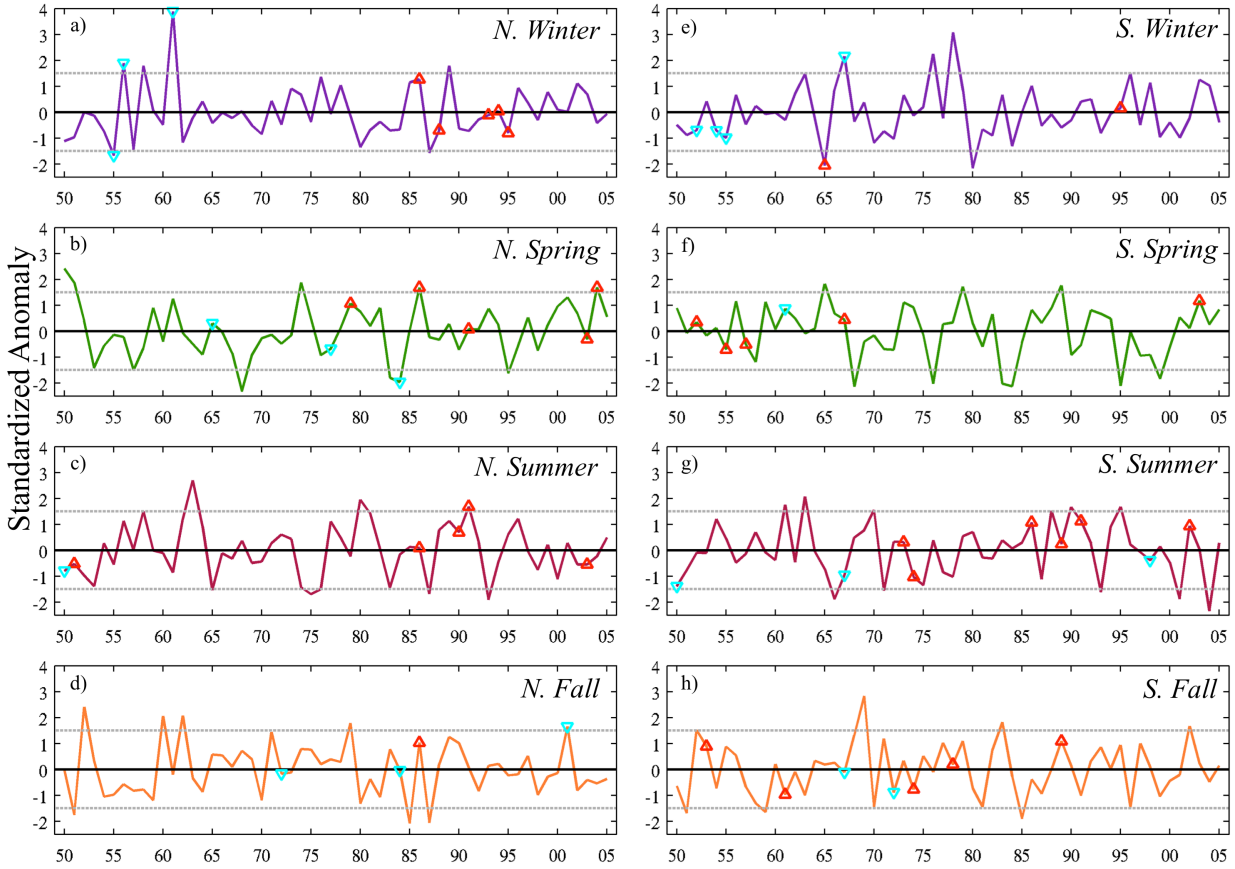

Figure 3.8. Wind friction anomalies and extremes by season. Wind friction velocity anomalies by season (winter: purple, spring: green, summer: red, and fall: orange) with a comparison of seasonal wind friction velocity and seasonal primary production extremes for both the northern (left) and southern (right) Bering Sea simulated by the CESM from 1950 to 2005. Extreme production seasons are marked as red (extreme positive) and cyan (extreme negative) triangles. A grey dashed line indicates 1.5 times the standard deviation from the seasonal mean.

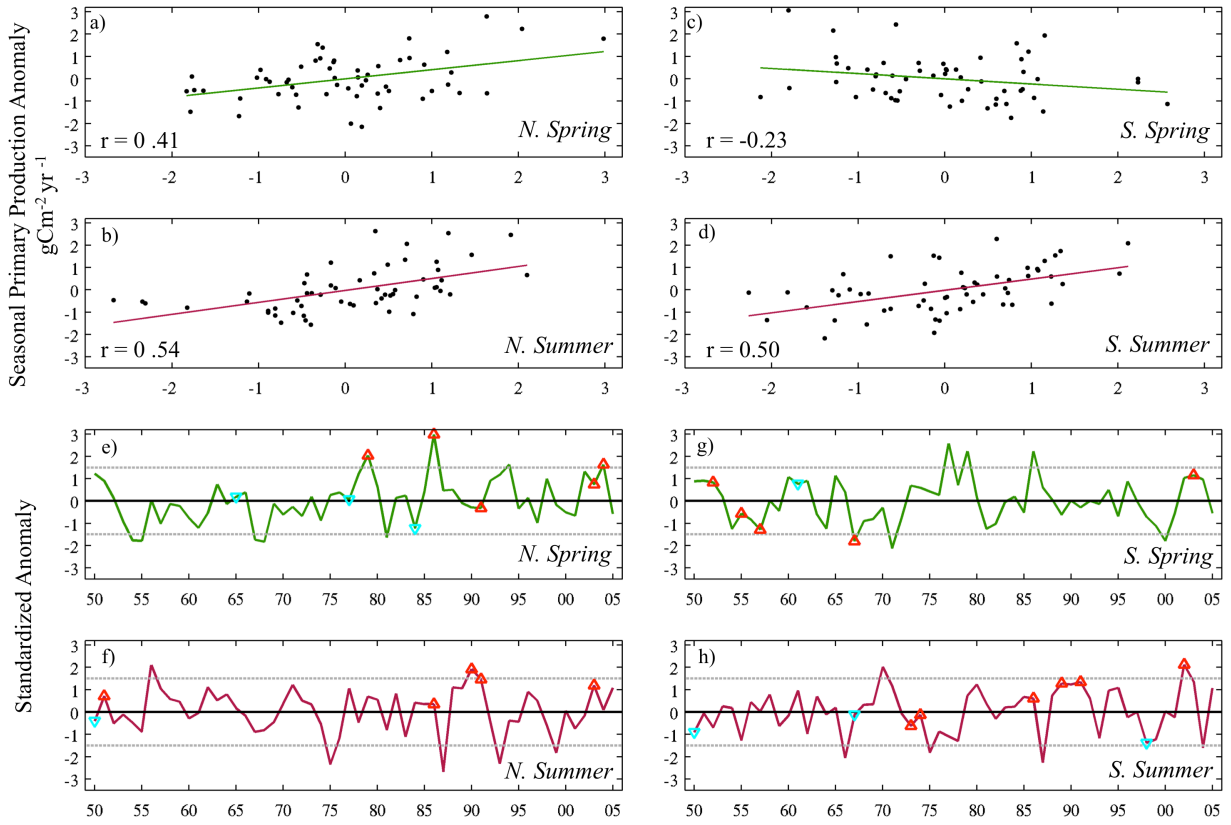

Figure 3.9. Spring and summer analysis of mixed layer depth. Simulated relationships between CESM1 (1950-2005) spring (a) and summer (b) mixed layer depth anomalies and seasonal primary production anomalies in the northern Bering Sea; similarly, for the southern Bering Sea spring (c) and summer (d). Relationships were determined by linear regression analysis via the least squares method. And spring (green line) and summer (red line) mixed layer depth anomalies in comparison to seasonal primary production extremes for both the northern (e and f) and southern (g and h) domains. Extreme production seasons are marked as red (extreme positive) and cyan (extreme negative) triangles. A grey dashed line indicates 1.5 times the standard deviation from the seasonal mean.

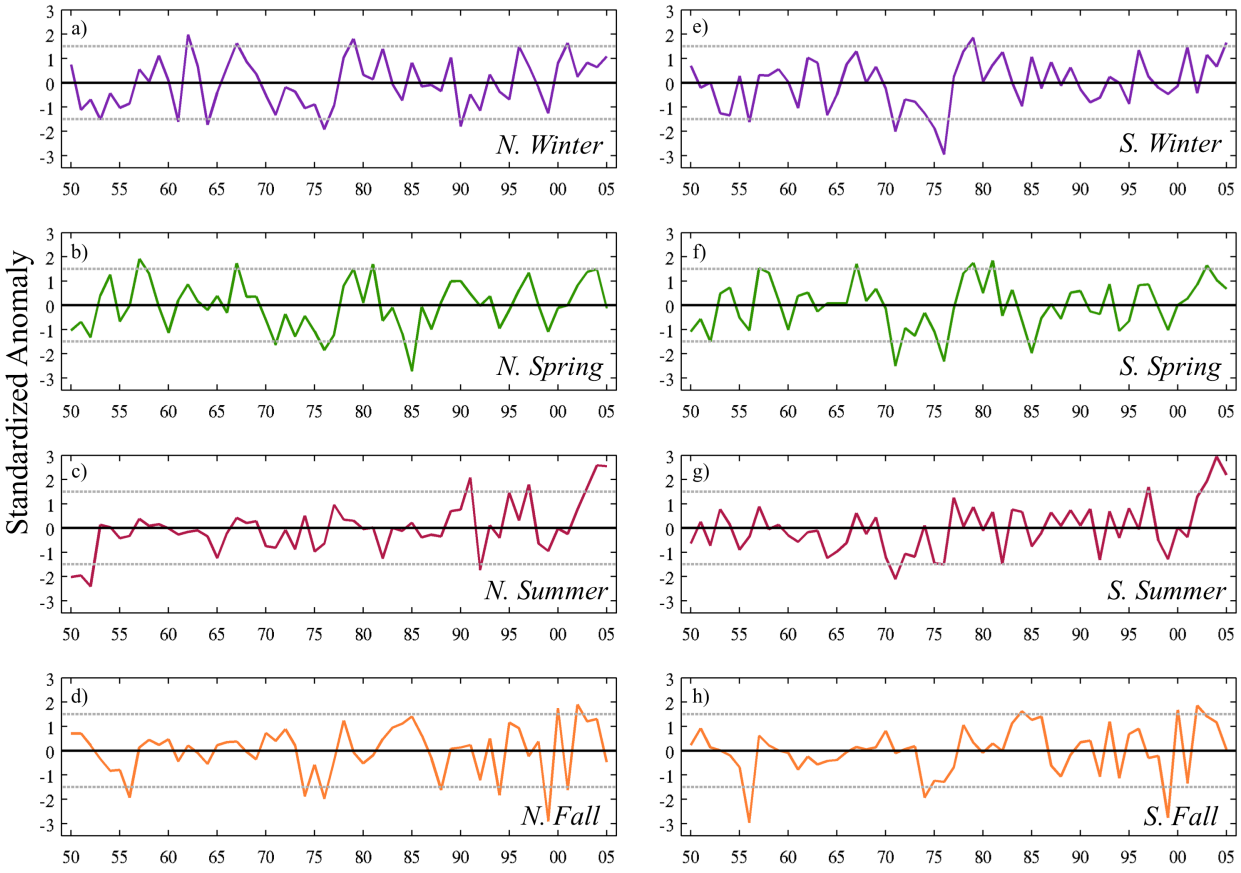

Figure 3.10. NCEP/NCAR reanalysis air temperature anomalies. NCEP/NCAR reanalysis air temperature anomalies from 1950 to 2005 by season (winter: purple, spring: green, summer: red, and fall: orange) for both the northern (left) and southern (right) Bering Sea. A grey dashed line indicates 1.5 times the standard deviation from the seasonal mean.

Table

Table 3.1. Analysis of variance (ANOVA). Analysis of variance (ANOVA) of multiple linear regression models representing a least squares fit for seasonally averaged forcing anomalies (air temperature, wind friction velocity, and sea ice area) and annual primary production anomalies for the northern (left) and southern (right) Bering Sea. The table presents the critical values for an *F*-distribution and corresponding *p*-values.

Table 1. Analysis of Variance (ANOVA)

	North		South	
Temperature	**F stat**	**pValue**	**F stat**	**pValue**
Winter	5.676	0.021	0.599	0.442
Spring	4.364	0.041	2.492	0.121
Summer	1.712	0.197	4.1	0.048
Fall	0.455	0.503	1.54	0.22
Sea Ice Area				
Winter	0.057	0.811	1.395	0.243
Spring	10.454	0.0021	0.396	0.532
Summer	1.866	0.177	0.064	0.801
Fall	1.282	0.263	0.316	0.577
Wind Friction Veleocity				
Winter	0.17	0.682	0.025	0.876
Spring	3.866	0.055	1.532	0.222
Summer	2.845	0.097	2.284	0.137
Fall	0.815	0.371	0.595	0.444

References

Beamish R J. 1993. Climate and exceptional fish production off the west coast of North America.*Canadian Journal of Fisheries and Aquatic Sciences* **50**: 2270-2291.

Beamish R J (ed.). 1995. Climate change and northern fish populations. Canadian Special Publication of Fisheries Aquatic Sciences **121**. 739 pp.

Bering Sea Interagency Working Group. 2006. Climate change and the Bering Sea ecosystem: an integrated, interagency-multi-institutional approach. AFSC Processed Report, 2006-01. Alaska Fisheries Science Center, National Marine Fisheries Service, NOAA: Seattle, WA, 30 pp.

Bond N A, Overland J E. 2005. The importance of episodic weather events to the ecosystem of the Bering Sea shelf. *Fisheries Oceanography* **14(**2), 97–111.

Bond N A, Overland J E, Spillane M., Stabeno P. 2003. Recent shifts in the state of the North Pacific. *Geophysical Research Letters* **30**(23): 2183. DOI:10.1029/2003GL018597.

Brown Z W, Arrigo K R. 2013. Sea ice impacts on spring bloom dynamics and net primary production in the Eastern Bering Sea. *Journal of Geophysical Research* **118**, 1–20. DOI:10.1029/2012JC008034.

Danabasoglu G, Yeager S G, Kwon Y O, Tribbia J J, Phillips A S, Hurrell J W. 2012. Variability of the Atlantic Meridional Overturning Circulation in CCSM4. *Journal of Climate* **25**(15): 5153–5172. DOI:10.1175/JCLI-D-11-00463.1.

De Boer G, Chapman W, Kay J E, Medeiros B, Shupe M D, Vavrus S, Walsh J. 2012. A Characterization of the Present-Day Arctic Atmosphere in CCSM4. *Journal of Climate* **25**(8): 2676–2695. DOI:10.1175/JCLI-D-11-00228.1.

Doney S C, Lima I, Moore J K, Lindsay K, Behrenfeld M J, Westberry T K, Mahowald N, Glover D, Takahashi T. 2009. Skill metrics for confronting global upper ocean ecosystem-biogeochemistry models against field and remote sensing data. *Journal of Marine Systems*, **76**: 95–112. DOI: 10.1016/j.jmarsys.2008.05.015.

Flato G M. 2011. Earth system models: an overview. *Wiley Interdisciplinary Reviews: Climate Change* **2**(6): 783–800. DOI:10.1002/wcc.148.

Fox-Kemper, B., R. Ferrari, and R. Hallberg, 2008: Parameteri- zation of mixed layer eddies. Part I: Theory and diagnosis. J. Phys. Oceanography **38**: 1145–1165.

Francis R C, Hare S R, Hollowed A B, Warren S. 1998. Effects of interdecadal climate variability on the oceanic ecosystems of the NE Pacific. *Fisheries Oceanography*, **7**(1): 1–21.

Gent P, Danabasoglu G, Donner L, Holland M, Hunke E, Jayne S, Lawrence D, Neale R, Rasch P, Vertenstein M, Worley P, Yang Z, ZhangM. 2011. The Community Climate SystemModel version 4. J. Clim. 24: 4973–4991, DOI: 10.1175/2011JCLI4083.1.

Grebmeier J, Overland J, Moore S, Farley E, Carmack E, Cooper L, Frey K, Helle J, McLaughlin F, McNutt S. 2006. A major ecosystem shift in the northern Bering Sea. Science 311: 1461–1464, DOI: 10.1126/ science.1121365.

Hunt G L, Coyle K O, Eisner L B, Farley E V, Heintz R A, Mueter F, Stabeno P. 2011. Climate impacts on eastern Bering Sea foodwebs: a synthesis of new data and an assessment of the Oscillating Control Hypothesis. *ICES Journal of Marine Science*, **68**(6): 1230–1243. DOI:10.1093/icesjms/fsr036.

Hunt G L, Stabeno P, Walters G, Sinclair E, Brodeur R D, Napp J M, Bond N A. 2002. Climate change and control of the southeastern Bering Sea pelagic ecosystem. *Deep Sea Research Part II: Topical Studies in Oceanography*, **49**(26): 5821–5853.

Hurrell J W, Holland M M, Gent P R, Ghan S, Kay J E, Kushner P J, Marshall S. 2013. The Community Earth System Model: A Framework for Collaborative Research. *Bulletin of the American Meteorological Society* **94**(9): 1339–1360. DOI:10.1175/BAMS-D-12-00121.1.

Jeffries M O, Richter-Menge J A, Overland J E (eds). 2013: Arctic Report Card 2013, http://www.arctic.noaa.gov/reportcard.

Kimura N, Wakatsuchi M. 2000. Relationship between sea-ice motion and geostrophic wind in the Northern Hemisphere. *Geophysical Research Letters*, **27**(22): 3735–3738. DOI:10.1029/2000GL011495.

Loughlin T, Sukhanova I, Sinclair E. 1999. Summary of Biological and Ecosystem Dynamics in the Bering Sea. Chapter 19 in Dynamics of the Bering Sea, Loughlin T, Ohtani K. (eds). Unniversity of Alaska Sea Grant, Ak-SG-99-03, Fairbanks. 838 pp. ISBN 1-56612-062-4.

Lomas M W, Moran S B, Casey J R, Bell D W, Tiahlo M, Whitefield J, Kelly R P, Mathis J T, Cokelet E D. 2012. Spatial and seasonal variability of primary production on the Eastern Bering Sea shelf. *Deep Sea Research Part II: Topical Studies in Oceanography* **65**(70): 126–140. DOI:10.1016/j.dsr2.2012.02.010.

Mantua N J, Hare S R, Zhang Y, Wallace J M, Francis R C. 1997. A Pacific Interdecadal Climate Oscillation with Impacts on Salmon Production. *Bulletin of the American Meteorological Society* **78**(6): 1069–1079.

Markus T, Stroeve J C, Miller J. 2009. Recent changes in Arctic sea ice melt onset, freezeup, and melt season length. *Journal of Geophysical Research* **114**(C12024). DOI:10.1029/2009JC005436.

Miller A J, Cayan D R, Barnett T P, Graham N E, Oberhuber J F. 1994. The 1976-77 Climate Shift if the Pacific Ocean. Oceanography **7**: 21–26.

Moore J K, Doney S C, Lindsay K. 2004. Upper ocean ecosystem dynamics and iron cycling in a global three-dimensional model. *Global Biogeochemical Cycles* **18**(GB4028). DOI:10.1029/2004GB002220.

Moore J K, Lindsay K, Doney S C, Long M C, Misumi K. 2013. Marine Ecosystem Dynamics and Biogeochemical Cycling in the Community Earth System Model [CESM1(BGC)]: Comparison of the 1990s with the 2090s under the RCP4.5 and RCP8.5 Scenarios. *Journal of Climate* **26**(23): 9291–9312. DOI:10.1175/JCLI-D-12-00566.1.

Moran S B, Lomas M W, Kelly R P, Gradinger R, Iken K, Mathis J T. 2012. Seasonal succession of net primary productivity, particulate organic carbon export, and autotrophic community composition in the eastern Bering Sea. *Deep Sea Research Part II: Topical Studies in Oceanography* **65–70**: 84–97. DOI:10.1016/j.dsr2.2012.02.011.

Napp J M, Hunt G L. 2001. Anomalous conditions in the south-eastern Bering Sea 1997: linkages among climate, weather, ocean, and Biology. *Fisheries Oceanography* **10**(1): 61–68. DOI:10.1046/j.1365-2419.2001.00155.

Niebauer H J, Alexander V, Henrichs S. 1990. Physical and Biological Oceanographic Interaction in the Spring Bloom at the Bering Sea Marginal Ice Edge Zone. *Journal of Geophysical Research* **95**(C12): 22,229–22,241. DOI:10.1029/JC095iC12p22229.

National Research Council. 1996. *The Bering Sea Ecosystem* . Washington, DC: The National Academies Press.

Overland J E, Nicholas A, Adams J M. 2001. North Pacific Atmospheric and SST Anomalies in 1997: Links to ENSO?. *Fisheries Oceanography* **10**(1): 69–80.

Perovich D, Gerland S, Hendricks S, Meier W, Nicolaus M, Richter-Menge J, Tschudi M. 2012. Sea Ice, in: Arctic Report Card 2012.

Solomon S, Qin D, Manning M, Chen Z, Marquis M, Averyt K, Miller H L. 2007. *Climate Change 2007: The Physical Science Basis*. Cambridge, United Kingdom and New York, NY, USA: Cambridge University Press. 996 pp.

Smith R D, Jones P, Briegleb B, Bryan F, Danabasoglu G, Dennis J, Dukowicz J, Eden C, Fox-Kemper B, Gent P, Hecht M, Jayne S, Jochum M, Large W, Lindsay K, Maltrud M, Norton N, Peacock S, Vertenstein M, Yeager S. 2010. The Parallel Ocean Program (POP) reference manual, ocean component of the Community Climate System Model (CCSM). Los Alamos National Laboratory, Technical Report LAUR-10-01853, 141 pp.

Stabeno P J, Bond N A, Kachel N B, Salo S A. 2001. On the temporal variability of the physical environment over the south-eastern Bering Sea. *Fisheries Oceanography* **10**(1): 81–98. DOI:10.1046/j.1365-2419.2001.00157.

Stabeno P J, Overland J E. 2001. Berig Sea Shifts to an Earlier Spring Transition. *EOS Transactions American Geophysical Union* **82**(29): 317–324.

Stabeno P, Napp J, Mordy C, Whitledge T. 2010. Factors influencing physical structure and lower trophic levels of the eastern Bering Sea in 2005: sea ice, tides, and winds. *Progress in Oceanography* **85**: 180-196. DOI:10.1016/j.pocean.2010.02.010.

Stabeno P, Farley E Jr, Kachel N, Moore S,Mordy C, Napp J, Overland J, Pinchuk A, Sigler M. 2012a. A comparison of the physics of the northern and southern shelves of the eastern Bering Sea and some implications for the ecosystem. Deep Sea Res. II Topical Stud. Oceanogr. **65–70**: 14–30, DOI: 10.1016/j.dsr2.2012.02.019.

Stabeno P, Kachel N, Moore S, Napp J, Sigler M, Yamaguchi A, Zerbini A. 2012b. Comparison of warm and cold years on the southeastern Bering Sea shelf and some implications for the ecosystem. *Deep Sea Research Part II: Topical Studies in Oceanography*, **65**: 31–45. DOI:10.1016/j.dsr2.2012.02.020.

Stafford K M, Moore S E, Stabeno P J, Holliday D V, Napp J M, Mellinger D K. 2010. Biophysical ocean observation in the southeastern Bering Sea. *Geophysical Research Letters* **37**(L02606). DOI:10.1029/2009GL040724.

Walston, J M, Gibson G A, Walsh J E. 2014. Performance assessment of the Community Climate System Model over the Bering Sea. *International Journal of Climatology*, in press. DOI:10.1002/joc.3954.

4 Conclusion

4.1 Summary

The goal of this thesis was to understand the predictive potential of complex interactions between the Arctic's physical and biological systems, concentrating primarily on the marine ecosystem of the eastern Bering Sea. This was achieved by completing two separate, but fundamentally linked, analyses. The first was accomplished through an assessment of the spatial and temporal variability in key atmospheric components relevant to marine ecosystems as simulated by CCSM4, the NCAR-developed general circulation model. Initially, model output was compared to NCEP/NCAR reanalysis data and its accuracy was assessed over a fifty-one-year climatological period. The CCSM4 has been further developed to include an interactive carbon cycling component and is now referred to as the Community Earth System Model (CESM1). Subsequent to the initial analysis, environmental (air temperature, wind mixing, sea ice cover, and mixed layer depth) extremes over a fifty-five-year climatological period, as simulated by the CESM1, were identified. The impact of these environmental extremes on simulated primary production extremes over interannual and seasonal scales throughout the eastern Bering Sea was explored. Key findings of this research is as follows:

- The spatial distribution of surface-air temperature was generally well simulated over the Arctic, though the simulated temperatures remain colder than the NCEP/NCAR reanalysis throughout most of the Arctic region.
- Over the Bering Sea, general temperature patterns, including spatial gradients, were accurately simulated compared to the reanalysis, although cold and warm biases still remain across climatological annual and seasonal means.

- The Beaufort High was nearly non-existent within simulated climatological monthly mean sea level pressure, corresponding to a large mass deficit in the Arctic domain.
- Across the entire northern half of the Bering Sea, a large northwest displacement of the Aleutian Low and a weaker-than-observed Siberian High resulted in a negative bias of up to 6 hPa. This shift in mass, along with a weaker anticyclone, produced errors in sea level pressure, and by implication, near-surface winds, in all seasons over the entire Bering Sea.
- Variability of simulated annually averaged surface-air temperature and sea level pressure over the Bering Sea exceeds that which is observed—nearly 1.5 and 2 times the observed variance, respectively.
- The model simulation of the 1950-2005 period shows trends towards higher temperatures (with fewer cold and more warm extremes) and a corresponding reduction of sea ice. Consistent with these trends, primary production in the northern Bering Sea shows a positive trend over the same period.
- The CESM simulates extremes in both forcing and primary production over the Bering Sea and relationships between the extremes are physically and biologically plausible, although seasonal extremes in the physical environment did not always correspond to seasons of extreme primary production.
- Seasonal extreme primary production did not always correspond to an annual extreme primary production.
- The strongest linear relationships between physical drivers and seasonal production were found in winter and spring simulated air temperature and sea ice cover. While simulated wind friction velocity (upper-ocean mixing) exhibited a positive linear correspondence with primary production only during summer in the southern domain.

- The inverse relationship between the amount of sea ice cover and spring production, found in the southern Bering Sea, is an indication that the CESM captures the importance of salinity stratification of the water column following sea ice retreat, initiating a spring bloom.

4.2 Discussion

4.2.1 Implications of air temperature biases

The overlying air temperature, in combination with ocean mixing, directly influences the temperature of the water column and impacts phytoplankton production. The relationship between temperature and production is complex; in addition to controlling metabolic processes of the marine biota, through thermal stratification, temperature impacts the stability of the water column and thus the vertical flux of nutrients essential for production. As such, to adequately simulate marine production in the eastern Bering Sea, or large marine ecosystems in general, it is critical to adequately represent spatial and temporal patterns of observed air temperature.

Over the broad Arctic domain the CSSM4 was found to under-simulate air temperature, resulting in a large cold bias throughout most of the Arctic. Despite the broad Arctic biases, spatial air temperature gradients from the third to fourth version of the CCSM have improved over the entire Bering Sea; however, warm and cold biases remain in every season simulated by the CSSM4. Air temperature, as a proxy for sea surface temperature, was used to infer the implications simulated biases may have on physical and biological processes of the Bering Sea. The impact of these biases on marine production will vary depending on which season they occurred in and which marine ecosystem component is considered. For example, the robust warm winter bias found in the northern Bering Sea would delay the formation and extent of sea ice, thus impacting simulations of the physical and biological structure of the water column.

Additionally, cold biases found during spring and summer would hinder the simulation of the phytoplankton and zooplankton metabolic rates, such as growth, respiration, and grazing, all of which are temperature dependent. These findings suggest the CCSM4 requires further development to reduce the robust air temperature biases during seasons critical for marine ecosystem dynamics in the Arctic and Bering Sea region.

4.2.2 Impacts of the simulated warming trend

The CESM1 simulated a trend towards warmer temperatures in every season over the eastern Bering Sea, with an increase in positive air temperature extremes occurring in the latter half of the evaluated period. A modest increase in summer air temperature has been observed over the entire Bering Sea since 1948 with a well-above-average warm period starting in the early 2000s (Brown and Arrigo, 2012). NCEP/NCAR reanalysis data over the Bering Sea does not show a warming trend in every season, but does show an upward trend in observed temperature during the summer. However, the magnitude of the CESM1 summer warming trend is greater than what is seen in the NCEP/NCAR reanalysis data. The exaggerated CESM1 warming trend may be partially due to natural variability in the model's simulation of air temperature. Moreover, Gent et al. (2011) suggest that the indirect effect of aerosols, which act as a cooling mechanism, is not included in the CESM1 atmospheric component and causes the globally averaged surface air temperature to increase at a faster rate compared to observations and its predecessor, the CCSM3.

The amplified air temperature trends and increase in temperature extremes found in the CESM1 may have implications for predictions of seasonal production over the eastern Bering Sea shelf. Statistically significant correlations between air temperature and production were seen during winter and spring in both north and south domains. Although it is likely that there is a

positive relationship between winter primary production and winter air temperature, with warmer temperature raising metabolic rates and increasing light availability through a reduction in sea ice cover, NCEP reanalysis data suggests that in reality winter temperatures have yet to increase (Figure 3.10). If such a warming were to occur, the resulting increase in winter production would remain a small fraction of the total annual production. This is because the solar angle during an Arctic/Subarctic winter does not enable enough solar heating nor does it provide a sufficient amount of light to sustain a prolonged period of primary production. However, a warming trend may have implications for ecosystem dynamics in the Subarctic, as an increase in production would increase the availability of energy to support over-wintering species in either the benthic or pelagic habitats. Even though both positive and negative correlations were distinguished between air temperature and primary production, there was a lack of correspondence between seasonal air temperature extremes and seasonal primary production extremes which indicates that additional environmental factors other than those examined may contribute to seasonal primary production extremes of the eastern Bering Sea in the model. However, it is also possible that the production response to environmental extremes occurs on timescales shorter than seasonal; this highlights the need to consider a range of ecosystem related timescales.

4.2.3 Implications of atmospheric circulation biases

As was the case for simulated air temperature, the CCSM4 captures spatial patterns of atmospheric circulation over the broad Arctic and has an improved representation of monthly mean sea level pressure over the Subarctic Pacific, relative to the CCSM3. However, there still remain substantial shortcomings in the CCSM4's ability to simulate the magnitude and placement of synoptic scale systems in the Arctic and Subarctic regions. The Beaufort High and Siberian High pressure centers, in the Arctic and Subarctic respectively, were correctly placed,

although considerably under simulated compared to the observational record. In contrast, the intensity of the low pressure centers in the Arctic and Subarctic domains exceeded observations. In a broad sense, the CESM1 captures the dipole characteristic between the Icelandic Low and Aleutian Low pressure centers in the Arctic and Subarctic, respectively. However, both simulated low pressure centers are laterally shifted from where they naturally reside.

These four pressure centers drive synoptic weather patterns over the Arctic and Subarctic domains. A misrepresentation of atmospheric circulation would impact the formation, melt and transport of sea ice (Maslowski et al., 2012), important physical mechanisms which high latitude marine ecosystems depend upon. A shifted Aleutian Low pressure center in combination with a weaker-than-average Siberian High pressure center caused biases in every season over the climatological period, in turn causing the seasonal patterns of geostrophic wind over the Bering Sea to differ from observations. Simulated sea level pressure was not spatially improved compared to CCSM3 during spring, a season of great importance to biological production in high latitudes. However, a large lateral displacement of the Aleutian Low should raise caution for ecosystem modelers because this shift promoted southwesterly winds spanning the entire Southern Bering Sea, compared to a northeasterly wind direction in reanalysis data. Changes in the direction of geostrophic wind could alter the dominant currents and impact simulations of nutrients and plankton transport.

4.2.4 Production response to wind mixing

During winter, the Bering Sea is well mixed due to convection, wind and tidal mixing, but as insolation increases and storms decrease in late spring and summer, the water column becomes stratified (Ladd and Stabeno, 2012). Stratification is initially beneficial to phytoplankton by confining their vertical position to the euphotic zone, however, phytoplankton become nutrient

limited because they quickly deplete the nutrient supply. In the summer, wind mixing breaks down thermal stratification and supplies nutrient-limited phytoplankton trapped in the upper mixed layer the resources they require. Hence, wind mixing and water column stability greatly impact the intensity and magnitude of primary production, which provides the energy driving pelagic and benthic habitats (Coyle et al., 2008).

Positive linear relationships between wind mixing and primary production were found during spring and summer in the north and south domains, respectively. Simulated summer wind mixing was found to be the most statistically significant environmental variable for summer production in the southern Bering Sea, supporting what is found in observations (Eisner et al., 2014 in press). Despite the positive correlation between summer wind mixing and summer production, there was a lack of correspondence between seasons of extreme wind mixing and seasons of extreme primary production. Wind mixing is proportional to the cubed root of the wind speed and thus storm events with stronger winds can have a large impact on the resultant wind mixing. Storms that last on the order of days to weeks pass over the Bering Sea shelf, and it is possible that the relationship between wind and the biological response to extremes would be more significant over shorter timescales.

The CESM's simulation of wind mixing should be treated with caution, since the models representation of atmospheric circulation has been shown to have several seasonal shortcomings. Atmospheric circulation establishes pressure gradients, which determine the strength of the wind stress, hence wind mixing at the ocean's surface. The CESM simulated summer atmospheric circulation with less skill than seen in any other season. Robust biases in the summer circulation produced a strong pressure gradient in the southern Bering Sea resulting in stronger zonal momentum than observed. This may result in an over estimation of wind mixing, leading to a

misrepresentation of the nutrient and light fields that the phytoplankton in the upper mixed layer are exposed to.

4.2.5 Mixed layer depth and primary production relationship

Primary production of the eastern Bering Sea is influenced by the interaction of several physical drivers. This research has focused on three physical features that are important to primary production in this region: sea ice, air temperature and wind mixing. The stability of the water column of the eastern Bering Sea is strongly influenced by temperature and salinity gradients caused by seasonal heating and the formation/melting of sea ice. Wind stress causes the upper surface layers of the ocean to mix and break down the stratification of the water column. The interaction between these three variables establishes the homogeneous upper mixed layer, which controls the amount of nutrients and light available for phytoplankton growth. As such the seasonal mixed layer depth reflects the balance of the physical environment and can be considered a composite property and key physical forcing variable for marine ecosystems.

Significant relationships were found between seasonal mixed layer depth and primary production simulated by the CESM1. The trend (positive or negative) of these relationships was dependent on the season and region of the Bering Sea. The relationship between summer primary production and summer mixed layer depths was positive in both the north and south Bering Sea. However, the relationship during spring was positive in the northern Bering Sea and negative in the southern. Despite these correlations, the lack of strong correspondence between production extremes and mixed layer depth extreme suggests that a time scale less than seasonal may be more representative of this important relationship. It may also imply that other factors, such as nutrient transport, light availability or even grazing pressure of zooplankton are contributing to primary production extremes.

4.2.6 Ecosystem variability

Variability of the physical environment can affect production of the eastern Bering Sea on multiple timescales. The physical features of the eastern Bering Sea exhibit strong year-to-year variation, especially the extent of sea ice, but shorter timescales of variability on the order of weeks to months can have a large effect on primary production in the eastern Bering Sea (Bond and Overland, 2005). Recent studies suggest that the Bering Sea has been experiencing a pattern of low frequency variability, with a multi-year pattern oscillating between warm (2000-2005) and cold (2007-2012) years (Overland et al., 2012; Stabeno et al., 2012b; Wendler et al., 2013). Wendler et al. (2013) propose the PDO as an appropriate explanation for the fluctuations between the warm and cold years, with the strength of the Aleutian Low determining advection of warm maritime air. Large marine ecosystems in high latitude seas exhibit similar scales of variability, with abrupt changes in the physical environment causing large shifts in the abundance and distribution of marine species (Mantua 1997; Grebmeier et al., 2006). For this reason, it is imperative for climate models, especially those used to drive marine ecosystem dynamics, to represent the timescales and modes of variability similar to those of the real world. Without data assimilation, models cannot be expected to match the timing of observed variability. However, Earth System Models need to be able to accurately simulate the magnitude and frequency of variations in the physical environment, at least in a statistical sense, if they are to accurately represent the observed variations of marine ecosystems.

Over the Bering Sea domain the interannual variability of air temperature and sea level pressure simulated by CSSM4 was found to be approximately 1.5 to 2 times the observed interannual variability. This inflation may have an impact on simulated annual extremes over the Bering Sea. On a seasonal basis, variations of air temperature were simulated well, suggesting

that the models representation of seasonal air temperature extremes was likely accurate. Sea level pressure did not share a similar result, with seasonal variability exceeding the observed. Increased variability of atmospheric circulation may have several implications for simulated sea ice dynamics and geostrophic winds, possibly leading to an over prediction of seasonal variability and extremes compared to reality.

4.3 Future work

The ability to validate ESM simulations of past and present state of the Bering Sea ecosystem is limited by the lack of long-term observations. Studies such as the one presented here also need long-term observations to better analyze long-duration anomalies over different scales of variability, including extreme events. Until a sufficient amount of data of the Bering Sea is available, model simulations will remain limited in this respect.

Model simulations are also limited by their relatively course resolution. GCM's, such as the CESM1/CCSM4, simulate or project climate scenarios over a global domain and therefore have difficulty resolving mesoscale features over regional or lesser scales (Randall et al., 2007). To overcome these issues climate studies often use downscaling techniques; such methods may prove to enhance the work presented here. Additionally, an extension of this research to examine variability of both primary production and physical drivers over shorter timescales to capture the sub seasonal variations (i.e. weekly and/or monthly) may prove to be very insightful.

The primary focus of this work was the physical impacts on primary production. The lack of robust correspondence between physical and production extremes suggests that a more comprehensive assessment, to include biological (i.e. zooplankton and upper trophic level species) and chemical (nutrients) influences, may be needed to ascertain the full extent of the effects of environmental variability on primary production variability in the eastern Bering Sea.

4.4 Closing remarks

The combination of the two studies that comprise this thesis represents a significant step towards understanding the ability of ESMs to predict the ecosystem response to variations of the physical environment. While the predictability of such systems is limited due to a mismatch in timescales of variability (Levin, 1992) and inherent nonlinearities of the natural system (Francis et al., 1998), ESMs have improved in their ability to systematically capture the climate dynamics over global and regional scales. Despite these improvements some caution should be taken to understand the skill of a global model when using it to drive regional models of ecosystem dynamics.

This research concludes that the CESM1's physical environment can be used to drive marine ecosystems in the Bering Sea region, although the biases found in atmospheric circulation and the increased of variability of key physical forcing variables still requires further development. While this research found linkages between physical environmental variability and marine ecosystem variability, it suggests that a seasonal resolution may not be a sufficient resolution for examining the biological response to certain physical extremes of the eastern Bering Sea. An immediate priority is the determination of the sensitivity of this study's findings to the temporal resolution of the data.

References

Bond N A, and Overland J E. 2005. The importance of episodic weather events to the ecosystem of the Bering Sea shelf. *Fisheries Oceanography* **14(**2): 97–111.

Brown Z W, Arrigo K R. 2012. Contrasting trends in sea ice and primary productionin the Bering Sea and Arctic Ocean. *ICES Journal of Marine Science*, **69**(7): 1180–1193. DOI:10.1093/icesjms/fssl13.

Coyle K, Pinchuk A, Eisner L, Napp J. 2008. Zooplankton species composition, abundance and biomass on the eastern Bering Sea shelf during summer: The potential role of water-column stability and nutrients in structuring the zooplankton community. *Deep Sea Research Part II: Topical Studies in Oceanography* **55**: 1775–1791. DOI:10.1016/j.dsr2.2008.04.029.

Gent P, Danabasoglu G, Donner L, Holland M, Hunke E, Jayne S, Lawrence D, Neale R, Rasch P, Vertenstein M, Worley P, Yang Z, ZhangM. 2011. The Community Climate SystemModel version 4. Journal of Climate **24:** 4973–4991, DOI: 10.1175/2011JCLI4083.1.

Grebmeier J, Overland J, Moore S, Farley E, Carmack E, Cooper L, Frey K, Helle J, McLaughlin F, McNutt S. 2006. A major ecosystem shift in the northern Bering Sea. *Science* **311**: 1461–1464, DOI: 10.1126/ science.1121365.

Eisner L B, Napp J M, Mier K L, Pinchuk A I, Andrews III A G. 2014. Climate mediated changes in zooplankton community structure for the eastern Bering Sea. *Deep Sea Research Part II*, in press.

Francis R C, Hare S R, Hollowed A B, Warren S. 1998. Effects of interdecadal climate variability on the oceanic ecosystems of the NE Pacific. *Fisheries Oceanography* **7**(1): 1–21.

Ladd C, Stabeno P. 2012. Stratification on the Eastern Bering Sea shelf revisited. *Deep Sea Research Part II: Topical Studies in Oceanography*, ***65***: 72–83. DOI:10.1016/j.dsr2.2012.02.009.

Levin S. 1992. The problem of pattern and scale in ecology. *Ecology*, **73**(6): 1943–1967.

Mantua N J, Hare S R, Zhang Y, Wallace J M, Francis R C. 1997. A Pacific Interdecadal Climate Oscillation with Impacts on Salmon Production. *Bulletin of the American Meteorological Society*,**78**(6): 1069–1079.

Maslowski W, Kinney J, Higgins M, Roberts A. (2012). The Future of Arctic Sea Ice. *Annual Review of Earth and Planetary Sciences* **40**: 625–654. DOI:10.1146/annurev-earth-042711-105345

Overland J E, Wang M, Wood K R, Percivial D B, Bond N A. 2012. Recent Bering Sea warm and cold events in a 95 year context. *Deep Sea Research Part II* **65-70**: 6–13.

Randall D A, Wood R A, Bony S, Colman R, Fichefet T, Fyfe J, Kattsov V, Pitman A, Shukla J, Srinivasan J, Stouffer R J, Sumi A, Taylor K E. 2007. Cilmate Models and Their Evaluation, in: Climate Change 2007: The Physical Science Basis. Contribution of Working Group I to the Fourth Assessment Report of the Intergovernmental Panel on Climate Change, Solomon S, Qin D, Manning M, Chen Z, Marquis M, Averyt K B, Tignor M, Miller H L (eds.), Cambridge University Press, Cambridge, United Kingdom and New York, NY, USA

Stabeno P, Kachel N, Moore S, Napp J, Sigler M, Yamaguchi A, Zerbini A. 2012b. Comparison of warm and cold years on the southeastern Bering Sea shelf and some implications for the ecosystem. *Deep Sea Research Part II: Topical Studies in Oceanography* **65**: 31–45. DOI:10.1016/j.dsr2.2012.02.020.

Wendler G, Chen L, Moore B. 2013. Recent sea ice increase and temperature decrease in the Bering Sea area, Alaska. *Theoretical and Applied Climatology* **114**, DOI: 10.1007/s00704-013-1014.